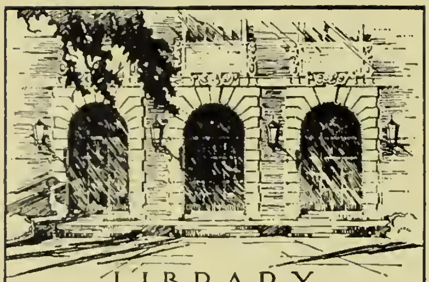

LIBRARY
OF THE
UNIVERSITY
OF ILLINOIS
621.365
Il655te
no. 2-14
cop. 3

Digitized by the Internet Archive
in 2013

http://archive.org/details/closelyspacedtra14hyne

Antenna Laboratory

Technical Report No. 14

CLOSELY SPACED TRANSVERSE SLOTS
in
RECTANGULAR WAVEGUIDE

by

R.F. Hyneman

10 December 1956

Contract AF33(616)-3220
Project No. 6(7-4600) Task 40572
WRIGHT AIR DEVELOPMENT CENTER

Electrical Engineering Research Laboratory
Engineering Experiment Station
University of Illinois
Urbana, Illinois

621.365
Il655te
no.4
cop.3

CONTENTS

Page

Abstract viii

Acknowledgement ix

List of Symbols x

I. Introduction 1

II. Discussion of the Problem 4

2.1 Simplifying Assumptions 4
2.2 Space Variation in the Fields 4
2.3 Integral Equation for the Aperture Field 10
2.4 Variational Solution for γ 11
2.5 Approximate Application of the Reaction Concept 13
2.6 Derivation of the Characteristic Equation for γ 16

III. Theoretical and Experimental Results for the Case of Slot Length Equal to Waveguide Width 25

3.1 Characteristic Equation for γ 25
3.2 Theoretical and Experimental Results 30
3.3 Aperture Distribution Synthesis 42
3.4 Surface Wave Mode 48

IV. Theoretical and Experimental Results for Small Slot Length 58

4.1 Characteristic Equation for γ 58
4.2 Theoretical and Experimental Results 60
4.3 Surface Wave Solution 66

V. Experimental Verification of the Theory 79

5.1 Details of Construction of the Model 79
5.2 Measurement of γ in Cases of Large α 81
5.3 Measurement of γ in Cases of Small α 83

VI. Conclusions and Recommendations for Further Investigation 85

References 87

Appendix A - Proof of the Stationary Properties of Equations 2-18 and 2-21 89

CONTENTS (CONTINUED)

Page

Appendix B - The Evaluation of I_n (β/k, L/λ) 93

Appendix C - Approximations for the Series S_3 and S_5 in Equation 3-3 103

Distribution List 113

ILLUSTRATIONS

Figure Number — *Page*

1. The Transversely Slotted Waveguide 5

2. The Traveling-Wave Slot Antenna 13

3. $F(\frac{W}{\lambda}) = j \frac{W}{\lambda} \frac{1}{1 - \frac{\lambda^2}{4W^2}} I_o (\frac{{}_o\beta}{k} \frac{W}{\lambda})$ 31

4. Attenuation Constant versus Frequency for Fixed Waveguide and Slot Dimensions 33

5. Velocity Ratio versus Frequency for Fixed Waveguide and Slot Dimensions 35

6. Attenuation Constant versus Frequency 36

7. Attenuation Constant versus Frequency for Fixed Waveguide and Slot Dimensions 37

8. Attenuation Constant versus Slot Spacing 38

9. Attenuation Constant versus Slot Spacing 39

10. Velocity Ratio versus Slot Spacing 40

11. Velocity Ratio versus Slot Spacing 41

12. Attenuation Function and Average Slot Spacing for Uniform Aperture Distribution 44

13. Polar Coordinate System for Pattern Measurements 45

14. E-Plane Radiation Patterns for Uniform Aperture Distribution (Figure 12) 46

15. Input Standing Wave Ratio versus Slot Spacing 47

16. Velocity Ratio versus Frequency for Surface Wave Mode 51

17. Axial Phase-Amplitude Distribution with Fundamental and Surface Wave Modes Present, $W < \lambda/2$ 53

ILLUSTRATIONS (continued)

Figure Number — *Page*

18. Measured Axial Phase-Amplitude Distribution under Conditions of Single Mode Propagation 54

19. Dielectrically Loaded Feed Section to Improve Surface Wave Launching Efficiency 55

20. Evidence of Asymmetrical Surface Wave Mode Resulting from Small Structural Dissymmetry when W/λ Near 1.0 56

21. Evidence of Third Order Surface Wave Mode for W/λ Near 1.5 57

22. Real Part of $I_0[({}_0\beta/k), (L/\lambda)]$ versus L/W 61

23. Imaginary Part of $I_0[({}_0\beta/k), (L/\lambda)$ versus L/W for $.02 \leq L/W \leq 0.25$ 62

24. Imaginary Part of I_0 $[({}_0\beta/k), (L/\lambda)$ versus L/W for $.02 \leq L/W \leq 1.0$ 63

25. $S' = \sum_{m=3}^{\infty} \frac{\cos^2 (m\pi L/2W)}{[1-(m^2L^2/W^2)^2]} \frac{[(m^2\lambda^2/4W^2) - 1]}{(m^2 - 1)^{1/2}}$ 64

26. $S' = \sum_{m=3}^{\infty} \frac{\cos^2 (m\pi L/2W)}{[1-(m^2L^2/W^2)^2]} \frac{[(m^2\lambda^2/4W^2) - 1]}{(m^2 - 1)^{1/2}}$ 65

27. Attenuation Constant versus Slot Length for Infinitesimally Spaced Slots, W/λ = 0.686 67

28. Attenuation Constant versus Slot Length for Infinitesimally Spaced Slots, W/λ = 0.95 68

29. Attenuation Constant versus Slot Length for Infinitesimally Spaced Slots, W/λ = 1.27 69

30. Velocity Ratio versus Slot Length for Infinitesimally Spaced Slots 70

ILLUSTRATIONS (continued)

Figure Number *Page*

31. Measured Axial Amplitude Distributions with Fundamental and Surface Wave Modes Present 73

32. Measured Axial Amplitude Distributions with Fundamental and Surface Wave Modes Present 74

33. E-Plane Radiation Patterns Showing Relative Excitation of Surface Wave versus L/λ as Frequency is Varied 76

34. E-Plane Radiation Patterns Showing Increase in Surface Wave Excitation with Decrease in D/λ. 78

35. The Experimental Model 80

36. Schematic of Experimental Setup for Phase-Amplitude Measurements 82

37. p_o (ℓ/d) 107

38. p_2 (ℓ/d) 108

39. p_4 (ℓ/d) 109

40. q_o (ℓ/d) 110

41. q_2 (ℓ/d) 111

42. q_4 (ℓ/d) 112

ABSTRACT

The traveling wave modes associated with the infinite, periodic structure consisting of closely spaced transverse slots in rectangular waveguide are considered. An approximate equation for the propagation constants of these modes for the case of infinitesimal thickness of the slotted wall is derived through Fourier Analysis techniques and an approximate application of the Reaction Concept. Theoretical results are given for two special cases, a) discretely spaced slots which extend completely across the broad face of the waveguide, and b) infinitesimally spaced slots of arbitrary length. In the homogeneous case considered, it is found that two dominant modes may exist, an attenuated fundamental mode representing a perturbation of the dominant TE_{10} mode in closed rectangular waveguide, and an unattenuated surface wave, with phase velocity less than that of free space, which is similar to the wave associated with a corrugated surface waveguide. Essentially independent control of the attenuation constant and phase velocity of the fundamental mode is possible over a wide range through the appropriate variation of the various physical parameters. Curves are given for the propagation constant in terms of these parameters, and the results of experimental measurements are shown to be in close agreement with the theory.

ACKNOWLEDGEMENT

The author wishes to acknowledge the guidance of Prof. V.H. Rumsey, without whose help this report would not have been possible. He is also indebted to Drs. R.H. Duhamel and E.J. Scott for their many helpful suggestions, to Mrs. Allen Blankfield, who performed most of the computations, and to Mr. J.J. Stafford who performed many of the experimental measurements.

LIST OF SYMBOLS

c	Free space velocity of propagation
c/v	Waveguide velocity ratio
d	Slot width (narrow dimension)
D	Waveguide depth (narrow dimension)
$H_o^{(2)}(z)$	Hankel Function of the second kind
$I_o(\frac{\beta}{k}, \frac{L}{\lambda})$	See Appendix B, page 99
j	$j = \sqrt{-1}$
k	Free space propagation constant, $k = \omega \sqrt{\mu_o \varepsilon_o}$
$K_o(z)$	Modified Hankel Function of the second kind.
ℓ	Slot spacing
L	Slot length (long dimension)
$\mathcal{L}$	Total length of aperture.
v	Waveguide phase velocity, $v = (\omega\lambda_g/2\pi)$
W	Waveguide width (large dimension)

α	Attenuation constant
α/k	Normalized attenuation constant (nepers per radian)
β_n	$\beta_n = k^2 - \sqrt{\gamma_n^2}$
β	$\beta \equiv \beta_o = \sqrt{k^2 - \gamma_n^2}$
γ_n	$\gamma_n = \gamma - (2n\pi/\ell)$
γ	$\gamma \equiv \gamma_o$, waveguide propagation constant, $\gamma = (\omega/v) - j\alpha$
${}_o\gamma$	Unperturbed γ for closed rectangular waveguide, ${}_o\gamma = \sqrt{k^2 - (\pi^2/W^2)}$
γ	Euler's constant, $\overline{\gamma} = .5772 \ldots$
Γ	Reflection coefficient at beginning of aperture
ε	Permittivity constant

$\zeta_{m,n}$	$\zeta_{m,n} = j\,\kappa_{m,n} = \sqrt{(m\pi/W)^2 + \gamma_n^2 - k^2}$
$\kappa_{m,n}$	$\kappa_{m,n} = \sqrt{k^2 - \gamma_n^2 - (m^2\pi^2/W^2)} = \sqrt{k^2 - (m\pi/W)^2 - \gamma_n^2}$
κ	$\kappa \equiv \kappa_{1,0} = \sqrt{k^2 - (\pi/W)^2 - \gamma^2}$
λ	Free space wavelength
λ_g	Guide wavelength
μ	Permeability constant
$\xi_{m,n}$	$\xi_{m,n} = 0$ for $m = 1$ when $n = 0$, $= 1$ otherwise.
ρ	$\rho = \sqrt{x^2 + (y - y')^2}$
σ_n	$\sigma_n = j\,\beta_n = \sqrt{\gamma_n^2 - k^2}$
ω	$\omega = 2\pi$ frequency

I. INTRODUCTION

The general subject of traveling-wave antennas has been of considerable interest for a long period of time. Early investigations have dealt with the characteristics of such long wire devices as the Beveridge Wave Antenna and the Rhombic. More recently, as the result of the trend to higher frequencies, attention has been primarily directed to studies of open, radiating waveguide systems.

Dielectric and corrugated surface waveguides[1-5] in their various forms belong to this latter class. Their usefulness arises from the existence of a guided wave mode of propagation for which the phase velocity is less than the free space velocity of light. Thus when employed in their rudimentary form as antenna elements, these structures possess essentially end-fire radiation characteristics. When an arbitrary radiation pattern is required, a surface waveguide may be employed as a transmission line for the excitation of a suitable configuration of discretely spaced radiating or scattering elements.[6-7]

The Channel Guide[8] and the Traveling Wave Slot Antenna[9-10] have also received considerable attention. Basically, these structures consist of conventional metallic, cylindrical waveguide in which the internal fields are coupled to the exterior, or free space region, by means of a continuous axial slot. In the homogeneous case, the propagation constant is complex and the traveling wave, which has a phase velocity greater than that of free space, is attenuated with distance along the guide. A useful means of radiation pattern control is available since the aperture illumination may be adjusted by suitably varying the transverse geometry of the waveguide and the width of the axial slot.[11] As a result, a wide variety of antenna patterns may be synthesized.

In recent papers[12-13], Elliott has reported on an investigation of the Serrated Waveguide Antenna. This structure is essentially a rectangular waveguide, having a corrugated surface for one of the interior broad faces. Transverse slots placed in this face at the bottom of the corrugations provide coupling to the exterior region. Because of computational difficulties, the analysis was limited to the case of infinitesimally spaced slots and corrugating teeth. For this case, the Serrated Waveguide is essentially a thick walled rectangular waveguide which has been pierced by a series of infinitesimally spaced transverse slots.

This report is concerned with the characteristics of finitely spaced transverse slots in a thin walled rectangular waveguide. Thus, from a physical standpoint, the structure is in some respects a complement of the one considered by Elliott. In addition, from an electrical point of view, the transversely slotted waveguide differs from the rectangular case of the Traveling Wave Slot Antenna only in the type of coupling mechanism which is employed The resulting differences between the characteristics of the two structures are in the modes of propagation and in the type of polarization of the radiated fields.

The radiating aperture of the transversely slotted waveguide consists of a collection of discretely spaced radiating elements. However, experiments have shown that when the slot spacing is less than one-half free-space wavelength, the character of the distant radiated field is approximately the same as for a continuous distribution that is the average of the discrete elements. Thus the existing techniques for antenna pattern synthesis which apply to the continuous or axial slot case give good results for the case of transverse slots. In order that these techniques may be employed, a knowledge of the attenuation constant and phase velocity of the traveling wave is necessary.

In the treatment of the uniform, infinite, periodically slotted case, Fourier Analysis techniques may be employed to obtain an approximate expression for the propagation constant. By following this procedure, the need for an explicit and difficult consideration of the large mutual coupling between the closely spaced slots is obviated.

Approximate theoretical results, which are in close agreement with experimental observations, are given for the attenuation constant and phase velocity as a function of the structure geometry. In addition, it is found that an unattenuated surface wave with velocity less than that of free space may exist under certain conditions. Thus the transversely slotted waveguide combines some of the characteristics of an open corrugated surface waveguide and the Traveling Wave Slot Antenna.

II. DISCUSSION OF THE PROBLEM

2.1 Simplifying Assumptions

A theoretical analysis of the problem is possible only for the infinite, uniform, periodic case. Although these conditions are not met in a physical situation, previous investigations have shown that the results of an analysis of the idealized case closely apply when the structure is long, and where any departure from uniformity and periodicity is gradual, in terms of wavelength.

Several simplifying assumptions are made. With reference to Figure 1, it is assumed that the slot length to width ratio L/d is sufficiently great, and d/λ is sufficiently small that only the z component of electric field in the slot is appreciable. The thickness of the slotted wall of the waveguide is taken to be infinitesimal. Finally, consideration is restricted to the case where the permittivity and permeability of the internal and external regions are equal to those of free space. However, the somewhat more general case where the two regions are individually taken to be homogeneous represents only a simple extension of the theory.

2.2 Space Variation of the Fields

All components in the internal and external regions can be written in terms of the unknown tangential $\underline{E}$ in the plane of the aperture. The imposition of continuity conditions on the various components at the aperture then leads to an integral equation for the unknown aperture distribution.

Under the initially assumed conditions of periodicity, it can be shown[14,15] that all field components may be expressed in terms of

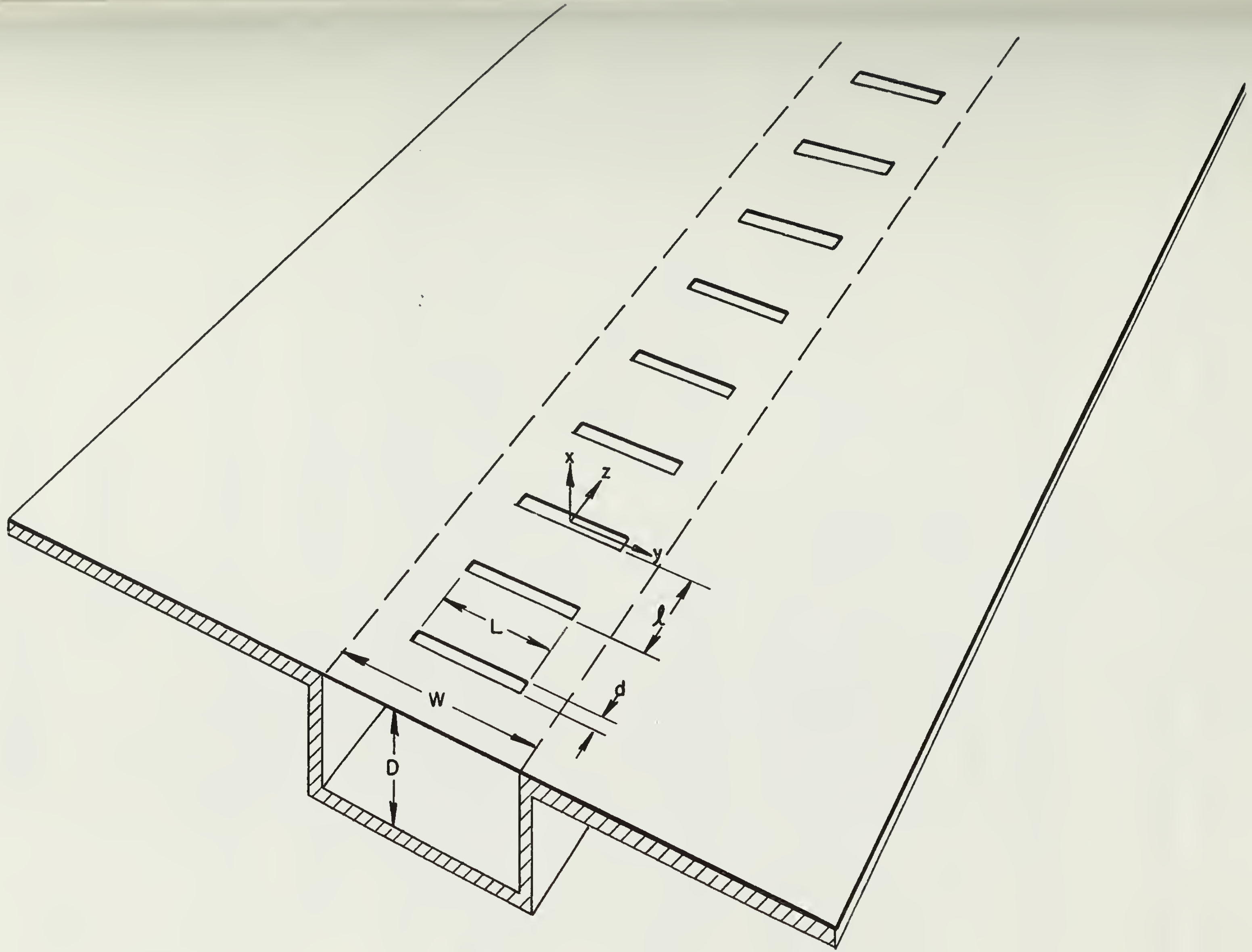

Figure I. The Transversely Slotted Waveguide

exponential and periodic functions of position. The space variation of the fields in both the external and internal regions is of the general form ($e^{+j\omega t}$ time convention),

$$\underline{F}(x,y,z) = \underline{G}(x,y,z)\, e^{-j\gamma z} \qquad (2\text{-}1)$$

where γ is independent of x and y, and $\underline{G}$ satisfies the relation

$$\underline{G}(x,y,z) = \underline{G}(x,y,z,\; z-\ell).$$

Let the origin be placed at the center of a typical slot as in Figure 1. Let the tangential electric field at x = 0 and within the period $-\ell/2 \leq z \leq \ell/2$ be given by

$$\begin{aligned} \underline{E}_{tan} = \underline{z}\, E_z(0,y,z) &= \underline{z}\; g(y,z) && \left\{\begin{matrix} 0 \leq |y| \leq L/2 \\ 0 \leq |z| \leq d/2 \end{matrix}\right\} \\ &= 0 && \left\{\begin{matrix} L/2 \leq |y| \\ d/2 \leq |z| \leq \ell/2 \end{matrix}\right\} \qquad (2\text{-}2) \end{aligned}$$

where g(y,z) is an unknown scalar function of position, and $\underline{z}$ is the unit vector in the z direction. In accordance with Equation 2-1, $E_z e^{+j\gamma z}$ is periodic, and thus may be expanded in a Fourier series valid for all z.

$$\begin{aligned} E_z(0,y,z) &= e^{-j\gamma z} \sum_{n=-\infty}^{\infty} a_n(y)\, e^{j(2n\pi z/\ell)} \\ &= \sum_{n=-\infty}^{\infty} a_n\,(y)\, e^{-j\gamma_n z}, \qquad (2\text{-}3) \end{aligned}$$

where

$$\gamma_n = \gamma - 2n\pi/\ell$$

and where

$$\begin{aligned} a_n(y) &= 1/\ell \int_{-\ell/2}^{\ell/2} E_z\,(0,y,z)\, e^{j\gamma z}\, e^{-j(2n\pi z/\ell)} dz \\ &= 1/\ell \int_{-d/2}^{d/2} g(y,z)\, e^{j\gamma_n z} dz && 0 \leq |y| \leq L/2, \\ &= 0. && L/2 \leq |y|. \; (2\text{-}4) \end{aligned}$$

The field components may be expressed in terms of the aperture field distribution through the use of the equivalent magnetic current sheets defined by

$$\underline{M} = \underline{E} \times \underline{n},$$

where $\underline{n}$ is the unit normal to the aperture pointing into the appropriate region. Thus in the internal and external regions respectively,

$$\underline{M}_{int} = -\underline{y}\, E_z(0,y,z) \qquad (2\text{-}5a)$$

$$\underline{M}_{ext} = \underline{y}\, E_z(0,y,z) \qquad (2\text{-}5b)$$

Let $\underline{F}$ be the magnetic vector potential defined by

$$\underline{E} = -\nabla \times \underline{F}.$$

From Equation 2-5 and in view of the symmetrical boundary considerations, $\underline{F}$ has only a $\underline{y}$ component,

$$\underline{F} = \underline{y}\, f.$$

Thus,

$$\underline{E} = -\nabla \times \underline{y}f = \underline{y} \times \nabla f = \underline{x}\,(\partial f/\partial z) - \underline{z}(\partial f/\partial x) \qquad (2\text{-}6)$$

and all fields are TE with respect to the y axis. Then

$$\begin{aligned}\underline{H} &= -1/j\omega\mu\; \nabla \times \underline{E} = -1/j\omega\mu\; (\nabla \times \bar{y}f)\\ &= -1/j\omega\mu\; [-\underline{x}(\partial^2 f/\partial x \partial y) + \underline{y}\cdot(\partial^2 f/\partial x^2 + \partial^2 f/\partial z^2) +\\ &\qquad - z\,(\partial^2 f/\partial y \partial z)]. \end{aligned} \qquad (2\text{-}7)$$

Since in any source-free region f must satisfy the scalar Helmholtz equation,

$$\nabla^2 f + k^2 f = 0,$$

then

$$H_y = 1/j\omega\mu\; (k^2 + \partial^2/\partial y^2) f. \qquad (2\text{-}8)$$

2.2.1 Internal Field Distribution

Since $\underline{E}_{tan}$ vanishes on the conducting surfaces, then from Equation 2-6, f must satisfy the following boundary conditions in the internal region:

$$\begin{aligned}
\partial f/\partial z &= 0 && y = \pm W/2 \\
\partial f/\partial x &= 0 && x = -D \\
\partial f/\partial x &= -E_z\ (0,y,z) && \\
&= -\sum_{n=-\infty}^{\infty} a_n\ (y)\ e^{-j\gamma_n z} && \left.\begin{array}{l} |y|\leq L/2 \\ \\ L/2\leq |y| \end{array}\right\} x=0. \\
&= 0 &&
\end{aligned}$$

It follows from the wave equation that f is of the form

$$f_{int.} = \sum_{m=1}^{\infty} \sum_{n=-\infty}^{\infty} c_{m,n} \cos m\pi y/W \frac{\cos \kappa_{m,n}(x+D)}{\kappa_{m,n} \sin \kappa_{m,n} D} e^{-j\gamma_n z}, \qquad (2\text{-}9)$$

where

$$\kappa_{m,n} = \sqrt{k^2 - (m\pi/W)^2 - \gamma_n^2},$$

and where

$$\begin{aligned}
c_{m,n} &= 2/W \int_{-L/2}^{L/2} a_n(y') \cos (m\pi y'/W)\, dy' \\
&= 2/\ell W \int_{-L/2}^{L/2} dy' \int_{-d/2}^{d/2} dz' \{g(y',z') \cos(m\pi y'/W)\ e^{j\gamma_n z}\} \quad \text{for m odd,} \\
&= 0 \qquad \text{for m even,} \quad (2\text{-}10)
\end{aligned}$$

since a symmetrical slot location has been assumed. The prime on sigma (Σ') denotes that only the odd numbered terms are included in the summation.

2.2.2 External Field Distribution

In the external region, $\underline{F}$ is obtained from

$$\underline{F} = 2\ \underline{F}_o,$$

where $\underline{F}_o$ is the "free space" magnetic vector potential resulting when the equivalent magnetic aperture current defined in Equation 2-5b is considered to oscillate in free space. This follows from the fact that the magnetic image current in the ground plane is coincident and in phase with the primary source.

The integral expression for $\underline{F}$ is thus

$$\underline{F}_{ext} = 1/2\pi \int_{-L/2}^{L/2} dy' \int_{-\infty}^{\infty} dz' \left\{ \frac{\underline{M}(0,y',z')\ e^{-jkR}}{R} \right\},$$

or, from Equations 2-3,5b,

$$\underline{F}_{ext} = \underline{y}(1/2\pi) \int_{-L/2}^{L/2} dy' \int_{-\infty}^{\infty} dz' \left\{ \frac{\sum_{n=-\infty}^{\infty} a_n(y') e^{-j\gamma_n z'} e^{-jkR}}{R} \right\} \quad (2\text{-}11)$$

where

$$R = \sqrt{x^2 + (y-y')^2 + (z-z')^2}.$$

For complex γ, Equation 2-11 does not converge, and hence is not a valid representation. However, the vector potential function for an infinite line source

$$\underline{y}\ M_y\ dy'\ e^{-j\gamma_n z'}$$

of arbitrary propagation constant γ_n can be determined.[16] For such a source in free space located at x', y', the potential function is given by

$$\underline{F} = \underline{y}\ M_y\ dy' (-j/4)\ H_o^{(2)}\ (\beta_n \rho)\ e^{-j\gamma_n z},$$

where

$$\beta_n = \sqrt{k^2 - \gamma_n^2},$$

$$\rho = \sqrt{(x-x')^2 + (y-y')^2}.$$

The radiation condition at infinity is satisfied when the root of $(k^2 - \gamma_n^2)$ having a positive real part is taken for β_n.

Upon substitution for M_y from Equations 2-3,4,5

$$f_{ext} = -j/2 \int_{-L/2}^{L/2} dy' \left\{ \sum_{n=-\infty}^{\infty} a_n (y') \, H_o^2 \, (\beta_n \rho) \, e^{-j\gamma_n z} \right\}$$

$$= -j/2\ell \int_{-L/2}^{L/2} dy' \left\{ \sum_{n=-\infty}^{\infty} \int_{-d/2}^{d/2} g(y', z') \, e^{-j\gamma_n (z-z')} \cdot H_o^2 \, (\beta_n \rho) \, dz' \right\} \qquad (2\text{-}12)$$

2.3 Integral Equation for the Aperture Field

From Equations 2-7,8 the condition

$$f_{ext} \, (0,y,z) = f_{int} \, (0,y,z)$$

for y,z in a slot region satisfies the requirement of continuity of tangential H. For this condition to be met, Equations 2-9,10,12 yield

$$\sum_{m=1}^{\infty} \sum_{n=-\infty}^{\infty} 2/\ell W \int_{-L/2}^{L/2} dy' \int_{-d/2}^{d/2} dz' \left\{ g(y', z') \, \frac{\cos \kappa_{m,n}(x+D)}{\kappa_{m,n} \sin \kappa_{m,n} D} \cos (m\pi y/W) \cos (m\pi y'/W) \, e^{-j\gamma_n (z-z')} \right\} + j/2\ell \int_{-L/2}^{L/2} dy' \left\{ \sum_{n=-\infty}^{\infty} \int_{-d/2}^{d/2} g(y', z') H_o^{(2)} \, (\beta_n \rho) \, e^{-j\gamma_n (z-z')} dz' \right\} \Bigg|_{x=0} = 0. \qquad (2\text{-}13)$$

Because of the singularity of $H_o^{(2)}$ $(\beta\rho)$ at the origin, some care must be excerised in interchanging the operations of summation and integration in Equation 2-13. However, it can be verified for a suitably well behaved $g(y', z')$ that both terms are uniformly convergent for any $x \neq 0$, $\rho = \sqrt{x^2 + (y-y')^2} > 0$. Thus, although not explicitly stated, a limiting process is assumed in the following whereby x→0 after the interchange of operations has taken place.

Hence, Equation 2-13 may be written

$$0=\int_{-L/2}^{L/2} dy' \int_{-d/2}^{d/2} dz' \left\{ g(y',z') \left[\sum_{n=-\infty}^{\infty} 2/\ell W \sum_{m=1}^{\infty} \frac{\cot \kappa_{m,n} D}{\kappa_{m,n}} \cos\ (m\pi y/W) \cos (m\pi y'/W) \cdot \right. \right.$$

$$\left. \left. \cdot\ e^{j\gamma_n(z-z')} + (j/2\ell)\ H_o^{2}(\beta_n |y-y'|) e^{-j\gamma_n(z-z')} \right] \right\}. \tag{2-14'}$$

Expression 2-14' is an equation of the form

$$0 = \int_{-L/2}^{L/2} dy' \int_{-d/2}^{d/2} dz' \left\{ g(y',z')\ K\ (y,z|y',z') \right\}. \tag{2-15}$$

There is an infinite number of solutions, each solution $g_p(y,z)$ associated with an eigennumber γ_p and related constants

$$\gamma_{p_n} = \gamma_p - (2n\pi/\ell).$$

However, the equation is not of standard form and no technique for exact solution exists. Thus a variational method will be explored for obtaining an approximate value of γ based on an assumed distribution function, g.

2.4 Variational Solution for γ

From Equation 2-14', we have that the kernel given by

$$K\ (y,z|y',z') = \sum_{n=-\infty}^{\infty} \left[(2/\ell W) \sum_{m=1}^{\infty}{}' \frac{\cot \kappa_{m,n} D}{\kappa_{m,n}} \cos\ (m\pi y/W)\ \cos\ (m\pi y'/W) \cdot \right.$$

$$\left. \cdot\ e^{-j\gamma_n(z-z')} + j/2\ell\ H_o^{(2)}\ (\beta_n |y-y'|)\ e^{-j\gamma_n\ (z-z')} \right] \tag{2-16}$$

where

$$\gamma_n = \gamma - (2n\pi/\ell),$$

$$\beta_n = \sqrt{k^2 - \gamma_n^2},$$

$$\kappa_{m,n} = \sqrt{k^2 - (m\pi/W)^2 - \gamma_n^2},$$

is not symmetrical, i.e.,

$$K(y,z|y',z') \neq K(y',z'|y,z).$$

This fact makes it rather difficult to establish a variational principal[17,18] for the general case where γ is complex. However, approximate formulas for γ may be obtained which do have stationary properties for the restricted conditions that γ be real, or that the slot spacing be infinitesimal.

For example, assume γ real and $\gamma > k$. Then

$$\beta_n = -j\sqrt{\gamma_n^2 - k^2},$$

$$\kappa_{m,n} = -j\sqrt{(m\pi/W)^2 + \gamma_n^2 - k^2}$$

are pure imaginary for all m,n. Since

$$j\,H_o(-jx) = -(2/\pi)\,K_o(x),$$

$$\frac{\cot(-jx)}{-jx} = -\frac{\coth x}{x}$$

are then pure real, it is readily verified that K is Hermitian, i.e.,

$$K(y,z|y',z') = K^*(y',z'|y,z). \qquad (2\text{-}17)$$

Under this condition, a stationary formula can be established directly from Equation 2-14.[19]

Let $h(y,z)$ be an approximation to the unknown $g(y,z)$. By making use of the property in Equation 2-17, it is shown in Appendix A that the value of γ which satisfies

$$\iiiint h(y',z')\ h^*(y,z)\ K(y,z|y',z')\ dy'\,dy\,dz'\,dz = 0 \qquad (2\text{-}18)$$

is stationary for small variations in h about the correct function g. Thus a first order error in the assumed aperture distribution leads to a second order error in the value of γ derived from Equation 2-18.

When γ is not real, an alternative formula having stationary properties for the case of infinitesimal slot spacing can be obtained from a consideration of the Reaction Concept.

2.5 Approximate Application of the Reaction Concept

Through the use of the Reaction Concept,[20] Rumsey has treated extensively the case of the continuous axial slot or the Traveling Wave Slot Antenna.[9] A sketch of this structure appears below.

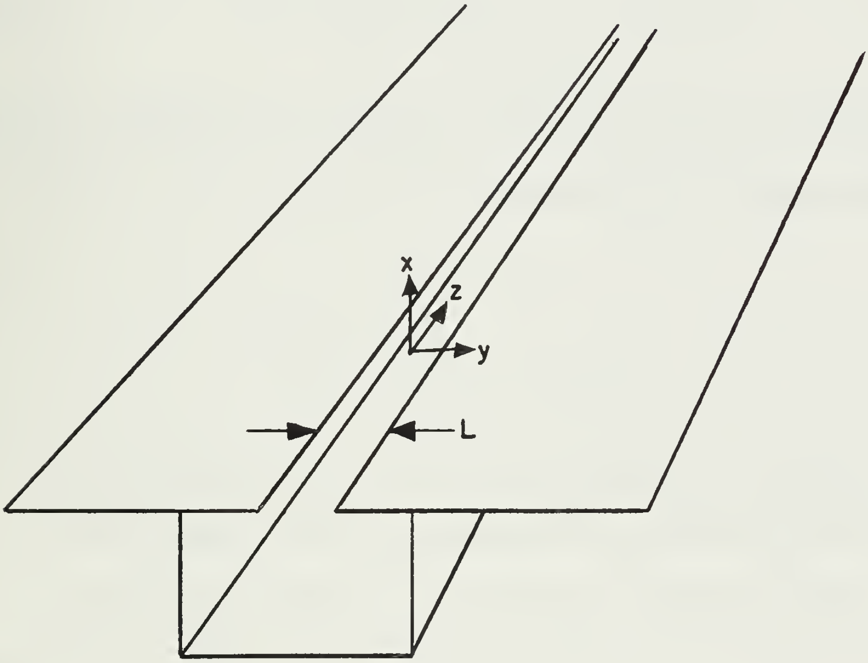

Figure 2. The Traveling-Wave Slot Antenna

In the continuous slot case, all fields vary with z as $e^{-j\gamma z}$. Let $\underline{E}_a$ (y) be an assumed tangential electric field distribution that is postulated to exist in the slot. Assuming that $\underline{E}_a$ is incorrect, the tangential components of the internal and external magnetic fields, $\underline{H}_{a_{int}}(y)$ and $\underline{H}_{a_{ext}}(y)$, that fit this distribution are discontinuous in the slot. Hence, an equivalent electric surface current distribution $\underline{J}_a(y)\, e^{j\gamma z}$ must be established in the slot to support the initially assumed $\underline{E}_a$. The required current distribution is obtained from

$$\underline{J}_a\,(y) = \underline{n} \times [\underline{H}_{a_{ext}}(y) - \underline{H}_{a_{int}}(y)], \qquad (2\text{-}19)$$

with $\underline{n}$ the unit outward normal.

The self reaction[20] of this surface current source distribution is given by

$$<a,a> = \int_{-L/2}^{L/2} [J_{a_y}E_{a_y} - J_{a_z}E_{a_z}]dy, \qquad (2\text{-}20)$$

where L is the width of the axial slot. Since $\underline{J}_a(y)$ includes γ as a parameter, enforcement of the condition

$$<a,a> = 0 \qquad (2\text{-}21)$$

leads to an expression for γ which is a function of the assumed field distribution. Rumsey has shown that this is a variational formula for γ which is stationary for small variations of the assumed aperture distribution about the correct distribution of an allowable mode of propagation. The proof of this result is repeated in Appendix A. It should be noted that this result holds when γ is complex. In cases where only an E_z component of tangential aperture field is present, Equations 2-20,21 give

$$0 = \int_{-L/2}^{L/2} E_{a_z} \, [H_{y_{ext}} - H_{y_{int}}] dy. \qquad (2\text{-}22)$$

Expression 2-22 does not apply to a periodic aperture distribution, since, in this case, E_{a_z} is a collection of traveling-wave fields of differing propagation constants γ_n, n=1,2,3, ...

A third aspect of the approximate method is brought out by considering the case of an aperture of finite extent, S'. In this case the conventional form of the reciprocity theorem applies,

$$0 = \iint_S (J_1 \cdot E_2 - J_2 \quad E_1) \, dS, \qquad (2\text{-}23)$$

and thus the self reaction of a source $\underline{J}_a$ is given by

$$<a,a> = \iint_{S'} J_a \cdot E_a \, dS. \qquad (2\text{-}24')$$

It is apparent that the application of Equation 2-24' to the transversely slotted waveguide is not strictly justifiable because of the infinite extent of the aperture. Thus, although the relation

$$0 = \iint_{S'} E_{a_z} [H_{y_{ext}} - H_{y_{int}}] dS', \qquad (2\text{-}25)$$

where S' is the infinite aperture, gives an approximate expression for γ in terms of the assumed field distribution, the expression is not necessarily stationary. However, in the limit as $\ell/\lambda \to 0$, Equation 2-25 reduces to Equation 2-22 since the aperture field then becomes essentially continuous and the z dependence can be eliminated. Thus γ derived from

Equation 2-25 is approximately stationary for small ℓ/λ. This contrasts with the characteristics of Equation 2-18, which is stationary for finite ℓ but only in the event γ is real.

The lack of exact stationary properties in the general case is probably not of great consequence since the degree of disparity between the actual field and any assumed field is unknown. Thus, experimental verification of the theory is necessary anyway.

There is some question as to whether Equation 2-18 or 2-25 provides the better approximation for γ. It would appear that Equation 2-25 more nearly fits the actual circumstances, since, in general, γ is complex. In addition, the limiting case of infinitesimal slot spacing is one of special interest.

2.6 Derivation of the Characteristic Equation for γ

The expression 2-25 is taken as the basis for an approximate formula for γ. The integration is to be performed over the infinite aperture surface, but since all fields vary between adjacent slots as $e^{-j\gamma\ell}$, 2-25 is equivalent to

$$0 = \sum_{p=-\infty}^{\infty} e^{-jp\gamma\ell} \int_{-L/2}^{L/2} dy \int_{-d/2}^{d/2} dz \left\{E_{a_z} \left(H_{y_{ext}} - H_{y_{int}}\right)\right\}, \qquad (2\text{-}26)$$

where the integration is performed over any typical slot, e.g., the slot centered at z=0. A sufficient condition for Equation 2-26 is, then,

$$0 = \int_{-L/2}^{L/2} dy \int_{-d/2}^{d/2} dz \left\{E_{a_z} \left(H_{y_{ext}} - H_{y_{int}}\right)\right\} . \qquad (2\text{-}27)$$

The approximation to E_{a_z} is taken as

$$E_{a_z} = g_a(y,z) = \cos(\pi y/L) \quad \begin{cases} |z| \le L/2 \\ |z| \le d/2 \end{cases} \qquad (2\text{-}28)$$

$$= 0 \quad \begin{cases} |y| \ge L/2 \\ d/2 \le |z| \le \ell/2 . \end{cases}$$

The substitution of Equation 2-28 into 2-8 and 2-10 gives for the y component of internal magnetic field at the aperture,

$$H_{y_{int}} = (1/j\omega\mu)\left[k^2+(\partial^2/\partial y^2)\right]\sum_{m=1}^{\infty}\ \sum_{n=-\infty}^{\infty} 2/\ell W \cos(m\pi y/W)\,\frac{\cos\kappa_{m,n}(x+D)}{\kappa_{m,n}\sin\kappa_{m,n}D}\,e^{-j\gamma_n z}\ \cdot$$

$$\cdot\int_{-L/2}^{L/2} dy'\int_{-d/2}^{d/2} dz'\left\{\cos(\pi y'/L)\cos(m\pi y'/W)\,e^{j\gamma_n z}\right\}. \tag{2-29}$$

Similarly, from Equations 2-8 and 2-12,

$$H_{y_{ext}} = (1/j\omega\mu)\left[k^2+(\partial^2/\partial y^2)\right] -j/2\ell\int_{-L/2}^{L/2} dy'\left\{\sum_{n=-\infty}^{\infty}\int_{-d/2}^{d/2}\cos(\pi y'/L)\ \cdot\right.$$

$$\cdot\, e^{j\gamma_n z}\, H_o^{(2)}(\beta_n\rho)\,dz', \tag{2-30}$$

where

$$\rho = \sqrt{x^2 + (y-y')^2}.$$

Upon substitution of Equations 2-29,30 into 2-27, with the results

$$\int_{-L/2}^{L/2}\cos(m\pi y/W)\cos(\pi y/L)\,dy = (2L/\pi)\,\frac{\cos(m\pi L/2W)}{1-(m^2L^2/W^2)}, \tag{2-31}$$

$$\int_{-d/2}^{d/2} e^{-j\gamma_n z}\,dz\int_{-d/2}^{d/2} e^{j\gamma_n z}\,dz = \frac{d^2\sin^2\left[(n\pi d/\ell)-(\gamma d/2)\right]}{\left[(n\pi d/\ell)-(\gamma d/2)\right]^2}, \tag{2-32}$$

and upon passing to the limit $x \to 0$, we obtain

$$0 = \sum_{n=-\infty}^{\infty} \frac{\sin^2[(n\pi d/\ell) - (\gamma d/2)]}{[(n\pi d/\ell) - (\gamma d/2)]} \left\{ (16L^2/\pi^2 W) \sum_{m=1}^{\infty} [k^2 - (m^2\pi^2/W^2)] \frac{\cos^2(m\pi L/2W)}{[1 - (m^2L^2/W^2)]^2} \cdot \right.$$

$$\cdot \frac{\cot \kappa_{m,n} D}{\kappa_{m,n}} + j \int_{-L/2}^{L/2} \int_{-L/2}^{L/2} \cos(\pi y/L) \cos(\pi y'/L) \cdot$$

$$\cdot [k^2 + (\partial^2/\partial y^2)] H_o^{(2)}(\beta_n |y-y'|) \, dy dz' . \tag{2-33}$$

The limiting process employed in Equation 2-33 is as previously stated in Section 2.3. Since the integrals in Equation 2-33 converge for $x=0$, the limit as $x \to 0$ exists.

It is convenient to consider the normalized propagation constant,

$$\gamma/k = c/v - j\, \alpha/k,$$

where c/v is the waveguide velocity ratio and α/k is the normalized attenuation constant in nepers per radian. Substitution for γ_n, where

$$\gamma_n = \gamma - (2n\pi/\ell) = k\,(c/v - j\,\alpha/k - n\lambda/\ell),$$

yields for γ and β,

$$\kappa_{m,n} = k \sqrt{1 - (n\lambda/\ell - c/v - j\alpha/k)^2 - (m\lambda/2W)^2},$$

$$\beta_n = k \sqrt{1 - (n\lambda/\ell - c/v - j\,\alpha/k)^2}.$$

Principal interest is attached to cases where $\ell < \lambda/2$ and $W < 1.5\lambda$. Thus, for reasonably small α/k, both $\kappa_{m,n}$ and β_n are approximately pure imaginary whenever $m \neq 1$ or $n \neq 0$. Under these conditions, it is convenient to let

$$\kappa_{m,n} = -j\,\zeta_{m,n} = -jk\sqrt{(n\lambda/\ell - \gamma/k)^2 + (m\lambda/2W)^2 - 1},$$

$$\beta_n = -j\,\sigma_n = -jk\sqrt{(n\lambda/\ell - \gamma/k)^2 - 1}, \qquad (2\text{-}34)$$

where the root having a positive real part is to be taken. With the first of these transformations,

$$\frac{\cot \kappa_{m,n} D}{\kappa_{m,n}} = -\frac{\coth \zeta_{m,n}}{\zeta_{m,n}}.$$

Thus, (2-33) may be written

$$\frac{\cot \kappa D}{\kappa D} = -\frac{\left(1-\frac{L^2}{W^2}\right)^2}{\cos^2\left(\frac{\pi L}{2W}\right)}\;\frac{\left(\frac{\gamma d^2}{2}\right)^2}{\sin^2\frac{\gamma d}{2}}\;\frac{1}{1-\frac{\lambda^2}{4W^2}}\sum_{n=-\infty}^{\infty}\frac{\sin^2\left(\frac{n\pi d}{\ell}-\frac{\gamma d}{2}\right)}{\left(\frac{n\pi d}{\ell}-\frac{\gamma d}{2}\right)^2}\left\{\sum_{m=1}^{\infty}{}' \xi_{m,n}\left(\frac{m^2\lambda^2}{4W^2}-1\right)\cdot\right.$$

$$\left.\frac{\cos^2\left(\frac{m\pi L}{2W}\right)}{\left(1-\frac{m^2L^2}{W^2}\right)^2}\;\frac{\coth \zeta_{m,n} D}{\zeta_{m,n} D} + j\,\frac{\pi^2}{16}\,\frac{W}{k^2L^2D}\int_{-L/2}^{L/2}\int_{-L/2}^{L/2}\cos\frac{\pi y}{L}\cos\frac{\pi y'}{L}\cdot\right.$$

$$\left.\cdot\left(k^2+\frac{\partial^2}{\partial y^2}\right) H_o^{(2)}(\beta_n|y-y'|)\,dy\,dy',\right. \qquad (2\text{-}35)$$

where

$$\xi_{m,n} = 0 \text{ for } m=0 \text{ and } n=1,$$

$$= 1 \text{ otherwise},$$

$$\kappa \equiv \kappa_{1,0} = k\sqrt{1-(\lambda/2W)^2-(\gamma/k)^2}.$$

Let

$$I_n = (1/4\pi)(\lambda/L)^2 \int_{-L/2}^{L/2} \int_{-L/2}^{L/2} \cos(\pi y/L)\ \cos(\pi y'/L)\ \left[k^2 + \partial^2/\partial y^2\right] \cdot$$

$$\cdot H_o^{(2)}\ (\beta_n |y-y'|) dy\ dy'. \qquad (2\text{-}36)$$

In Appendix B, I_n is approximately evaluated in closed form for $n \neq 0$. The result is given in Equation B-18 as

$$I_n \simeq j(\pi/kL) \Big\{ \left[1-(\lambda^2/4L^2)\right](k/\sigma_n)[1-1/8(\lambda/L)^2(k/\sigma_n)^2] +$$

$$+ (\lambda/L)^3 \quad [1/2\pi^2\ (k/\sigma_n)^2\ (1/8\pi^3)(\lambda/L)^2(k/\sigma_n)^4] \Big\}. \qquad (2\text{-}37)$$

This approximation is good for cases where

$$|\sigma_n L| > 3\pi$$

which in turn approximately holds for all cases where $L > 3/2\ \ell$ and $\ell < \lambda/2$. Thus no additional limitation has been imposed, since the analysis was initially restricted to cases of narrow, closely spaced slots.

It does not appear possible to extend the approximate evaluation of Equation 2-36 to the case n=0. Instead, the power series representation of $H_o(\beta_n)$ is substituted and the resulting series is integrated term by term. This work is also performed in Appendix B. The formal result from Equation B-19 is:

$$I_o(\beta/k, L/\lambda) = \sum_{i=0}^{\infty} (-1)^i\ (\beta/k, L/\lambda)^{2i} \Big\{ [1-j\ 2(\overline{\gamma}/\pi) - j(2/\pi)\ \ln(\beta/k)(L/\lambda)] \cdot$$

$$\cdot Q_{2i} + j\ R_{2i} \Big\}, \qquad (2\text{-}38)$$

where

$$\bar{\gamma} = \text{Euler's constant} = .5772\ldots,$$

$$\beta/k \equiv \beta_o/k = \sqrt{1-(\gamma/k)^2},$$

and Q_{2i}, R_{2i} are functions of L/λ that are defined in Equations B-19,20 and tabulated for i through 10 in Table I, Page 102.

If Equations 2-37, 38 are inserted in Equation 2-35, the following approximate expression for γ results:

$$\frac{\cot \kappa D}{\kappa D} \simeq - \frac{1}{1-(\lambda^2/4W^2)} \frac{(1-L^2/W^2)^2}{\cos^2(\pi L/2W)} \frac{\lambda}{2\pi D} \left\{ \frac{(\gamma d/2)^2}{\sin^2(\gamma d/2)} \sum_{n=-\infty}^{\infty} \right.$$

$$\bullet \frac{\sin^2(n\pi D/\ell - \gamma d/2)}{(n\pi d/\ell - \gamma d/2)^2} \left[\!\left[\sum_{m=1}^{\infty} \xi_{m,n} (m^2\lambda^2/4W^2 - 1) \frac{\cos^2(m\pi L/2W)}{[1-(m^2L^2/W^2)]^2} (k/\zeta_{m,n}) \bullet \right.\right.$$

$$\bullet \coth \zeta_{m,n} D + -\xi_{1,n} (\pi^2 W/16L) \left[(1-\lambda^2/4L^2) \left(\frac{k}{\sigma_n} - \frac{1}{8} \frac{\lambda^2}{L^2} \frac{k^3}{\sigma_n^3} \right) + \right.$$

$$\left.\left.\left. + (1/2\pi^2)(\lambda/L)^3 (k/\sigma_n)^2 - (1/8\pi^3)(\lambda/L)^5 (k/\sigma_n)^4 \right] \right]\!\right] +$$

$$\left. + j (\pi^2/8)(W/\lambda) I_o (\beta/k, L/\lambda) \right\}, \qquad (2\text{-}39)$$

where

$$\kappa = k\sqrt{1 - (\lambda/2W)^2 - (\gamma/k)^2},$$

$$\beta = k\sqrt{1 - (\gamma/k)^2},$$

$$\zeta_{m,n} = k\sqrt{(n\lambda/\ell - \gamma/k)^2 + (m\lambda/2W)^2 - 1},$$

$$\sigma_n = k\sqrt{(n\lambda/\ell - \gamma/k)^2 - 1}.$$

When solved, Equation 2-39 yields solutions for γ corresponding to those modes whose internal field distribution is approximately cosinusoidal with y. For the lowest order mode, Equation 2-39 may be easily put in perturbation form.

It is assumed that this mode represents a small perturbation of the closed-waveguide $TE_{1,0}$ mode, and that there is a correspondingly small perturbation of γ. Thus, let

$$\gamma = {}_o\gamma + \delta\,(\gamma),$$

where

$${}_o\gamma = k\sqrt{1 - (\lambda^2/4W^2)}.$$

For small $\delta(\gamma)$,

$$\gamma \simeq {}_o\gamma^2 + 2\ {}_o\gamma\ \delta(\gamma),$$

and

$$\begin{aligned}\kappa &= \sqrt{k^2 - (\pi^2/W^2) - \gamma^2}\\ &\simeq \sqrt{-2\ {}_o\gamma\ \delta(\gamma)}\,.\end{aligned}$$

Using the first two terms of the power series expansion for (cot z/z) gives approximately

$$(\cot \kappa D)/(\kappa D) \simeq -\left(1/[2\,{}_o\gamma\ D^2\ \delta(\gamma)]\right) - 1/3.$$

Substitution of Equation 2-41 for the left hand side of Equation 2-39 then gives

$$\begin{aligned}\frac{1}{\delta(\gamma/k)} \simeq & -\frac{8}{3}\ \pi^2\left(\frac{D}{\lambda}\right)^2\sqrt{1-\frac{\lambda^2}{4W^2}} + \frac{4\pi D}{\lambda}\ \frac{1}{\sqrt{1-(\lambda^2/2W^2)}}\ \frac{[1-(L^2/W^2)]^2}{\cos^2(\pi L/2W)}\ \cdot\\ & \cdot\left\{\frac{(\gamma d/2)^2}{\sin^2(\gamma d/2)}\ \sum_{n=-\infty}^{\infty}\frac{\sin^2(m\pi d/\ell - \gamma d/2)}{(n\pi d/\ell - \gamma d/2)^2}\left[\!\!\left[\sum_{m=1}^{\infty}{}'\ \xi_{m,n}\left(\frac{m^2\lambda^2}{4W^2}-1\right)\cdot\right.\right.\right.\\ & \cdot\frac{\cos^2(m\pi L/2W)}{[1-(m^2L^2/W^2)]^2}\ \frac{k}{\zeta_{m,n}}\ \coth \zeta_{m,n}D - \xi_{1,n}(\pi^2/16\cdot L)\left([1-(\lambda^2/4L^2)](k/\sigma_n)\cdot\right.\\ & \left.\left.\left.\cdot\left[1-\frac{1}{8}\ \frac{\lambda^2}{L^2}\ \frac{k^2}{\sigma_n{}^2}\right] + \frac{\lambda^3}{L^3}\left[\frac{1}{2\pi^2}\left(\frac{k}{\sigma_n}\right)^2 - \frac{1}{8\pi^3}\left(\frac{\lambda}{L}\right)^2\left(\frac{k}{\sigma_n}\right)^4\right]\right) + j\ \frac{\pi^2}{8}\ \frac{W}{\lambda}\ I_o\left(\frac{\beta}{k}, \frac{L}{\lambda}\right)\right]\!\!\right]\right\}\end{aligned}$$

(2-42)

where

$$\delta(\gamma/k) = \delta(c/v) - j(\alpha/k).$$

The first order approximation to γ is obtained by using ${}_{o}\gamma$ in the right hand side of Equation 2-42,

$$(\gamma/k)_1 = {}_{o}\gamma/k + \delta_o\,(\gamma/k) = {}_{o}\gamma/k + F({}_{o}\gamma/k).$$

Better approximations to the exact solution of Equation 2-39 are obtained from successive iterations of the form

$$(\gamma/k)_{i+1} = {}_{o}\gamma/k + \delta_i\,(\gamma/k) = {}_{o}\gamma/k + F({}_{i}\gamma/k).$$

However, since Equation 2-39 is based on an approximate field distribution, an exact solution is of no particular advantage. In practice, one or two iterations give sufficient accuracy for most cases of interest. Observe that for almost all m and n, $\zeta_{m,n}$ and σ_n in Equation 2-42 are relatively insensitive to changes in γ, so that a recomputation of these terms for succeeding iterations is usually not necessary.

Unfortunately, the use of either Equation 2-39 or Equation 2-42 is quite tedious because of the slow convergence of the infinite series for cases of small L/W and d/ℓ. Under some conditions, alternative series representations which have more favorable convergence properties may be obtained. An example is the series derived by means of the Euler-Maclauren transformation, whose rate of convergence varies inversely with L/W and d/ℓ. The first term of this series is essentially the integral approximation of the infinite sum. Unfortunately, the evaluation of this integral presents considerable difficulty in the application of the transformation to Equations 2-39,42.

The double sum in Equations 2-39, 42 reduces to a single sum for either of two cases of special interest; 1) for $L=W$, and 2) for the limiting case as $\ell/\lambda \rightarrow 0$. These special cases are considered in further detail in the following sections.

III. THEORETICAL AND EXPERIMENTAL RESULTS FOR THE CASE OF SLOT LENGTH EQUAL TO WAVEGUIDE WIDTH.

3.1 Characteristic Equation for γ.

In Equation 2-39, let $L \rightarrow W$. Since

$$\lim_{L \rightarrow W} \frac{\cos \frac{m \pi L}{2W}}{1 - \frac{m^2 L^2}{W^2}} = \pi/4 \qquad m = 1,$$

$$= 0 \qquad m \neq 1,$$

Equation 2-39 becomes

$$\frac{\cot \kappa D}{\kappa D} \cong \frac{\lambda}{2\pi D} \left\{ \frac{(\gamma d/2)^2}{\sin^2 \left(\frac{\gamma d}{2}\right)} \sum_{n=-\infty}^{\infty} \xi_n \frac{\sin^2 (n\pi d/\ell - \gamma d/2)}{(n\pi d/\ell - \gamma d/2)^2} \left[(k/\zeta_n) \coth \zeta_n D + (k/\sigma_n) + \right.\right.$$

$$\left. - \frac{1}{8} \left(\frac{\lambda}{W}\right)^2 \left(\frac{k}{\sigma_n}\right)^3 + \frac{1}{1 - \frac{\lambda^2}{4W^2}} \left(\frac{1}{2\pi^2} \frac{\lambda^3}{W^3} \frac{k^2}{\sigma_n{}^2} - \frac{1}{8\pi^3} \frac{\lambda^5}{W^5} \frac{k^4}{\sigma_n{}^4} \right) \right] +$$

$$\left. -j \frac{2}{1 - \frac{\lambda^2}{4W^2}} \frac{W}{\lambda} I_o \left(\frac{\beta}{k}, \frac{W}{\lambda} \right) \right\}, \tag{3-1}$$

where

$$\xi_n = 0 \qquad n = 0,$$

$$= 1 \qquad n \neq 0,$$

$$\kappa = k \sqrt{1 - \left(\frac{\lambda}{2W}\right)^2 - \left(\frac{\gamma}{k}\right)^2},$$

$$\beta = k \sqrt{1 - \left(\frac{\gamma}{k}\right)^2},$$

$$\zeta_n = k \sqrt{\left(\frac{n\lambda}{\ell} - \frac{\gamma}{k}\right)^2 + \left(\frac{\lambda}{2W}\right)^2 - 1},$$

$$\sigma_n = k \sqrt{\left(\frac{n\lambda}{\ell} - \frac{\gamma}{k}\right)^2 - 1}.$$

Since it has already been assumed that $\ell < \frac{\lambda}{2}$, and since, in general, $|\gamma/k| \leqslant 1$, then assuming $Re\,(\frac{\gamma}{k}) > 0$,

$$\left|\frac{n\lambda}{\ell} - \frac{\gamma}{k}\right| > 2 \qquad (3\text{-}2)$$

for all n(n = 0 excluded), except for possibly n = ± 1. Without excessive error in the final results, it can be assumed that Equation 3-2 holds for $n \neq 0$ Then in the first two terms in the right hand side of Equation 3-1,

$$\frac{k}{\sigma_{\pm n}} = \frac{1}{\left(\frac{n\lambda}{\ell} \mp \frac{\gamma}{k}\right)\sqrt{1 - \frac{1}{\left(\frac{n\lambda}{\ell} \mp \frac{\gamma}{k}\right)^2}}}$$

$$\simeq \frac{1}{\left(\frac{n\lambda}{\ell} \mp \frac{\gamma}{k}\right)}\left[1 + \frac{1}{2\left(\frac{n\lambda}{\ell} \mp \frac{\gamma}{k}\right)^2}\right]$$

and

$$\frac{k}{\zeta_{\pm n}} \simeq \frac{1}{\left(\frac{n\lambda}{\ell} \mp \frac{\gamma}{k}\right)}\left[1 + \frac{1 - \frac{\lambda^2}{4W^2}}{2\left(\frac{n\lambda}{\ell} \mp \frac{\gamma}{k}\right)^2}\right],$$

where in each case n is now restricted to positive values only.

Since the remaining terms under the summation sign in Equation 3-1 are demonstrably small compared with the first two, they may be treated even more approximately For these terms, the approximations

$$\left(\frac{k}{\sigma_{\pm n}}\right)^{\nu} \simeq \frac{1}{\left(\frac{n\lambda}{\ell} \mp \frac{\gamma}{k}\right)^{\nu}}$$

are used

As a further consequence of Equation 3-2, it can be verified that

$$\left|\zeta_n D\right| > \frac{2.5\ nD}{\ell}$$

Since, assuming reasonably small α, ζ_n is approximately a positive real for all $|n| \geq 1$, then for $D \geq \frac{\ell}{2}$,

$$\coth \zeta_n D \simeq 1.$$

Finally, since small slot widths have been assumed,

$$\frac{d}{\lambda} < \frac{1}{8}$$

$$\left|\frac{\gamma d}{2}\right| < \pi \left|\frac{\gamma}{k}\right| \frac{d}{\lambda} < \frac{\pi}{8}$$

and

$$\frac{\sin \frac{\gamma d}{2}}{\frac{\gamma d}{2}} \simeq 1.$$

With these approximations, 3-1 gives

$$\begin{aligned}
\frac{\cot \kappa D}{\kappa D} \simeq \frac{\lambda}{2\pi D} \left(\frac{\ell}{\lambda}\right) \left(\frac{\ell}{\pi d}\right)^2 \Bigg\{ \sum_{n=1}^{\infty} & \left[\frac{\sin^2 \left(\frac{n\pi d}{\ell} - \frac{\gamma d}{2}\right)}{n^3 \left(1 - \frac{1}{n} \frac{\ell}{\lambda} \frac{\gamma}{k}\right)^3} + \frac{\sin^2 \left(\frac{n\pi d}{\ell} + \frac{\gamma d}{2}\right)}{n^3 \left(1 + \frac{1}{n} \frac{\ell}{\lambda} \frac{\gamma}{k}\right)^3} \right] + \\
+ \frac{1}{\frac{4W^2}{\lambda^2} - 1} \frac{\ell}{\pi^2 W} \sum_{n=1}^{\infty} & \left[\frac{\sin^2 \left(\frac{n\pi d}{\ell} - \frac{\gamma d}{2}\right)}{n^4 \left(1 - \frac{1}{n} \frac{\ell}{\lambda} \frac{\gamma}{k}\right)^4} + \frac{\sin^2 \left(\frac{n\pi d}{\ell} + \frac{\gamma d}{2}\right)^2}{n^4 \left(1 + \frac{1}{n} \frac{\ell}{\lambda} \frac{\gamma}{k}\right)^4} \right] + \\
+ \frac{1}{2} \left(\frac{\ell}{\lambda}\right)^2 \left(1 - \frac{\lambda^2}{4W^2}\right) \sum_{n=1}^{\infty} & \left[\frac{\sin^2 \left(\frac{n\pi d}{\ell} - \frac{\gamma d}{2}\right)^2}{n^5 \left(1 - \frac{1}{n} \frac{\ell}{\lambda} \frac{\gamma}{k}\right)^5} + \frac{\sin^2 \left(\frac{n\pi d}{\ell} + \frac{\gamma d}{2}\right)^5}{n^5 \left(1 + \frac{1}{n} \frac{\ell}{\lambda} \frac{\gamma}{k}\right)} \right] + \\
+ \frac{1}{\frac{4W^2}{\lambda^2} - 1} \frac{1}{4\pi^3} \left(\frac{\ell}{W}\right)^3 \sum_{n=1}^{\infty} & \left[\frac{\sin^2 \left(\frac{n\pi d}{\ell} - \frac{\gamma d}{2}\right)}{n^6 \left(1 - \frac{1}{n} \frac{\ell}{\lambda} \frac{\gamma}{k}\right)^6} + \frac{\sin^2 \left(\frac{n\pi d}{\ell} + \frac{\gamma d}{2}\right)^6}{n^6 \left(1 + \frac{1}{n} \frac{\ell}{\lambda} \frac{\gamma}{k}\right)} \right] \Bigg\} + \\
- j \frac{W}{\pi D} \frac{1}{1 - \frac{\lambda^2}{4W^2}} I_o \left(\frac{\beta}{k}, \frac{W}{\lambda}\right) & \qquad \text{(3-3a)}
\end{aligned}$$

$$= \frac{\ell}{\pi D}\left(\frac{\ell}{\pi D}\right)^2 \left\{ S_3 + \frac{1}{\frac{4W^2}{\lambda^2}-1}\;\frac{\ell}{\pi^2 W}\; S_4 + \tfrac{1}{2}\left(\frac{\ell}{\lambda}\right)^2 \left(1-\frac{\lambda^2}{4W^2}\right) S_5 + \frac{1}{\frac{4W^2}{\lambda^2}-1}\;\frac{1}{4\pi^3}\left(\frac{\ell}{W}\right)^3 S_6 \right. +$$

$$- j\,\frac{W}{\pi D}\;\frac{1}{1-\frac{\lambda^2}{4W^2}}\; I_o\left(\frac{\beta}{k},\frac{W}{\lambda}\right) \qquad (3\text{-}3b)$$

where S_3, S_4, S_5, S_6 are defined by this equation.

For $W < .7\lambda$, it is readily verified that each term of S_4 and S_6 is negligible compared with the corresponding terms of S_3 and S_5. Computations have also shown that for smaller W/λ, the final term of Equation 3-3 becomes dominant, and S_4 and S_6 are then negligible with respect to that term. Thus, in the following, only S_3 and S_5 are considered. These are expanded and approximately summed in Appendix C. Polynomial representations are given, which are of the form

$$S_3 \simeq 2\left(\frac{\pi d}{\ell}\right)^2 \left[p_0 + p_2\left(\frac{\ell}{\lambda}\,\frac{\gamma}{k}\right)^2 + p_4\left(\frac{\ell}{\lambda}\,\frac{\gamma}{k}\right)^4\right]$$

$$S_5 \simeq 4\left(\frac{\pi d}{\ell}\right)^2 \left[q_0 + q_2\left(\frac{\ell}{\lambda}\,\frac{\gamma}{k}\right)^2 + q_4\left(\frac{\ell}{\lambda}\,\frac{\gamma}{k}\right)^4\right]$$

where the p_i, q_i are functions of ℓ/d that are defined in Equations C-4 and C-6 and graphed in Figures 37-42. Substituting S_3 and S_5 into Equation 3-3 gives

$$\frac{\cot \gamma D}{\gamma D} \simeq \frac{2\ell}{\pi D}\left\{\sum_{i=0}^{2} p_{2i}\left(\frac{\ell}{\lambda}\,\frac{\gamma}{k}\right)^{2i} + \left(\frac{\ell}{\lambda}\right)^2\left(1-\frac{\lambda^2}{4W^2}\right)\sum_{i=0}^{2} q_{2i}\left(\frac{\ell}{\lambda}\,\frac{\gamma}{k}\right)^{2i}\right\} +$$

$$- j\,\frac{W}{\pi D}\;\frac{1}{1-\frac{\lambda^2}{4W^2}}\; I_o\left(\frac{\beta}{k},\frac{W}{\lambda}\right), \qquad (3\text{-}4)$$

where

$$\kappa = k \sqrt{1 - \left(\frac{\lambda}{2W}\right)^2 - \left(\frac{\gamma}{k}\right)^2} ,$$

$$\beta = k \sqrt{1 - \left(\frac{\gamma}{k}\right)^2} ,$$

and $I_o \left(\frac{\beta}{k} \frac{W}{\lambda}\right)$ is given in Appendix B.

The corresponding perturbation formula, obtained from Equation 3-4 using Equation 2-41, is

$$\delta \left(\frac{\gamma}{k}\right) = \delta \left(\frac{c}{v}\right) - j \frac{\alpha}{k} \simeq \frac{1}{8\pi \sqrt{1 - \frac{\lambda^2}{4W^2}}} \frac{\lambda}{D} \left\{ \frac{\pi D}{3\lambda} - 2\frac{\ell}{\lambda} \left[\sum_{i=0}^{2} p_{2i} \left(\frac{\ell}{\lambda} \frac{\gamma}{k}\right)^{2i} + \left(1 - \frac{\lambda^2}{4W^2}\right) \left(\frac{\ell}{\lambda}\right)^2 \bullet \sum_{i=0}^{2} q_{2i} \left(\frac{\ell}{\lambda} \frac{\gamma}{k}\right)^{2i} \right] + j \frac{W}{\lambda} \frac{1}{1 - \frac{\lambda^2}{4W^2}} I_o \left(\frac{\beta}{k}, \frac{W}{\lambda}\right) \right\}^{-1} \qquad (3\text{-}5)$$

Because α assumes relatively large values for the case L = W, the practical value of Equation 3-5 is somewhat questionable. However, Equation 3-5 is of interest in that it shows the general dependence of γ on the various physical parameters.

Both α and $\delta(c/v)$ increase with a decrease of D/λ or of ℓ/λ. For small ℓ/λ, the term in Equation (3-5) within the brackets [ ] is given approximately by

$$-2 \frac{\ell}{\lambda} p_o .$$

From Equation C-4,

$$p_o = \ln \frac{2.23\ell}{\pi d} + \frac{6.4}{2\pi^2} \left(\frac{d}{\ell}\right)^2 .$$

Thus large values of ℓ/d enter Equation 3-5 only as the logarithm. It follows that for ℓ/λ held constant, α is relatively insensitive to changes in d/λ. Further, from Equation 3-5, α is independent of ℓ/d in the limit as $\frac{\ell}{\lambda} \rightarrow 0$.

The last term of Equation 3-5,

$$F\,(\beta,W) = j\,\frac{W}{\lambda}\,\frac{1}{1-\frac{\lambda^2}{4W^2}}\,I_o\left(\frac{\beta}{k},\,\frac{W}{\lambda}\right)$$

is plotted against W/λ in Figure 3, with β equal to its unperturbed value

$$_o\beta = k\sqrt{1-\left(\frac{_o\gamma}{k}\right)^2} = \frac{\pi}{W},$$

The real part of $F(_o\beta W)$ is relatively small compared with the first three terms of Equation 3-5, the sum of which is approximately real. The imaginary part of F is relatively constant with W/λ. Hence, for small perturbation of γ, so that

$$\beta \simeq {_o\beta},$$

that quantity in Equation 3-5 contained in the braces {} is relatively slowly varying with changes in W/λ. Under these conditions, α is approximately proportional to $\left(1-\frac{\lambda^2}{4W^2}\right)^{-1/2}$, if all other dimensions are held constant. Since the variation of this latter factor is slight except for W in the vicinity of $\lambda/2$, α is relatively insensitive to changes of W/λ. Thus a measure of independent control over α and c/v exists, since, to the first order, c/v depends on W/λ only.

3.2 Theoretical and Experimental Results.

Expression 3 4 was solved for the lowest order root giving the propagation constant for the fundamental mode. Because of the transcendental nature of the expression, the University of Illinois automatic digital computer (ILLIAC) was employed in the solution.

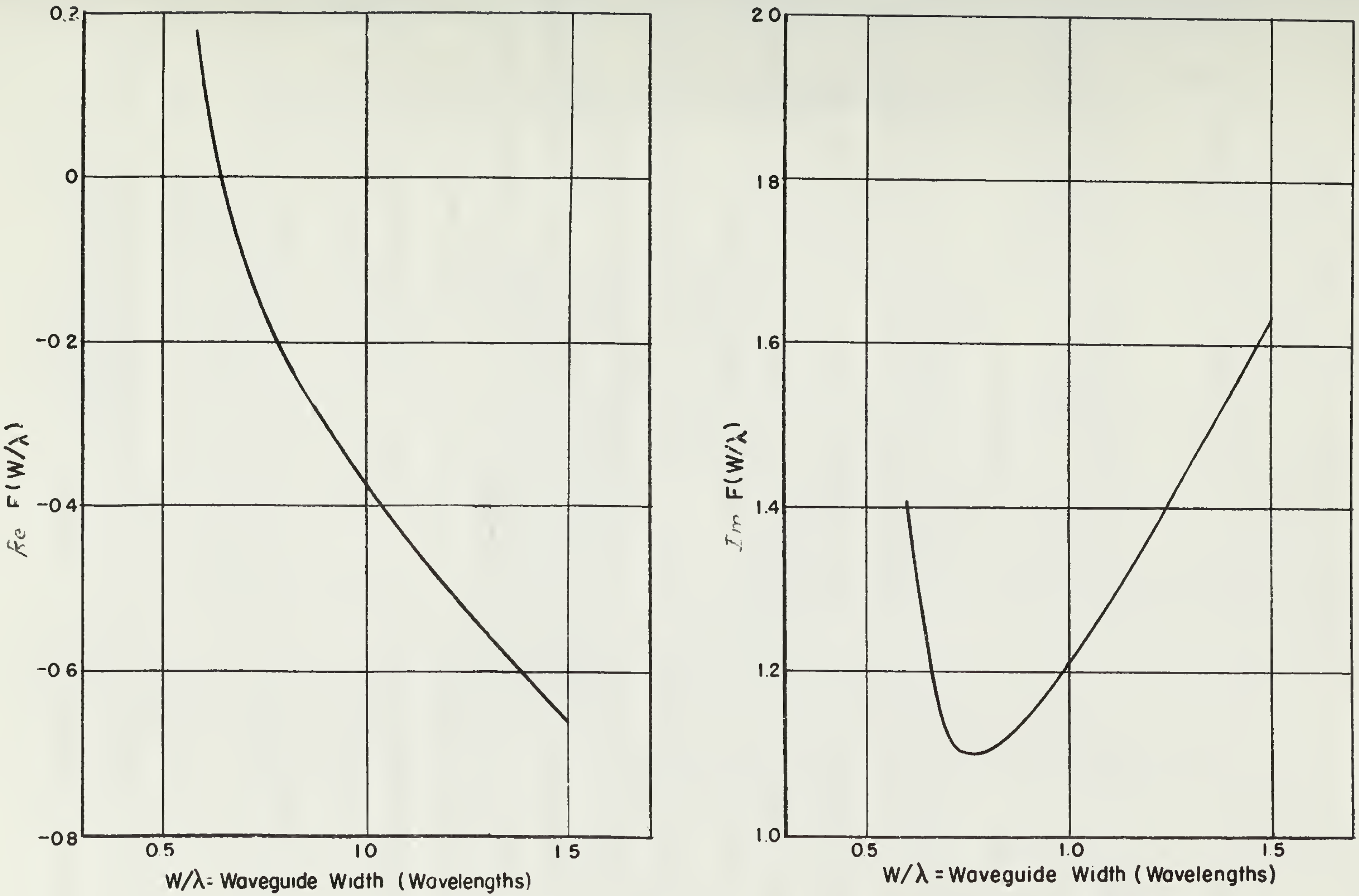

Figure 3. $F(W/\lambda) = j(W/\lambda)\left(\frac{1}{1-(\lambda^2/4W^2)}\right) \; I_0[({}_0\beta/k)(W/\lambda)]$

Theoretical results showing the variation of γ with changes in the various parameters are presented in Figures 4-16. The results of experimental measurements are also given to provide a check on the validity of the approximate theory. A discussion of the experimental procedure is given in Section V.

Figure 4 shows the variation of α with frequency for a typical fixed waveguide and slot configuration. Agreement between the observed and predicted values is good at all frequencies.

Of particular interest in Figure 4 is the behavior of α in the vicinity of the unperturbed cutoff frequency, since this result contrasts with that obtained for the axially slotted guide. In the latter case, α increases indefinitely with decrease in frequency as cutoff is approached. In the unperturbed waveguide, all fields are TEM with respect to the y axis exactly at the cutoff frequency. Since in the transversely slotted case the long dimensions of the slots are thus parallel with the direction of current flow on the broad face of the guide, the perturbation of the fields would appear to be small, and the radiation losses minimal. Exactly at cutoff, Equation 3-4 predicts zero α. Measurements made at this frequency show a small value of α that varies erratically with distance along the waveguide. The variation of α is apparently the result of minor nonuniformities in the construction of the experimental model.

At frequencies below unperturbed cutoff, the fields decay more rapidly than in the unperturbed waveguide because of the radiation losses. In addition, c/v is finite in this region instead of remaining zero as in the lossless unperturbed case. However, the signs of c/v and α are

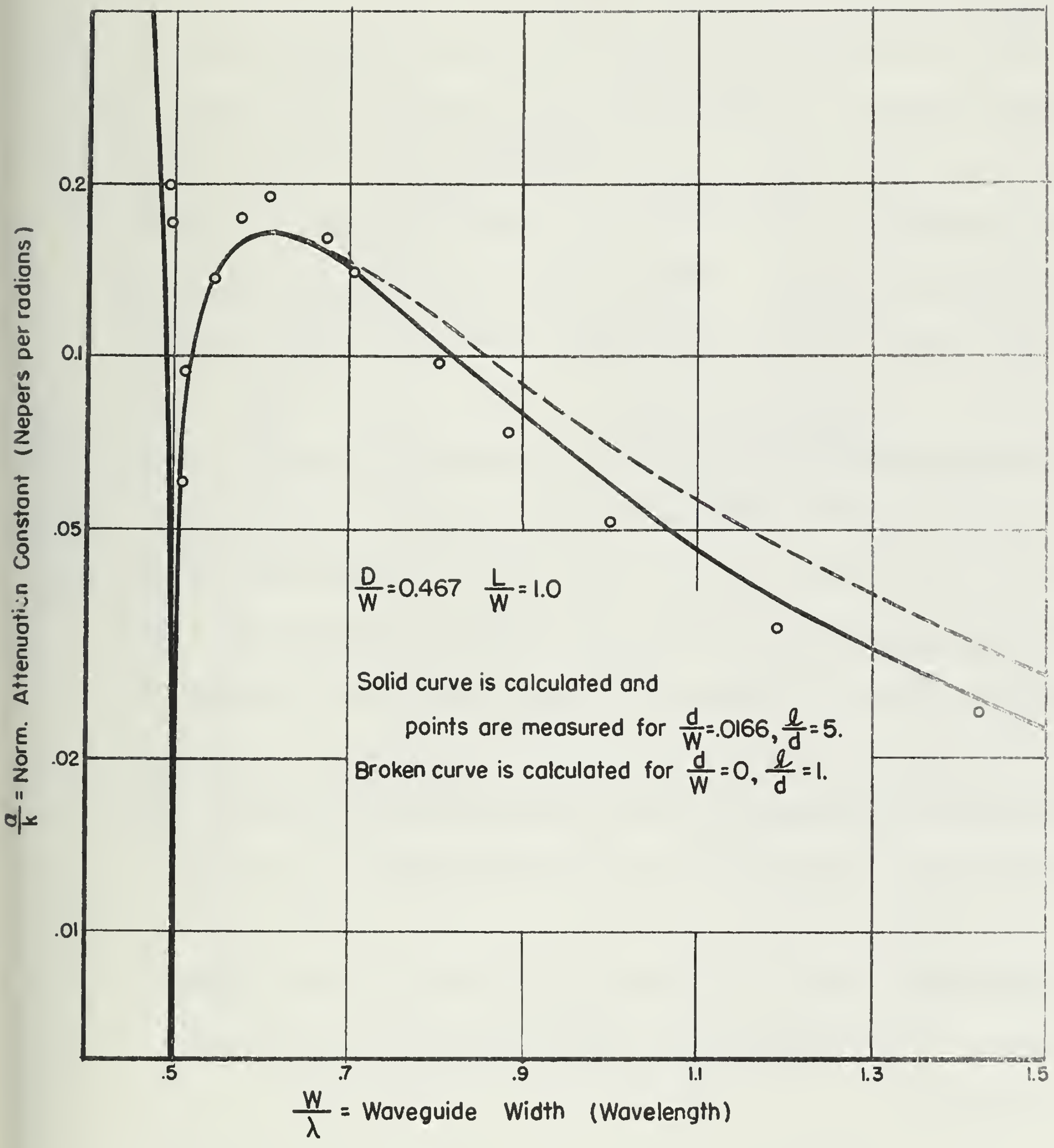

Figure 4. Attenuation Constant versus Frequency for Fixed Waveguide and Slot Dimensions

opposite, so that the direction of decreasing phase is opposite to the direction of decreasing amplitude. A comparison of the perturbed and unperturbed c/v ratios is given in Figure 5.

Several curves in Figure 7 are of particular interest in that they show the relative insensitivity of α to changes in ℓ/d. The broken curve in that figure, which is calculated for zero ℓ/λ and the maximum possible ℓ/d ($\ell/d = 1$) gives the largest attainable α for the given waveguide dimensions. Curves 3 and 4, which are for impractically small values of d, are only slightly below this curve of maximum α.

A moderate degree of control over α is available through the variation of ℓ/λ. Typical results are given in Figure 8. The maximum range of α for variation of ℓ/λ alone is seen to be approximately 10:1. However, this range can be increased by allowing a simultaneous variation of D. Curves for different W/λ and D/λ are given in Figure 9. Because of the relative insensitivity of α to W and d, fairly accurate results can be interpolated for most cases from Figures 8 and 9. An indication of the corresponding perturbations of the c/v ratio is given in Figures 10 and 11.

The waveguide depth is limited by the need to suppress higher order modes. The unperturbed cutoff value of D for the next higher mode is given by

$$\left(\frac{D}{\lambda}\right)_{c.o} = \frac{1}{2\sqrt{1 - \left(\frac{\lambda}{2W}\right)^2}} .$$

Experimental measurements have shown this value may be exceeded by

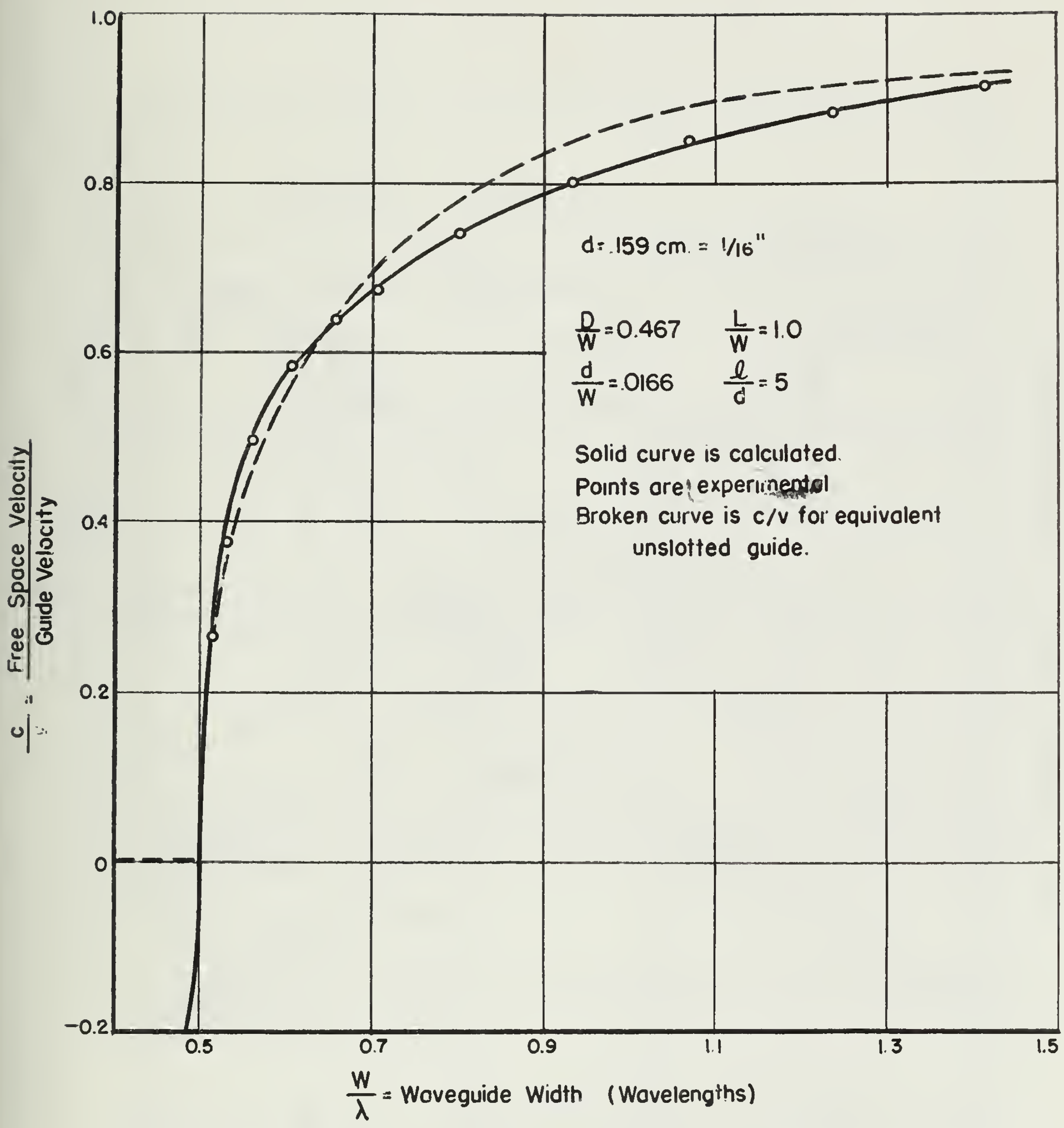

Figure 5. Velocity Ratio versus Frequency for Fixed Waveguide and Slot Dimensions

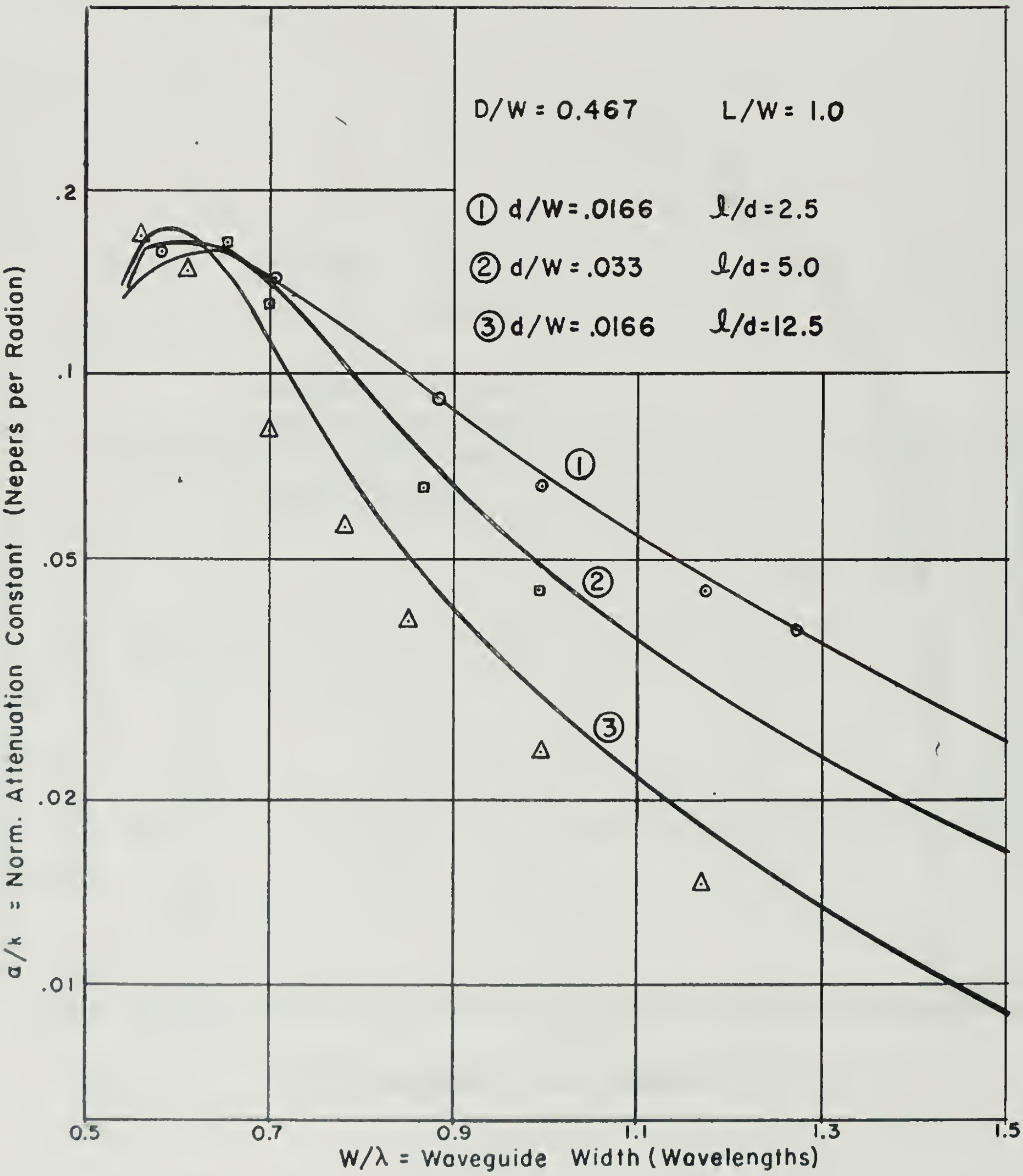

Figure 6. Attenuation Constant versus Frequency

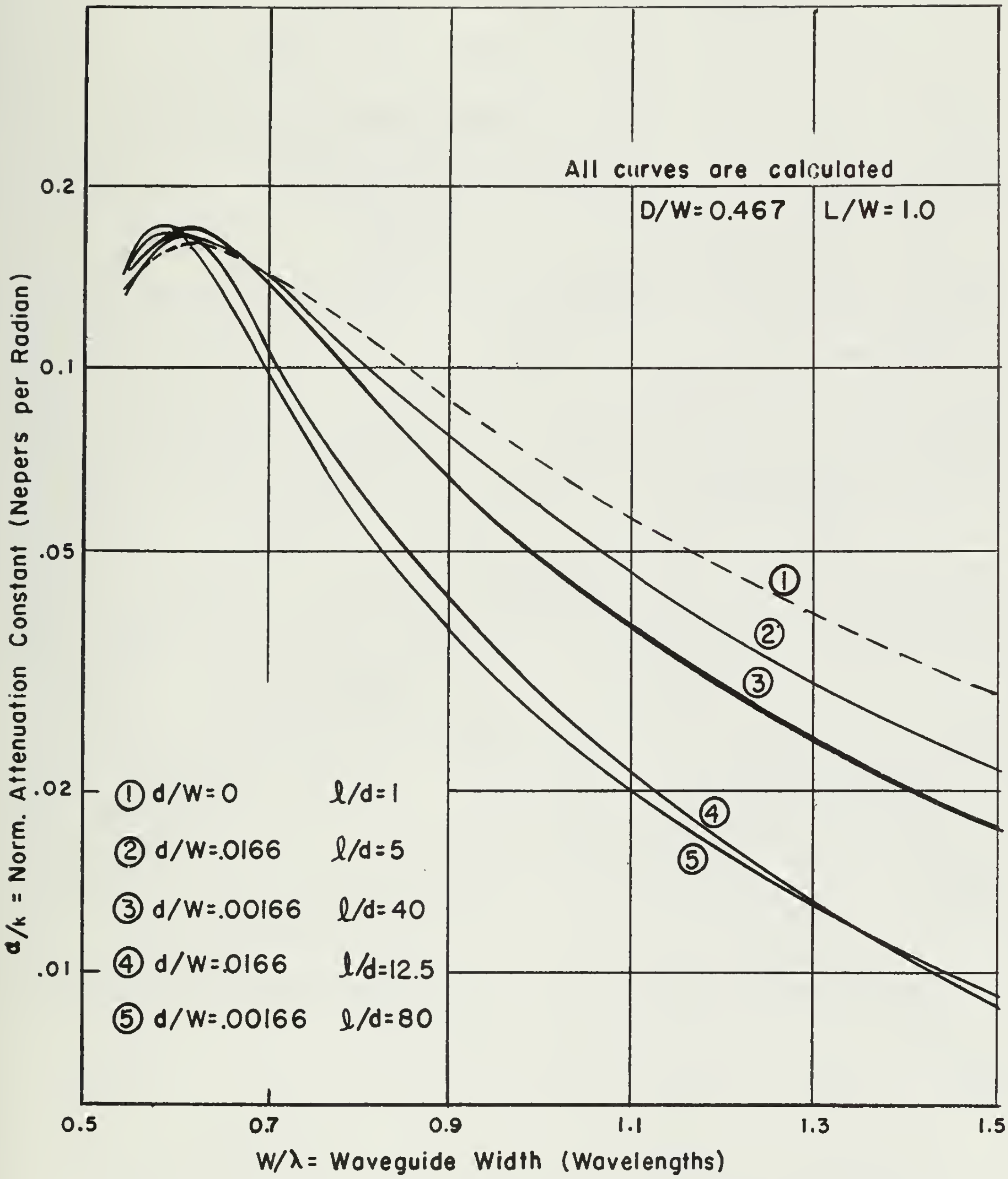

Figure 7. Attenuation Constant versus Frequency for Fixed Waveguide and Slot Dimensions

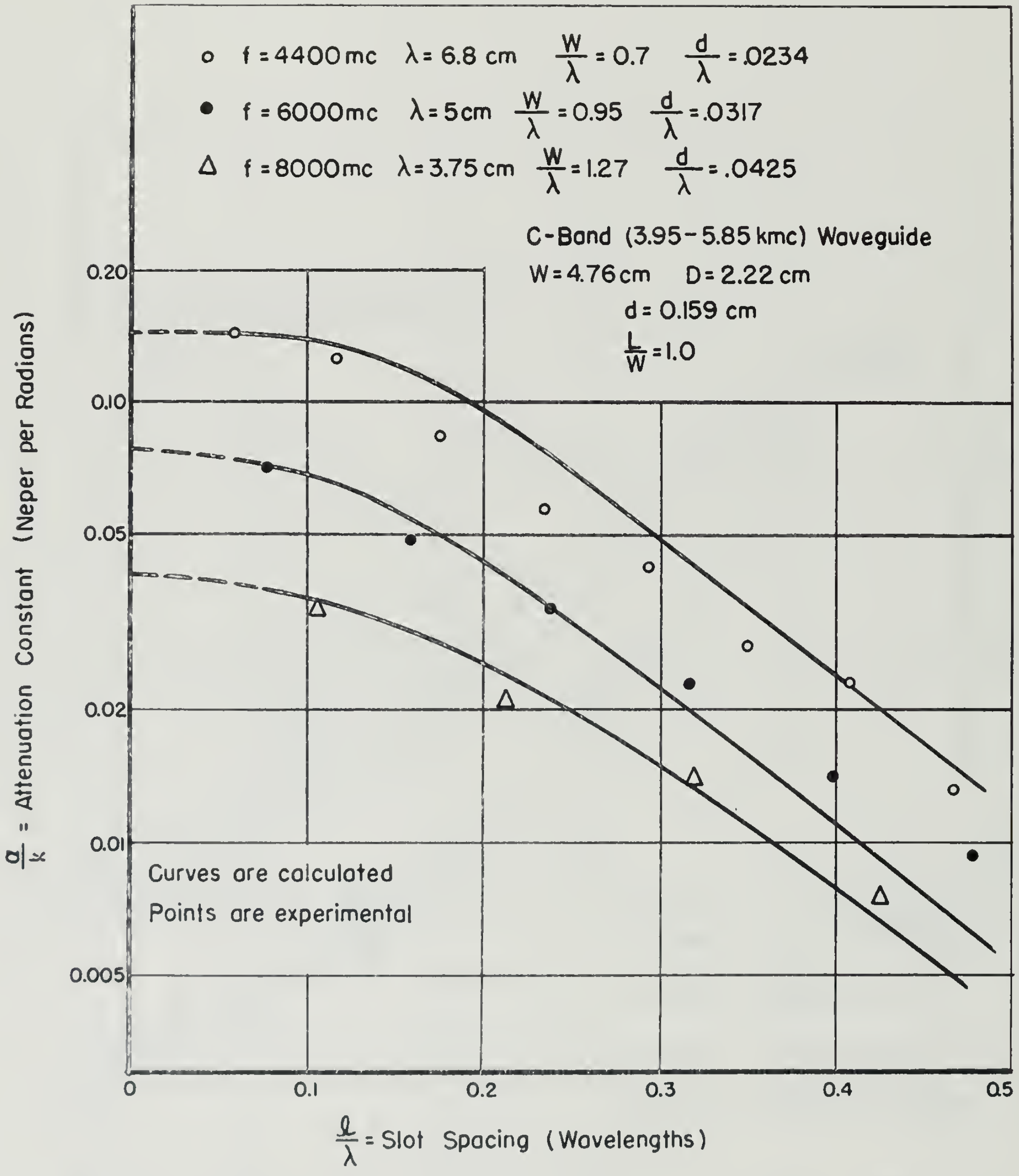

Figure 8 Attenuation Constant versus Slot Spacing

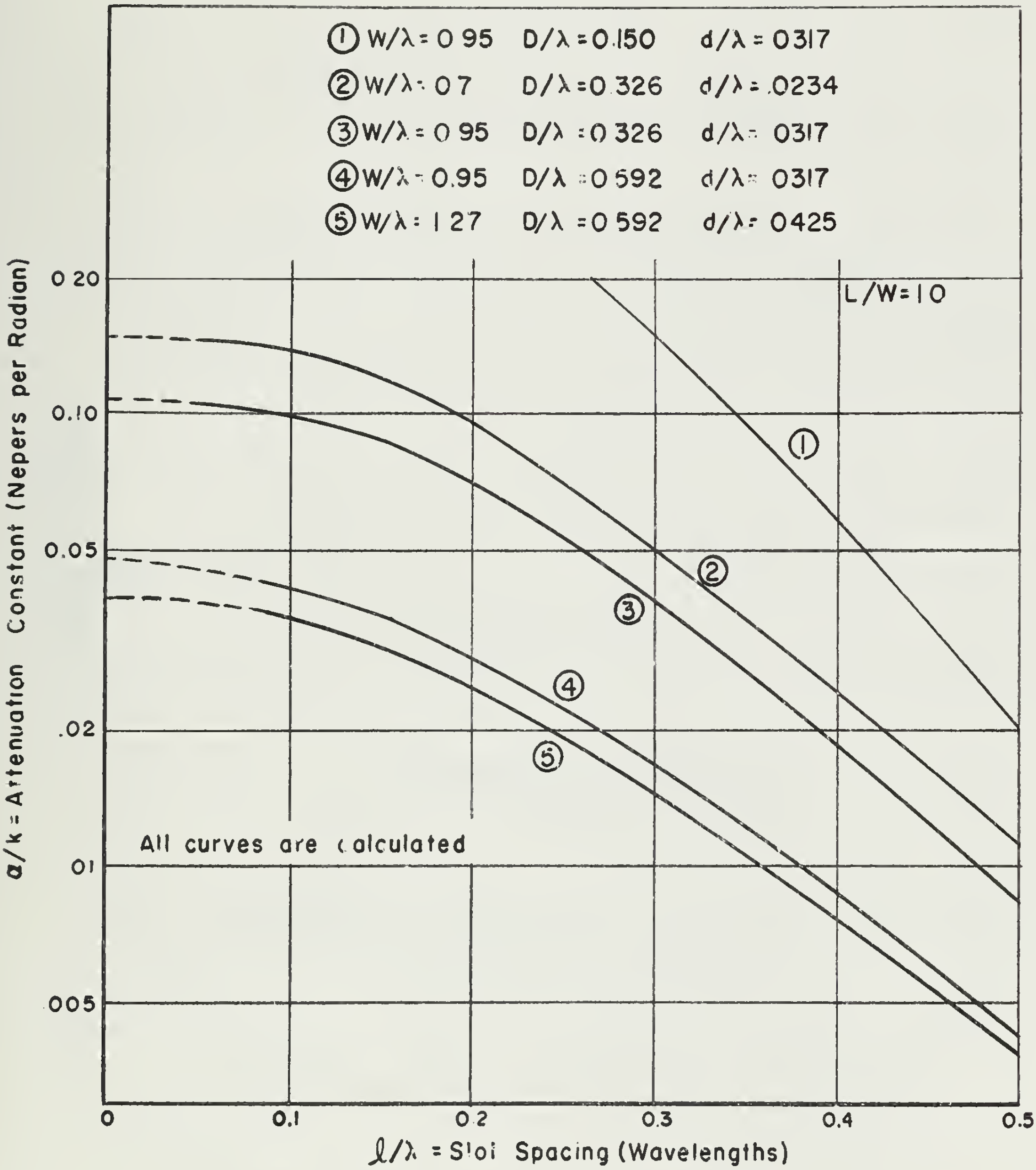

Figure 9. Attenuation Constant versus Slot Spacing

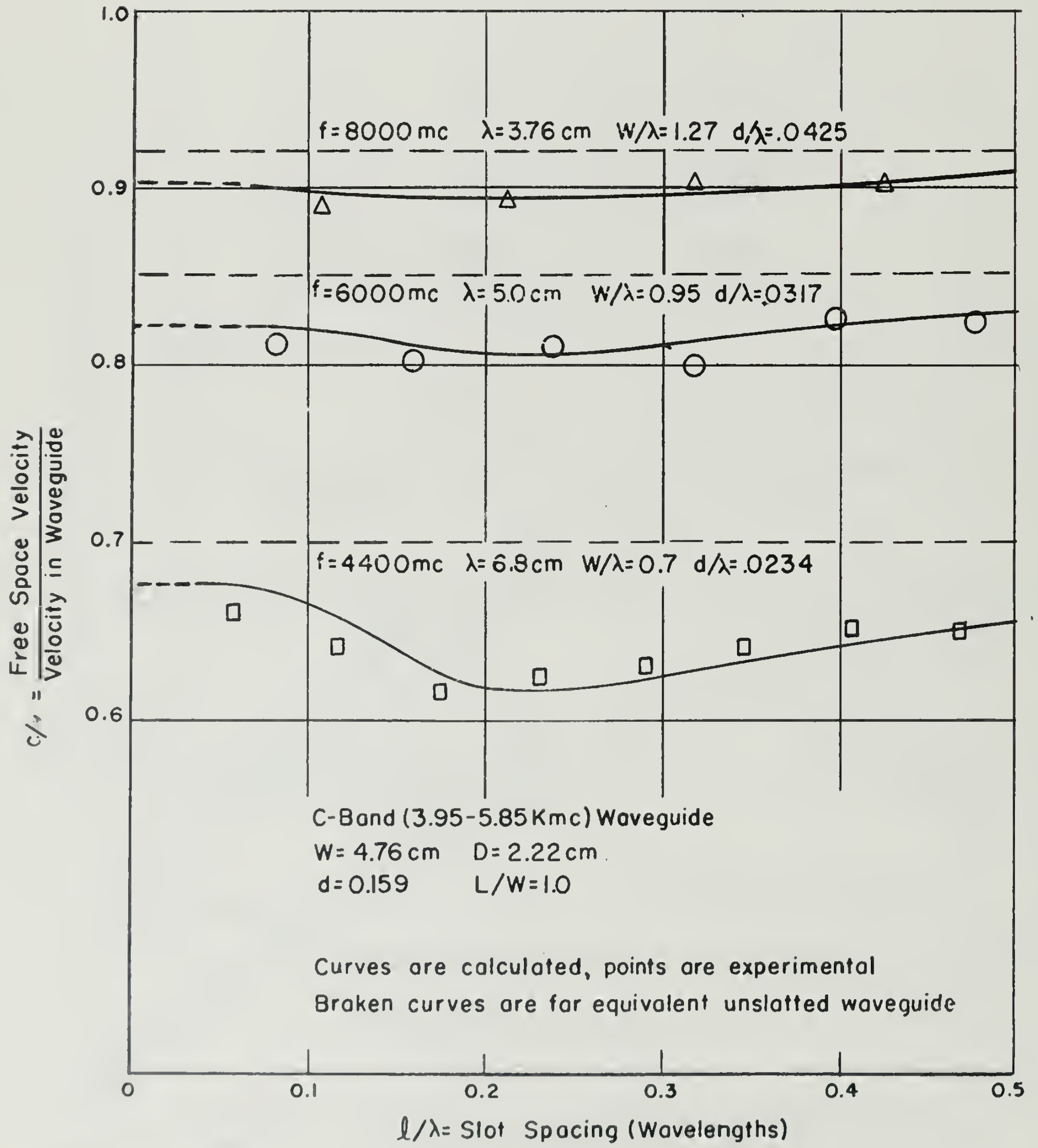

Figure 10 Velocity Ratio versus Slot Spacing

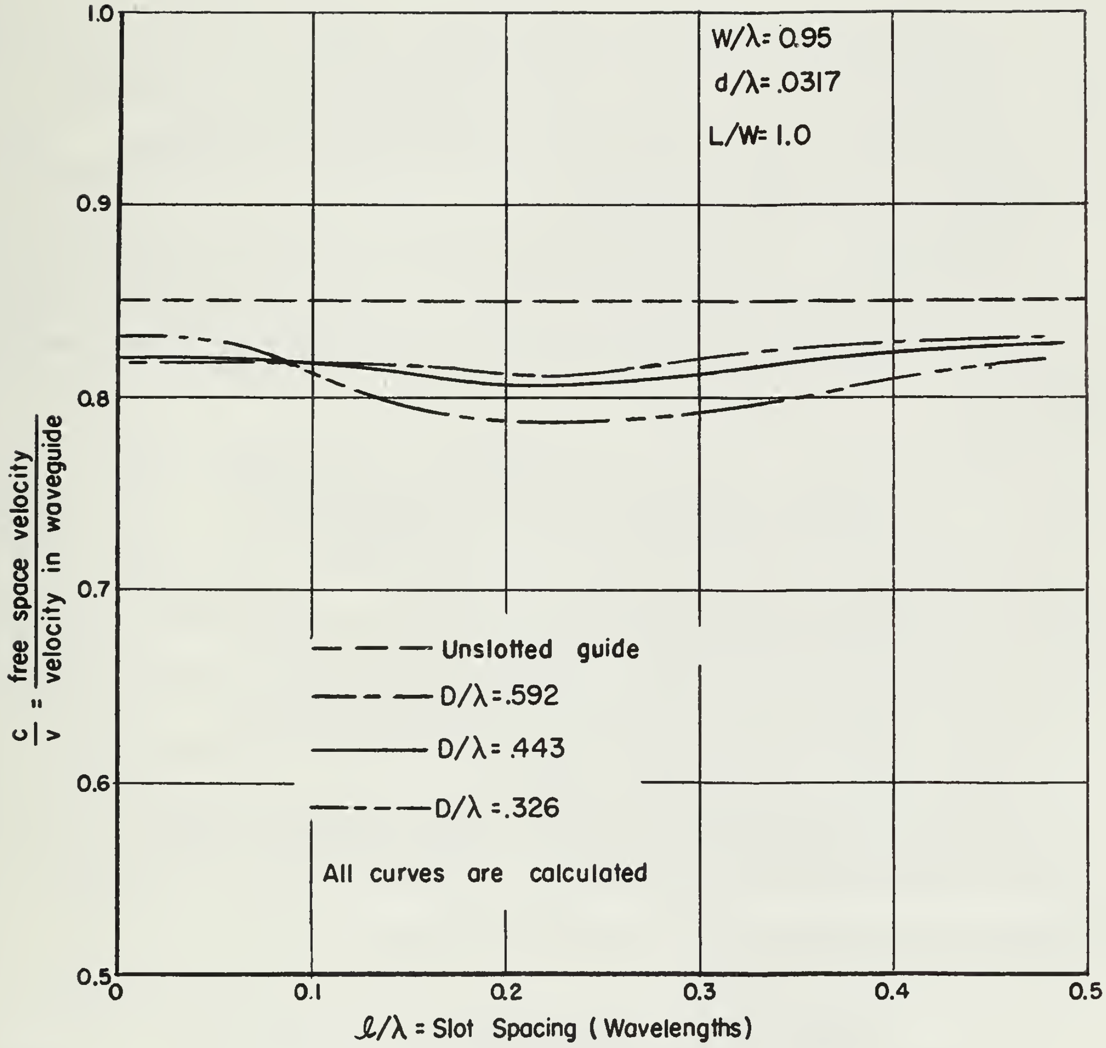

Figure 11. Velocity Ratio versus Slot Spacing

roughly 25% before the excitation of this mode by an incident $TE_{1,0}$ field reaches an objectionable level.

This limitation on D/λ, together with the requirement that $\ell \leq \lambda/2$, results in a minimum α of about .005. This in turn restricts the use of structure to applications where the aperture length is of the order of eight wavelengths or less. An increased dynamic range of α can be obtained by varying $\frac{L}{\lambda}$, as considered in the following section.

3.3 Aperture Distribution Synthesis

An approximate formula relating the aperture illumination to the attenuation factor as a function of distance along the guide has been given[11] as

$$2\alpha(z) = \frac{A^2(z)}{1/(1-f)\int_0^L A^2(z) - \int_0^z A^2(z)dz}, \qquad (3\text{-}6)$$

where z is the distance along the aperture,

A(z) is the desired aperture amplitude function,

L is the total aperture length,

f is the fraction of incident power remaining in the waveguide at the end of the aperture.

Expression 3-6 may be written in normalized form,

$$\frac{\alpha}{k}(z) = \frac{1}{4\pi}\,\frac{A^2(z)}{1/(1-f)\int_0^L A^2(z')dz' - \int_0^{z'} A^2(z')dz'}, \qquad (3\text{-}7)$$

where all distances are now in terms of wavelengths. Within certain limitations, a function A(z) can be obtained for a desired radiation pattern using conventional pattern synthesis techniques.[21,22]

For the case of discrete slot spacing, (Equations 3-6,7) apply on an average basis. The uniform aperture distribution is used as a demonstration of this application.

Standard C-band waveguide is used, with an excitation frequency of 6,000 mc. From Figure 9, this gives a c/v ratio of approximately .81, which corresponds to a beam maximum approximately 36 degrees away from end-fire. The proportion of the incident power which is to be dissipated in the load is chosen as 1/7. Substitution into Equation 3-6 for a total aperture length of seven wavelengths and with A(z) = 1 gives

$$\frac{\alpha}{k}(z) = \frac{\lambda}{4\pi}\,\frac{1}{\frac{7}{6}\,7 - z} = \frac{.157}{15.6 - z} \qquad (3\text{-}8)$$

for $\lambda = 1.97$ inches. The required variation of α is plotted in Figure 12a. The average slot spacing as a function of distance along the aperture is determined from Figure 8 and plotted in Figure 12b. The actual slot spacing is then taken as a stepwise approximation to this curve.

The polar coordinate system used in the measurement of the radiation pattern is defined in Figure 13. The principal plane measured and predicted patterns ($\varphi = 0$, E_θ polarization) are given in Figure 14. In view of the neglect of the variation of c/v which accompanies the variation of α, the agreement as to both beam shape and side lobe level is very good.

Because of the approximate basis of the procedure, this result cannot be taken as further corroboration of the theory, but only as a demonstration of its application to cases of discrete slot spacing.

A crude estimation of the mismatch caused by the discontinuity at the beginning of the aperture can be obtained by considering this point

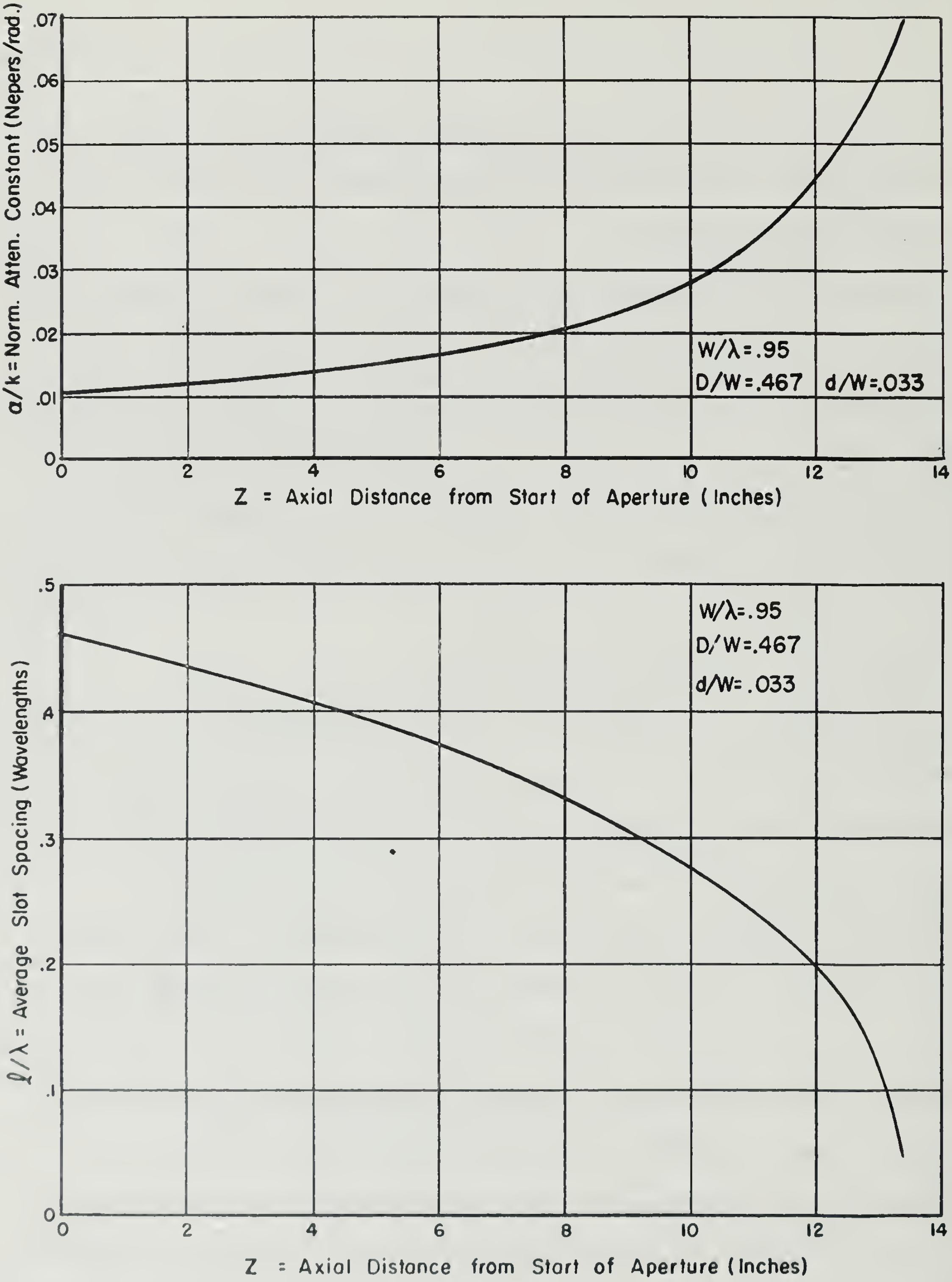

Figure 12 Attenuation Function and Average Slot Spacing for Uniform Aperture Distribution

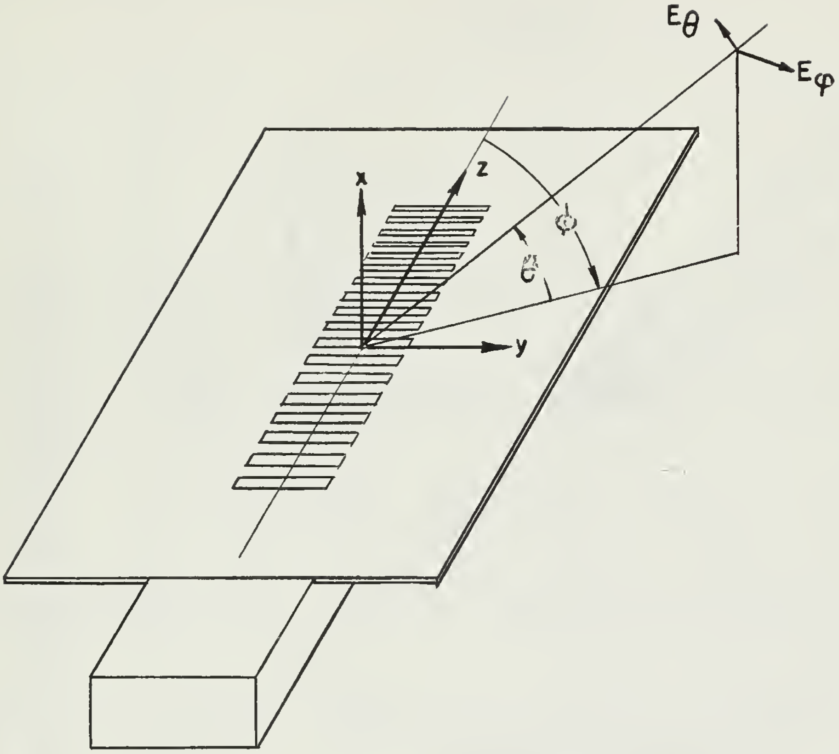

Figure 13. Polar Coordinate System for Pattern Measurements

as the junction of two equivalent transmission lines having different characteristic impedances. Define the characteristic impedance Z by

$$Z = \frac{E_{x_0}}{H_{y_0}},$$

where E_{x_0} and H_{y_0} are fundamental (n=0) components of the internal waveguide field

From Equation 2-6,

$$E_{x_0} = \frac{\partial f_0}{\partial z} = -j\gamma f_0,$$

$$H_{y_0} = \frac{1}{j\omega\mu}\left(k^2 + \frac{\partial^2}{\partial y^2}\right) f_0 = \frac{1}{j\omega\mu}\left(k^2 - \frac{\pi^2}{W^2}\right) f_0.$$

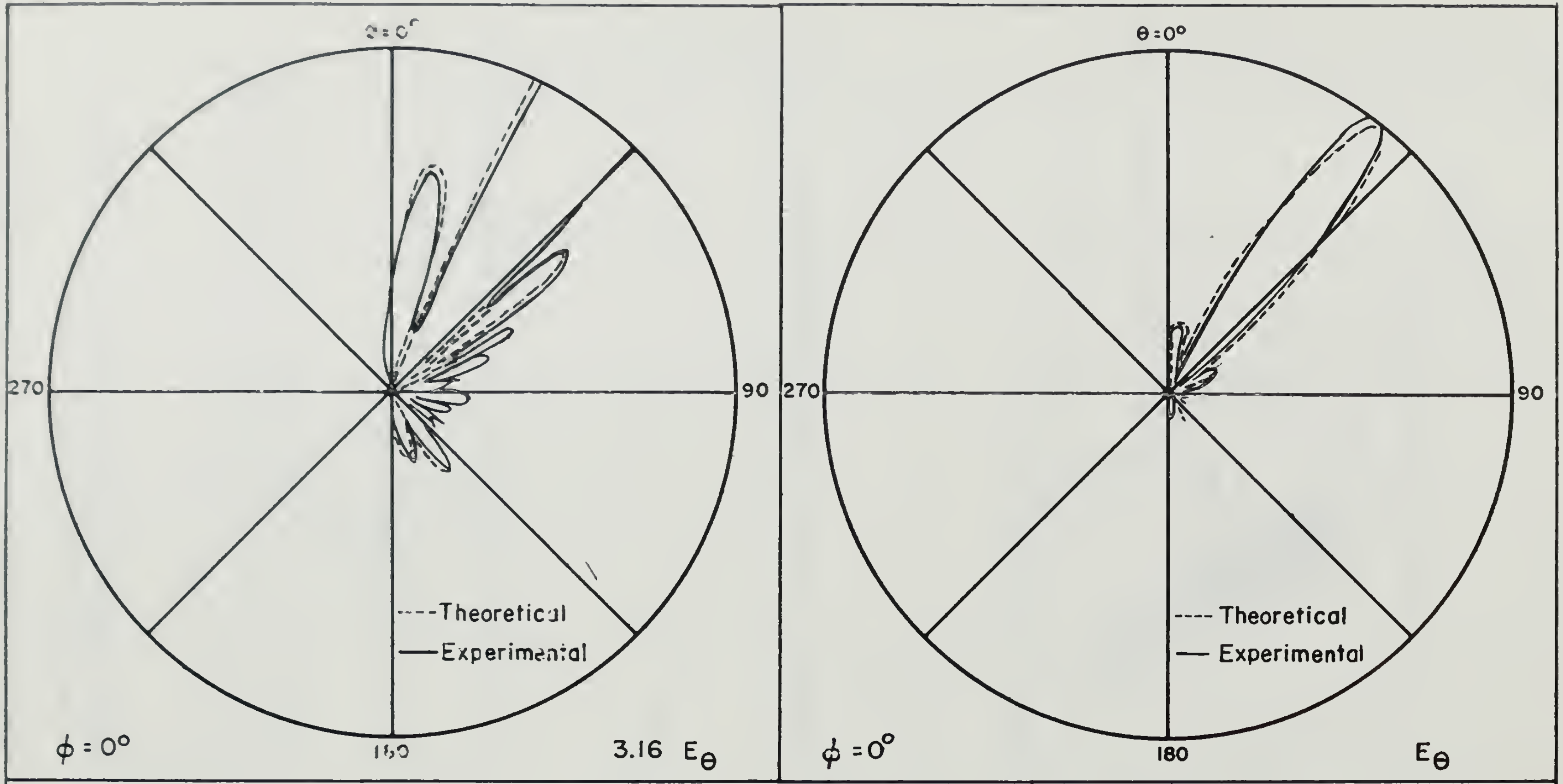

Figure 14. E-Plane Radiation Patterns for Uniform Aperture Distribution (Figure 12).

Thus,

$$\frac{Z_1}{Z_2} = \frac{\gamma_1}{\gamma_2}$$

where the subscripts 1 and 2 refer respectively to the unslotted and slotted regions of the waveguide. Then Γ , the reflection coefficient at the junction, is given approximately by

$$\Gamma = \frac{Z_2 - Z_1}{Z_2 + Z_1} = \frac{\gamma_2/\gamma_1 - 1}{\gamma_2/\gamma_1 + 1}, \qquad (3\text{-}9)$$

where $\gamma_1 = k\sqrt{1-(\lambda/2W)^2}$ and γ_2 are the propagation constants in regions 1 and 2.

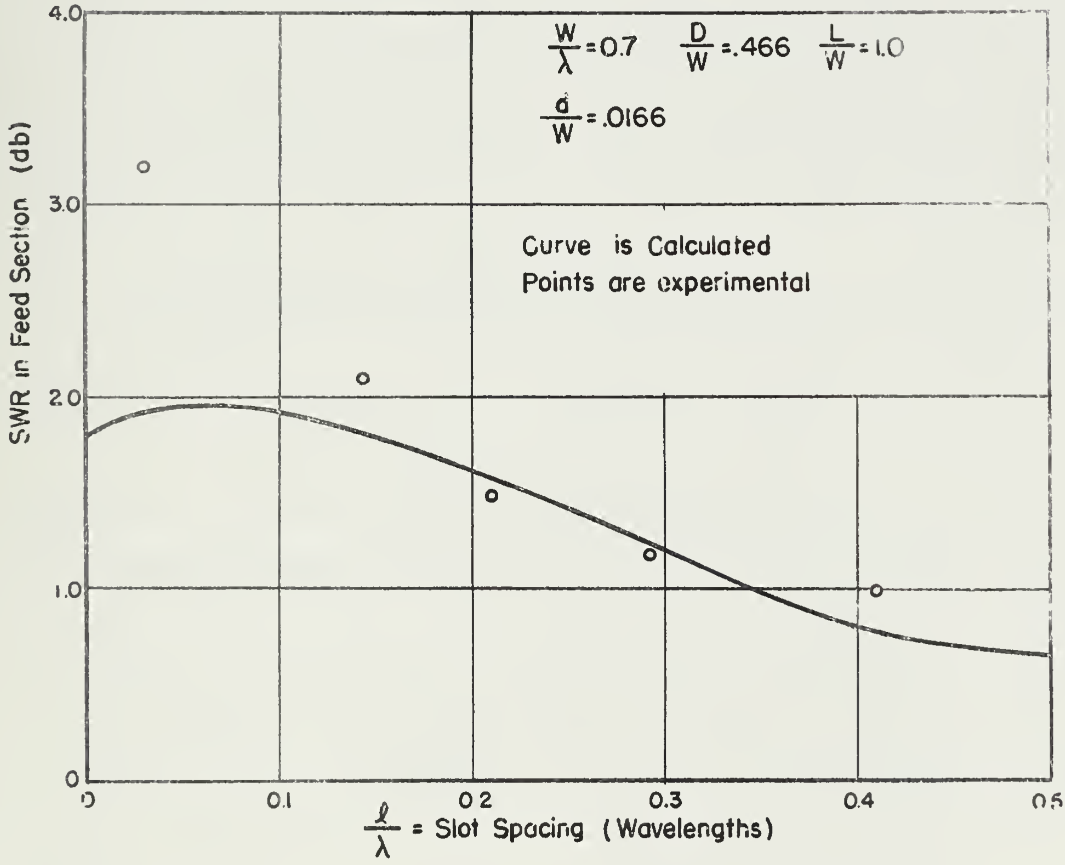

Figure 15. Input Standing Wave Ratio Versus Slot Spacing

The calculated results for a typical case with variable ℓ/λ, are given in Figure 15. The measured results show reasonable agreement with the theory except in the range of small ℓ/λ, where the perturbation of the fields by the slots is relatively great. The failure of Equation 3-9 in this region is not surprising since the presence of higher order modes and the differences in the transverse distributions of the fields in the perturbed and unperturbed regions are not taken into account.

In the majority of antenna applications ℓ/λ is large at the start of the aperture, and thus a fairly good match is obtained.

3.4 Surface Wave Mode.

In view of the physical similarities between a corrugated surface and the transversely slotted rectangular waveguide, it is instructive to examine Equation 3-4 for a possible unattenuated surface wave solution. Toward this end, assume

$$\gamma/k = c/v > 1.$$

In this case, both β and κ are pure imaginary and may be written

$$\beta = -jk\sqrt{(c/v)^2-1} = -j\sigma$$

$$\kappa = -jk\sqrt{(c/v)^2+(\lambda/2W)^2-1} = -j\zeta \qquad (3\text{-}10)$$

where both σ and ζ are positive real. With these transformations, Equation 3-4 becomes

$$\frac{\coth \zeta D}{\zeta D} = -\frac{2\ell}{\lambda D}\left\{\sum_{i=0}^{2} p_{2i}\left(\frac{\ell}{\lambda}\frac{\gamma}{k}\right)^2 + \left(\frac{\ell}{\lambda}\right)^2\left(1-\frac{\lambda^2}{4W^2}\right)\sum_{i=0}^{2} q_{2i}\left(\frac{\ell}{\lambda}\frac{\gamma}{k}\right)^2 + \right.$$

$$\left. + j\,\frac{W}{\pi D}\,\frac{1}{1-\frac{\lambda^2}{4W^2}}\,I_0\left(-j\frac{\sigma}{k}, \frac{W}{\lambda}\right)\right. \qquad (3\text{-}11)$$

From Equation B-7, for $L = W$,

$$I_0\left(-j\frac{\sigma}{k}\frac{W}{\lambda}\right) = j\frac{2}{\pi}\int_0^{\pi} K_0\left(\frac{\sigma W r}{\pi}\right)\left[\left(1-\frac{\lambda^2}{4W^2}\right)\left(1-\frac{r}{\pi}\right)\cos r + \frac{1}{\pi}\left(1+\frac{\lambda^2}{4W^2}\right)\sin r\right]dr, \tag{3-12}$$

since

$$H_0^{(2)}(-j\sigma) \doteq j\frac{2}{\pi}K_0(\sigma).$$

For any fixed σ, define $F(\frac{W}{\lambda})$ as

$$F\left(\frac{W}{\lambda}\right) = j\frac{W}{\pi D}\,\frac{1}{1-\frac{\lambda^2}{4W^2}}\,I_0\left(-j\frac{\sigma}{k}\frac{W}{\lambda}\right)$$

$$= -\frac{W}{\pi D}\int_0^{\pi} K_0\left(\frac{\sigma W r}{\pi}\right)\left[\left(1-\frac{r}{\pi}\right)\cos r + \frac{1}{\pi}\,\frac{1+\frac{\lambda^2}{4W^2}}{1-\frac{\lambda^2}{4W^2}}\sin r\right]dr. \tag{3-13}$$

The function $K_0(\frac{\sigma W r}{\pi})(1-\frac{r}{\pi})$ is a positive, real monotone decreasing function for $0 \leq r \leq \pi$. Hence in Equation 3-13,

$$\int_0^{\pi} K_0\left(\frac{\sigma W r}{\pi}\right)\left(1-\frac{r}{\pi}\right)\cos r\, dr > 0,$$

and, for $W > \lambda/2$,

$$F(W/\lambda) < 0.$$

Thus, for $W > \lambda/2$, both terms on the right hand side of Equation 3-11 are negative and no solution giving a real value of ζ is possible.

For values of W less than, but sufficiently close to $\lambda/2$, the second term in the integrand of Equation 3-13 is dominant and negative. Thus for any given σ, $F(W/\lambda)$ can be made positive and as large as desired by the proper choice of W/λ. Alternatively, it can be shown that for sufficiently small W,

$$\int_0^{\pi} K_0\,(\sigma Wr/\pi)\ [1 - (r/\pi)]\cos r\,dr > 1/\pi \int_0^{\pi} K_0(\sigma Wr/\pi)\ \sin r\,dr,$$

since

$$K_0\ (\sigma Wr/\pi) \rightarrow \ln\ (\pi/\sigma Wr)\ \text{as}\ W/\lambda \rightarrow 0.$$

Hence, $F(W/\lambda)$ again becomes negative when W/λ is taken sufficiently close to zero. Thus, for given $\gamma > k$ (assuming always that $\gamma\ell < \pi$), and therefore given σ and ζ, there is a value of $W < \lambda/2$ which will satisfy Equation 3-11 and a surface wave solution is possible. The variation of c/v versus frequency obtained from Equation 3-11 is given in Figure 16 for a typical waveguide and slot configuration.

For the limiting case of $\ell/\lambda \rightarrow 0$, Equation 3-11 reduces to

$$(\coth \zeta D)/\zeta D = j\ (W/\pi D)[1/1 - (\lambda^2/4W^2)]\ I_0\ [(-j\sigma/k),\ (W/\lambda)]. \qquad (3\text{-}14)$$

For this case, there is no lower frequency limit for progagation of the surface wave mode, i.e., c/v approaches 1 as $\omega \rightarrow 0$. An expression which is asymptotic to Equation 3-14 is easily developed. Since $c/v \rightarrow 1$ as $W/\lambda \rightarrow 0$, then, from Equation 3-10,

$$\zeta/k \rightarrow \lambda/2W,$$

$$(\coth \zeta D)/\zeta D \rightarrow [\coth\ (\pi D/W)\ /(\pi D/W)]$$

$$\sigma/k = \sqrt{(c/v)^2 - 1} \rightarrow \sqrt{2(c/v - 1)}. \qquad (3\text{-}15)$$

For small σ, only the first term of I_0 is appreciable. From Appendix B, Equation B-19, and Table 1,

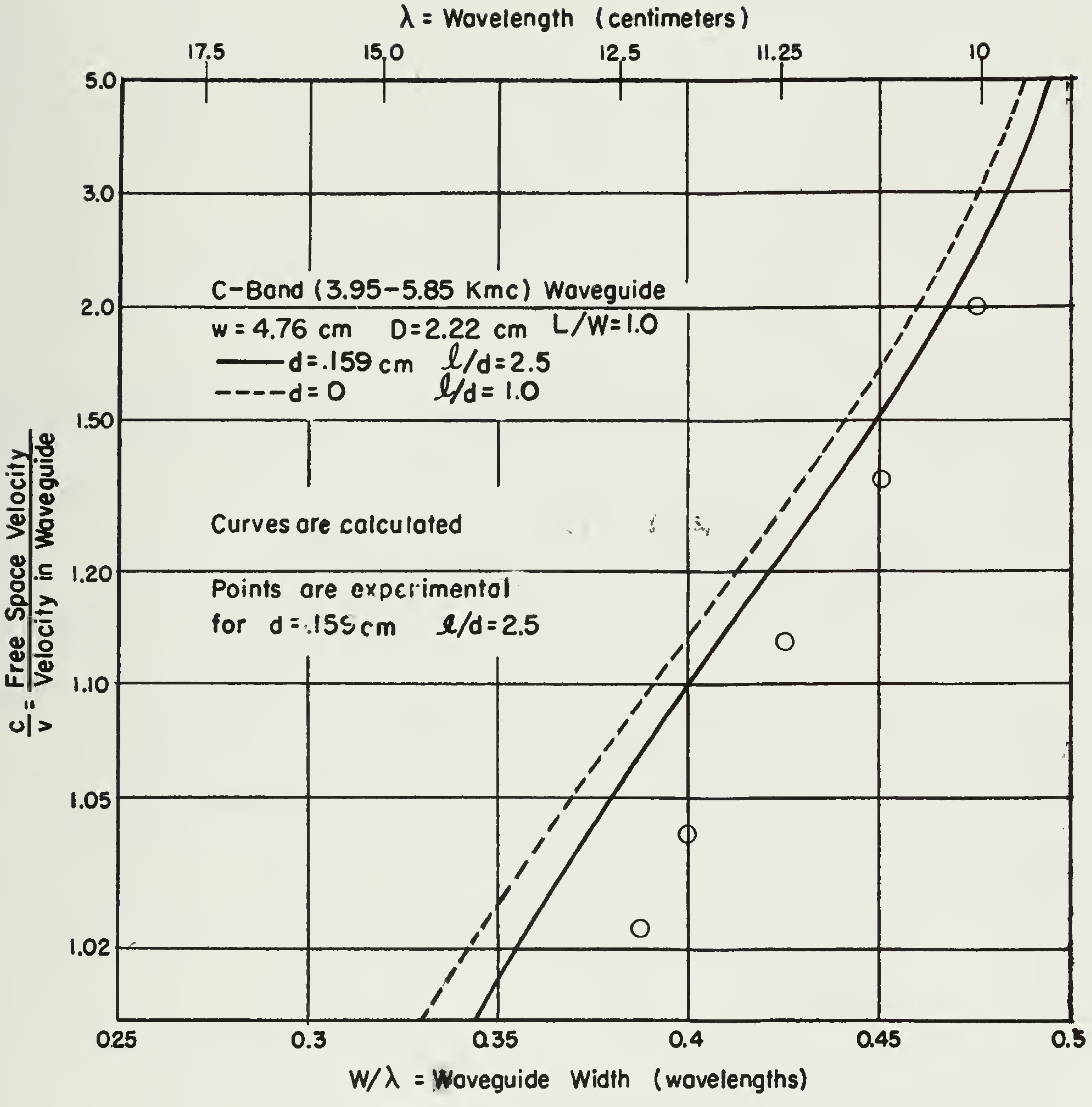

Figure 16. Velocity Ratio versus Frequency for Surface Wave Mode

UNIVERSITY OF ILLINOIS
LIBRARY

$$I_0 \left(-j\frac{\sigma}{k}, \frac{W}{\lambda}\right) \simeq -j\frac{2}{\pi} \left\{ (1.273)\left[\overline{\gamma} + \ln \frac{\sigma}{k}\frac{W}{\lambda}\right] - .807 + 1.215 \frac{\lambda}{2/W^2}\right\}. \qquad (3\text{-}16)$$

Substituting into (3-14) gives

$$\frac{\coth \frac{\pi D}{W}}{\frac{\pi D}{W}} \simeq \frac{2}{\pi^2}\frac{W}{D}\frac{1}{1-\frac{\lambda^2}{4W^2}} \left\{ (1.273)\left[\overline{\gamma} + \tfrac{1}{2}\ln\frac{4W^2}{\lambda^2} - \tfrac{1}{2}\ln 2 + \tfrac{1}{2}\ln (c/v - 1)\right] - .807 + 1.215 \frac{\lambda^2}{4W^2}\right\},$$

which simplifies to

$$c/v = 1 + \exp\left\{.808 - 1.91(\lambda^2/4W^2) - (\pi^2/4)(\lambda^2/4W^2 - 1)\coth \pi D/W + \ln \lambda^2/4W^2\right\}. \qquad (3\text{-}17)$$

Both the rapidly damped fundamental and the surface-wave modes are excited by an incident $TE_{1,0}$ field when $W < \lambda/2$. For this condition, typical variations of measured phase and amplitude with axial distance along the waveguide are given in Figure 17. The computed curves in these figures were obtained by taking a solution of Equation 3-4 for γ for the fundamental mode,

$$\gamma/k = -.190 - j.438,$$

and the measured value of

$$\gamma/k = 1.77$$

for the surface wave. Relative phase and amplitude of these fields were adjusted to give the best fit with the measured results. The poor agreement at the beginning of the aperture is possibly due to the presence of higher order evanescent modes. For comparison, typical measured results under conditions of single mode propagation ($W > \lambda/2$) are given in Figure 18.

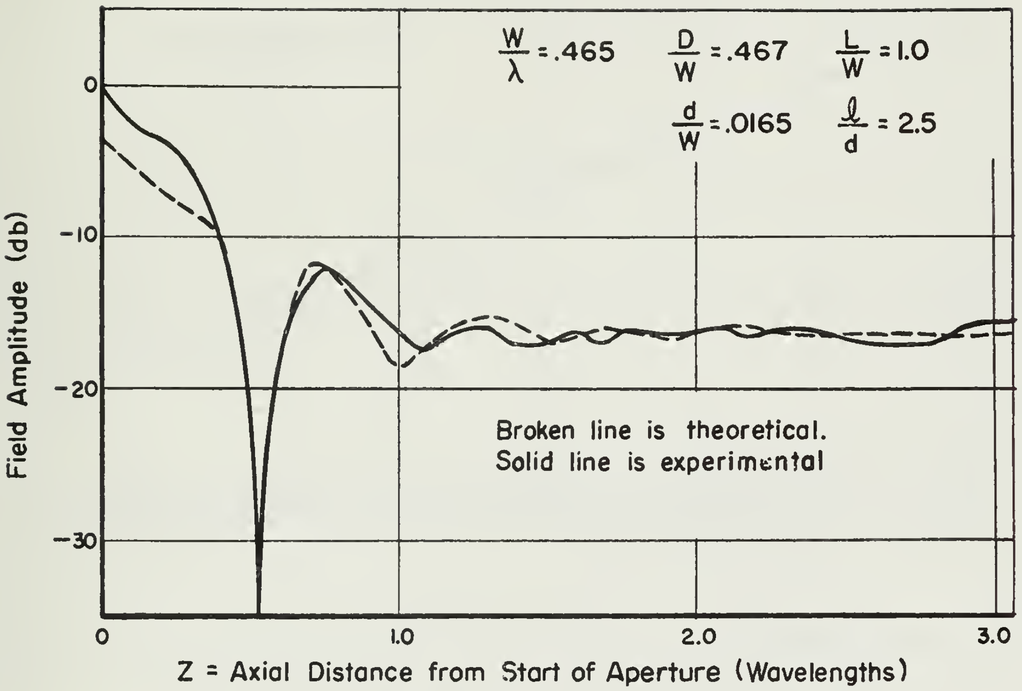

a) Axial Amplitude Distribution

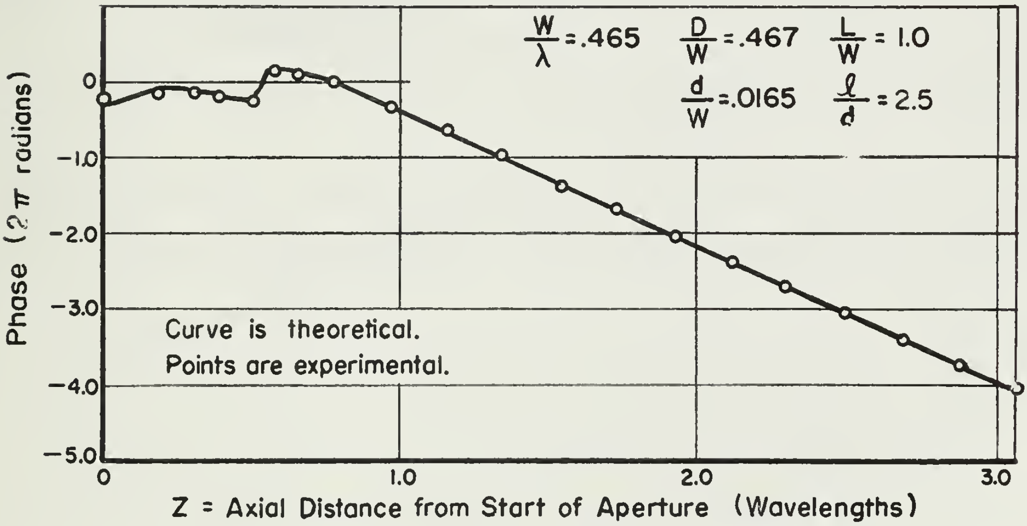

b) Axial Phase Distribution

Figure 17. Axial Phase-Amplitude Distribution with Fundamental and Surface Wave Modes Present, $W<\lambda/2$

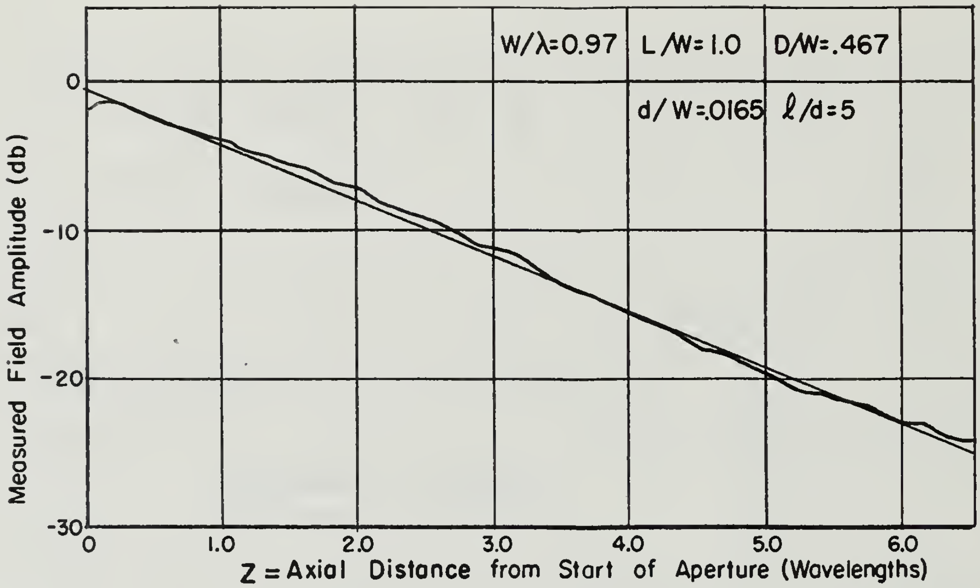

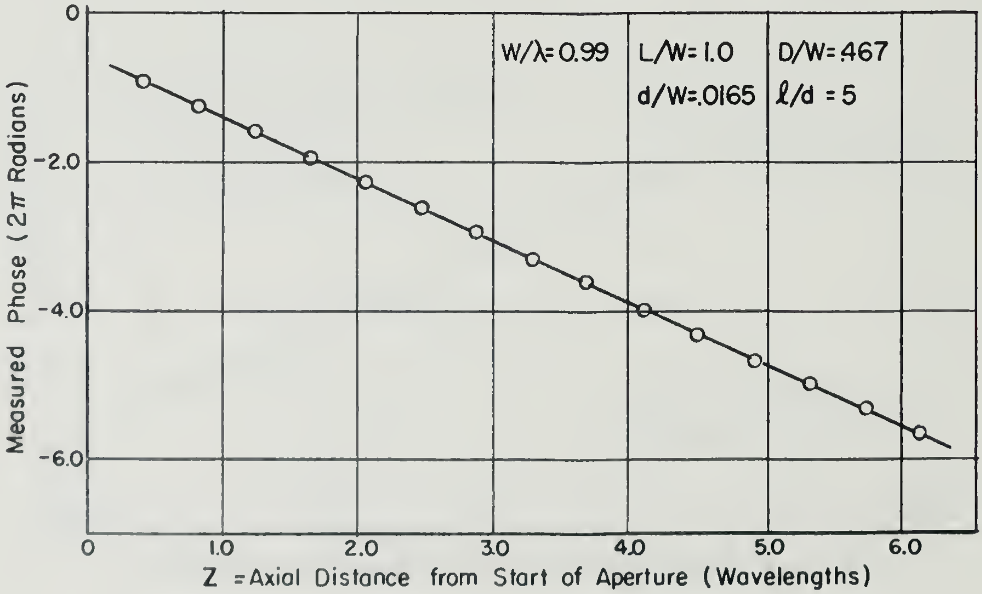

Figure 18. Measured Axial Phase-Amplitude Distribution Under Conditions of Single Mode Propagation

As inferred from Figure 17, the surface wave launching efficiency is relatively low when the slotted guide is excited internally by an evanescent $TE_{1,0}$ field. Dielectrically loading the feed section as indicated in Figure 19 gives some improvement in the launching efficiency. However, it appears that an external surface wave launcher, such as a waveguide horn, is necessary for relatively high excitation levels for this mode.

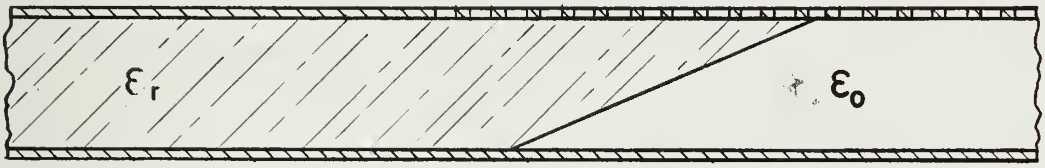

Cut Away Side View.

Figure 19. Dielectrically Loaded Feed Section to Improve Surface Wave Launching Efficiency

There are also a number of higher order surface wave modes. For example, Figure 20 shows evidence of the lowest order asymmetrical mode for W/λ near unity. Initial excitation is the result of a slight dissymmetry in the waveguide structure. Similarly, a higher order symmetrical mode is excited when W is slightly less than $1.5\ \lambda$ (See Figure 21). The excitation level of this latter mode by an incident $TE_{1,0}$ field appears to be of an objectionable level for $1.4 < W/\lambda < 1.5$. Thus, unless effective measures for its suppression are taken, the presence of this mode restricts use of the structure to cases where $W < 1.4\ \lambda$.

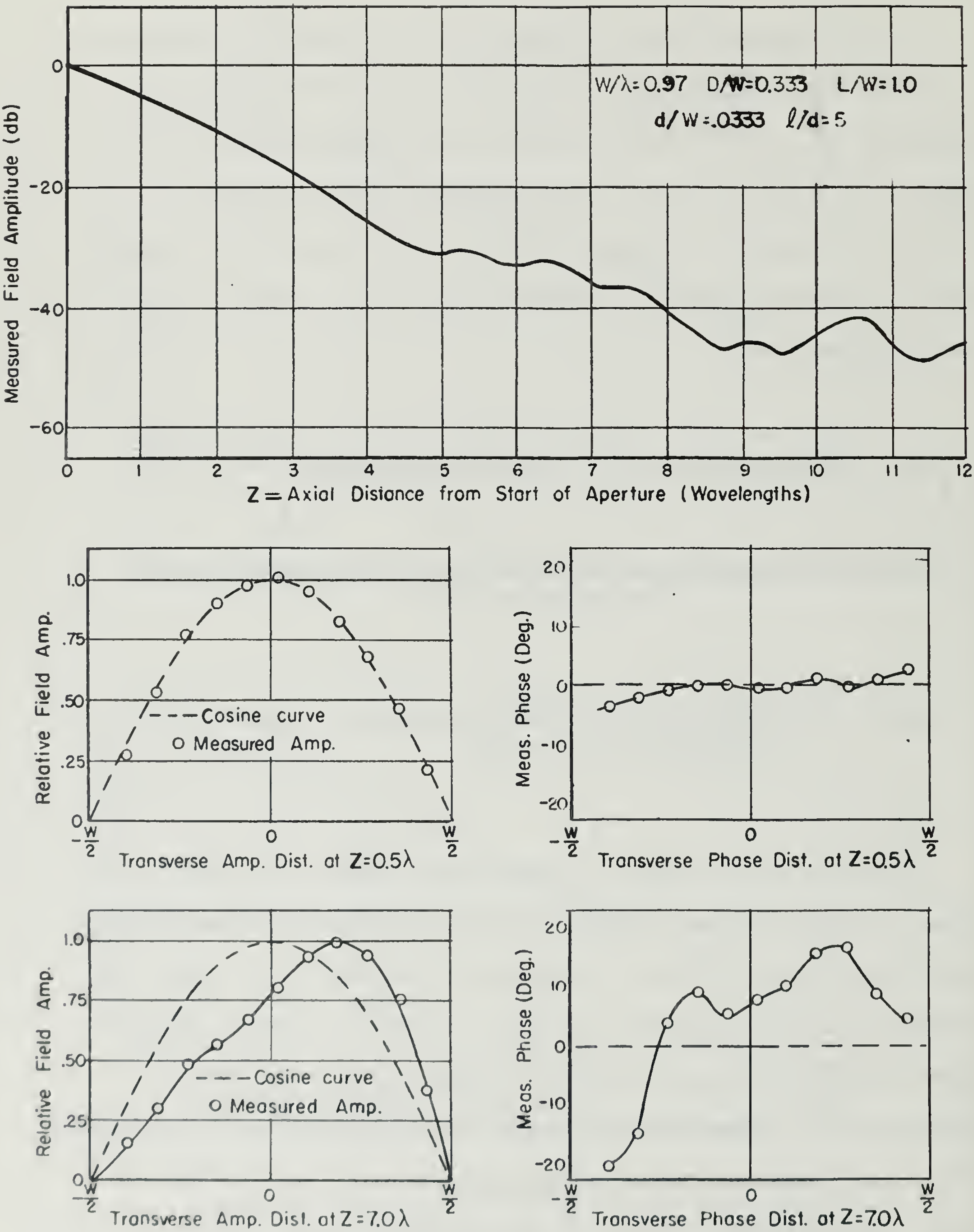

Figure 20 Evidence of Asymmetrical Surface Wave Mode Resulting from Small Structural Dissymmetry When W/λ Near 1.0

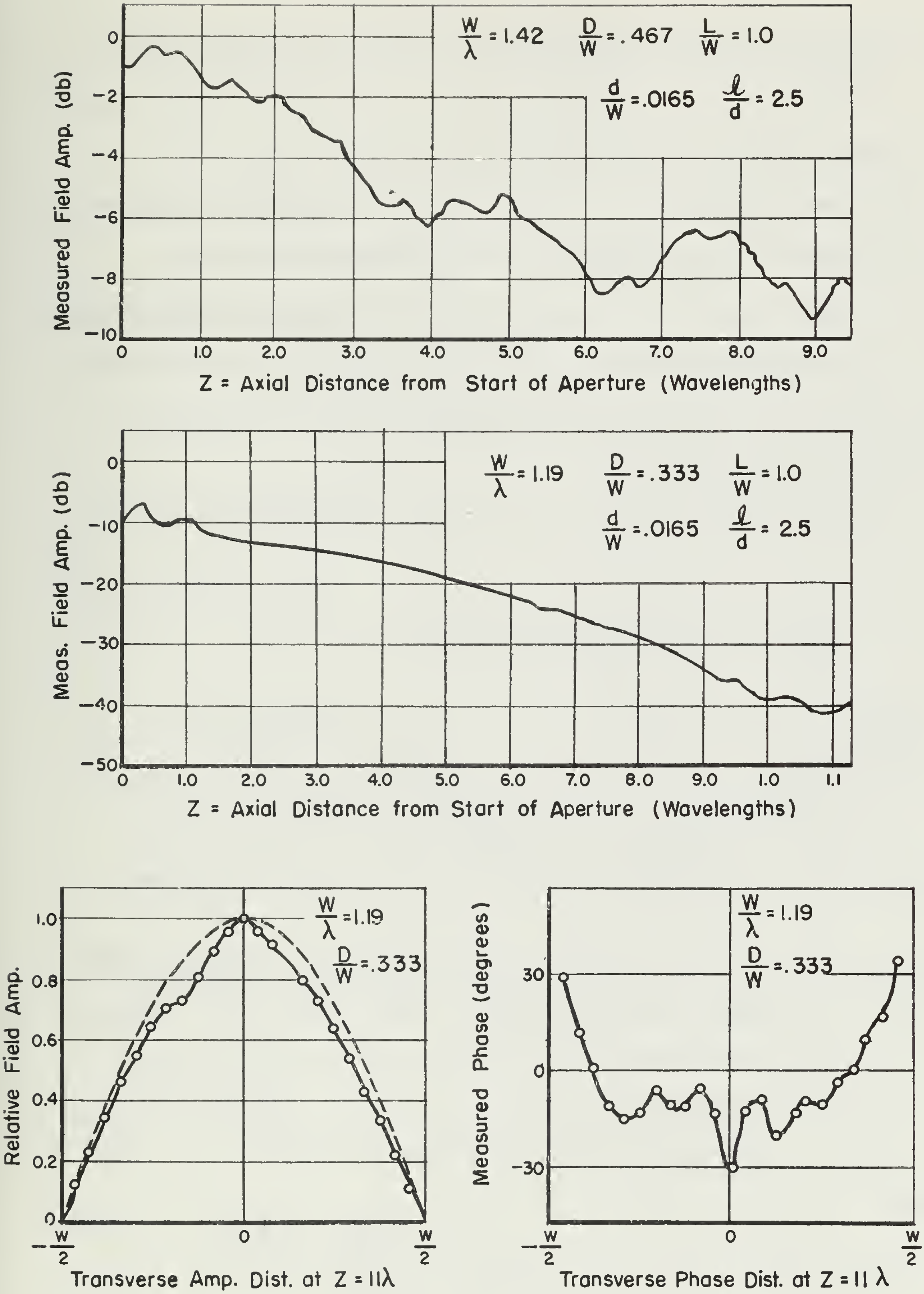

Figure 21 Evidence of Third Order Surface Wave Mode for W/λ Near 1.5

IV. THEORETICAL AND EXPERIMENTAL RESULTS FOR SMALL SLOT LENGTH

4.1 Characteristic Equation for γ.

The results of Section III show that γ is relatively insensitive to the values of ℓ and d when $\ell \lesssim \lambda/10$. Although these results strictly apply only for L = W, approximately the same condition should exist for arbitrary L provided that L/ℓ is large. Thus the simplified form of the characteristic equation (2-39) for the limiting case of $\ell/\lambda = 0$ is of special interest.

In Equation 2-39, let $\ell/\lambda \to 0$, with ℓ/d remaining finite. Since

$$\lim_{\frac{\ell}{\lambda}\to 0} k/\sigma_n = \lim_{\frac{\ell}{\lambda}\to 0} \frac{1}{\sqrt{(n\lambda/\ell - \gamma/k)^2 - 1}} = 0, \quad n \neq 0,$$

$$\lim_{\ell\to 0} k/\zeta_{m,n} = \lim_{\ell\to 0} \frac{1}{\sqrt{(n\lambda/\ell - \gamma/k)^2 + (m\lambda/2W)^2 - 1}} = 0, \quad n \neq 0,$$

then only the n = 0 term is non zero. Thus Equation 2-39 becomes

$$\frac{\cot \kappa D}{\kappa D} \quad \frac{1}{1 - (\lambda^2/4W^2)} \quad \frac{(1 - L^2/W^2)^2}{\cos^2(\pi L/2W)} \quad \frac{\lambda}{2\pi D}\left\{ \sum_{m=3}^{\infty}{}' \frac{m^2\lambda^2}{4W^2} - 1 \quad \frac{\cos^2(m\pi L/2W)}{(1 - m^2L^2/W^2)^2} \right.$$

$$k/\zeta_m \coth \zeta_m D + j \frac{\pi^2}{8} \frac{W}{\lambda} I_0 (\beta/k,\ L/\lambda), \tag{4-1}$$

where

$$\kappa = k\sqrt{1 - (\lambda/2W)^2 - (\gamma/k)^2},$$

$$\beta = k\sqrt{1 - (\gamma/k)^2} \quad ,$$

$$\zeta_m = k\sqrt{(\gamma/k)^2 + (m\lambda/2W)^2 - 1} \ ,$$

and where $\vec{I}_0\ (\beta/k,\ L/\lambda)$ is given in Appendix B.

The corresponding perturbation formula is obtained using Equation 2-41. Also, with

$$\gamma/k = ({}_0\gamma/k) + \delta\,(\gamma/k),$$

where $\delta(\gamma/k)$ is small,

$$\begin{aligned}\zeta_n &\simeq k\sqrt{({}_0\gamma/k)^2 + 2({}_0\gamma/k)\delta(\gamma/k) + (m\lambda/2W)^2 - 1} \\ &\simeq \lambda/2W\ \sqrt{m^2 - 1} \qquad \text{for } m \geq 3.\end{aligned} \tag{4-2}$$

Thus

$$\delta(\gamma/k) = \delta(c/v) - j\,\frac{\alpha}{k}$$

$$\begin{aligned}\simeq \frac{\sqrt{1 - (\lambda^2/4W^2)}}{8\pi}(\lambda/D)(\lambda/W)\Bigg\{ &- \pi/3(1 - \lambda^2/4W^2)\ D/W + \frac{(1 - L^2/W^2)^2}{\cos^2(\pi L/2W)}\, \bullet \\ &\bullet \sum_{m=3}^{\infty}{}' (m^2\lambda^2/4W^2 - 1)\ \frac{\cos^2\frac{m\pi L}{2W}}{(1 - m^2L^2/W^2)^2}\ \frac{\coth \pi D/W\sqrt{m^2 - 1}}{\sqrt{m^2 - 1}} + \\ &+ j\,\frac{\pi^2}{16}\,\frac{(1 - L^2/W^2)^2}{\cos^2(\pi L/2W)}\, I_0\left(\frac{\beta}{k}, \frac{L}{\lambda}\right)\Bigg\}^{-1}.\end{aligned} \tag{4-3}$$

The first order approximation to γ is obtained by using ${}_0\gamma/k = \sqrt{1 - (\lambda/2W)^2}$ in the right hand side of Equation 4-3. Thus

$$(\gamma/k)_1 = {}_0\gamma/k + \delta_0\,(\gamma/k) = {}_0\gamma/k + F\,({}_0\beta/k), \tag{4-4}$$

where

$${}_0\beta = k\sqrt{1 - ({}_0\gamma/k)^2} = k\sqrt{1 - 1 + (\lambda/2W)^2} = k\frac{\lambda}{2W}.$$

Better approximations to the exact solution of Equation 2-39 are obtained from successive iterations of the form

$$(\gamma/k)_{i+1} = {}_0\gamma/k + \delta_i(\gamma/k) = {}_0\gamma/k + F({}_i\beta/k)$$

where

$${}_{(i+1)}\beta = k\sqrt{1 - (\gamma/k)_{i+1}} = k\sqrt{1 - \left[({}_0\gamma/k) + \delta_i\ (\gamma/k)\right]}$$

$$\simeq k(\lambda/2W)\sqrt{1 - 8(1 - \lambda^2/4W^2)^{1/2}\ (W/\lambda)^2\ \delta_i\ (\gamma/k)}.$$

For use in the first iteration, curves of I_0 (${}_0\beta/k$, W/λ) with W/λ as parameter are given in Figures 22-24.

The first N terms of the infinite series of Equations 4-1,3 were summed for $N = 5\,\frac{W}{L}$. The results are given in Figures 25-26. In the course of these computations, the coefficients

$$\frac{(m^2\ \lambda^2/4W^2) - 1}{(m^2 - 1)^{1/2}}$$

were treated correctly for the first three terms of the series. For the remaining terms, the approximation

$$(m\ \lambda^2)/4W^2$$

was employed. In addition, the approximation

$$\coth(\pi D/W)\ \sqrt{m^2 - 1} \simeq 1.0$$

was used for all terms. The results given are estimated to be within about 5% of the exact value of the infinite sum for cases where $D/W \geq 0.2$. For smaller D, the hyperbolic cotangent approximation is invalid and correction terms are necessary.

4.2 Theoretical and Experimental Results

Two iterations using Equation 4-3 were employed for the results in

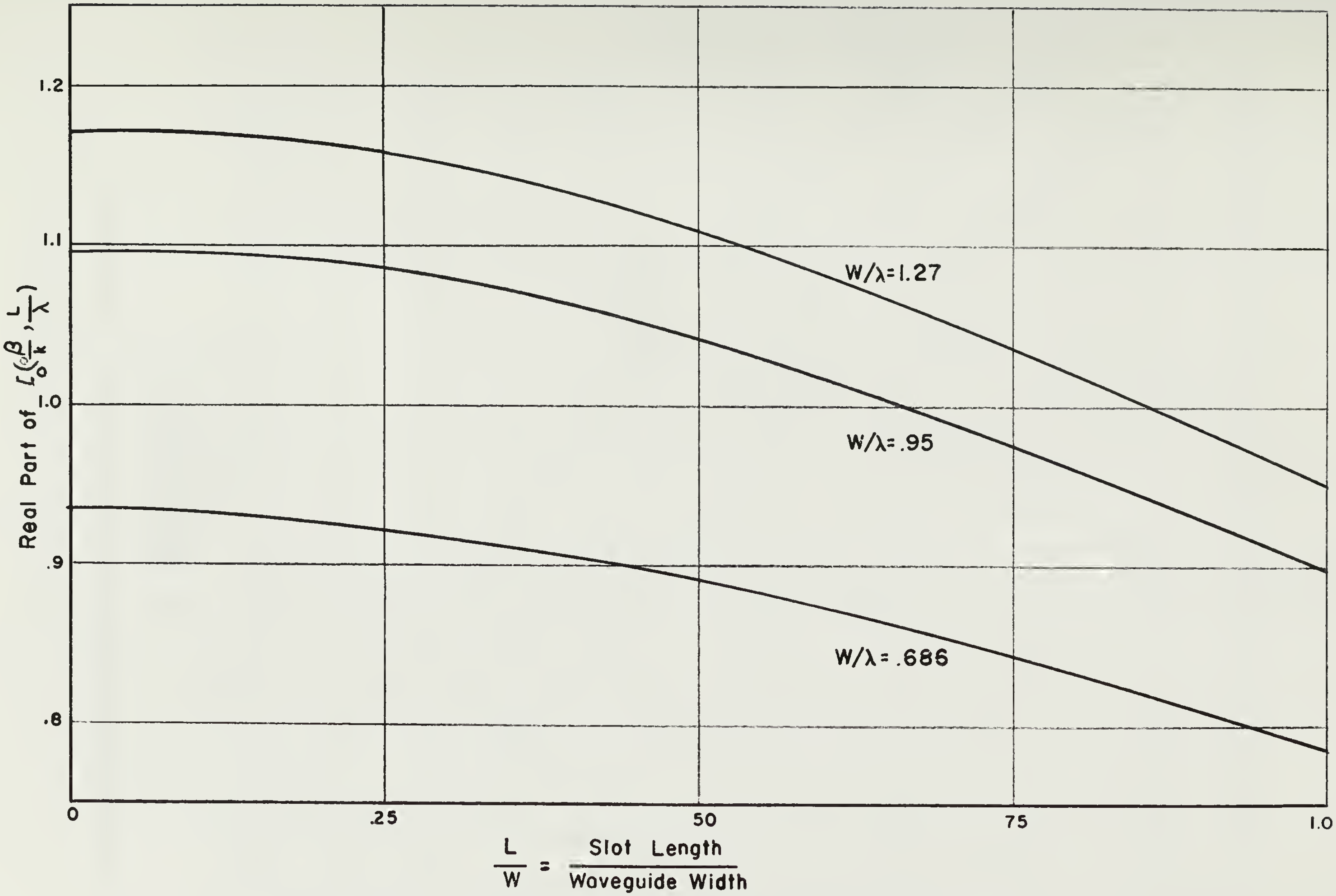

Figure 22 Real Part of I_0 $({}_0\beta/k,\ L/\lambda)$ versus L/W

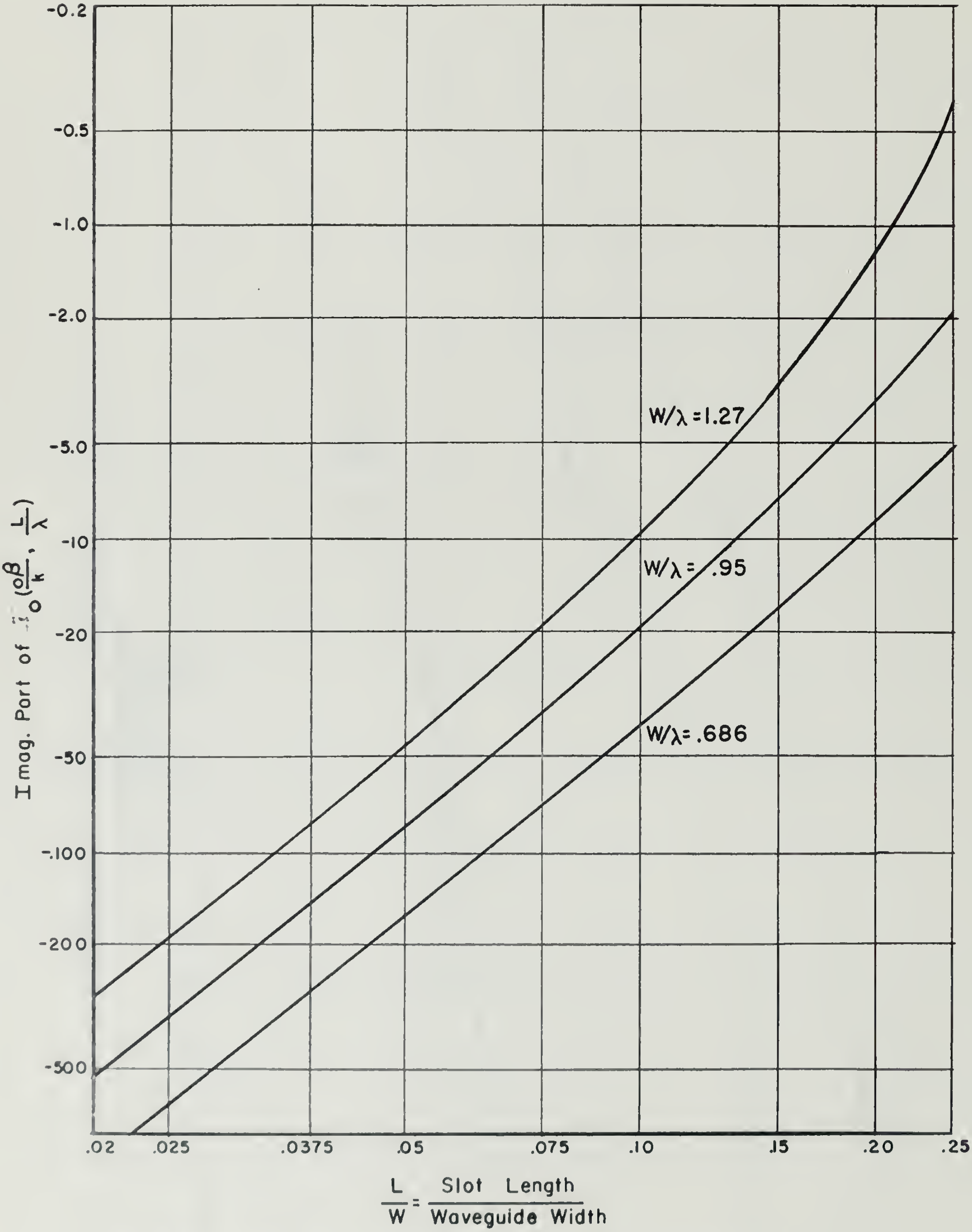

Figure 23 Imaginary Part of I_0 $(_0\beta/k,\ L/\lambda)$ versus L/W for $.02 \leq L/W \leq 0.25$

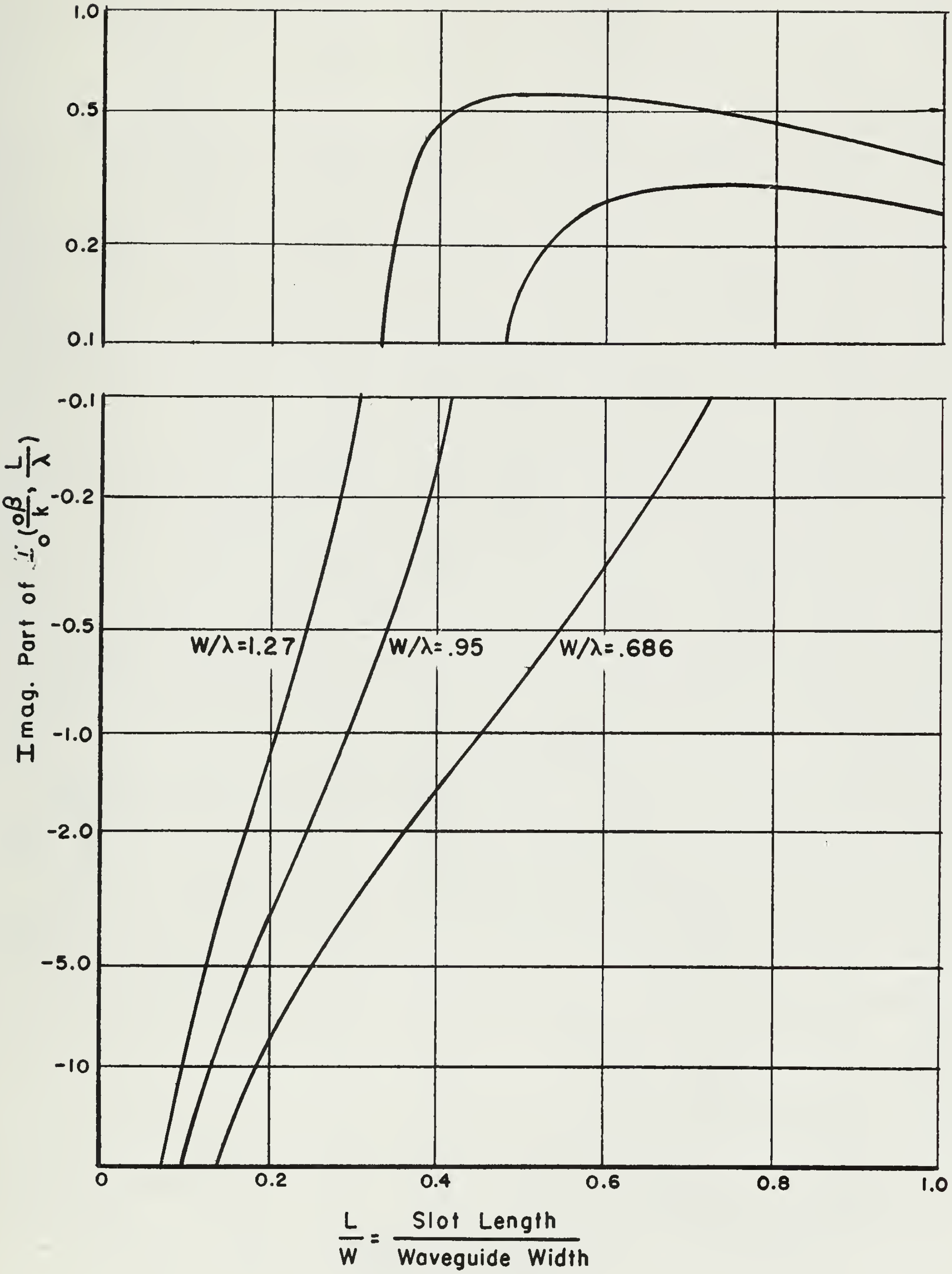

Figure 24. Imaginary Part of I_0 $({}_0\beta/k,\ L/\lambda)$ versus L/W for $0.2 \leq L/W \leq 1.0$

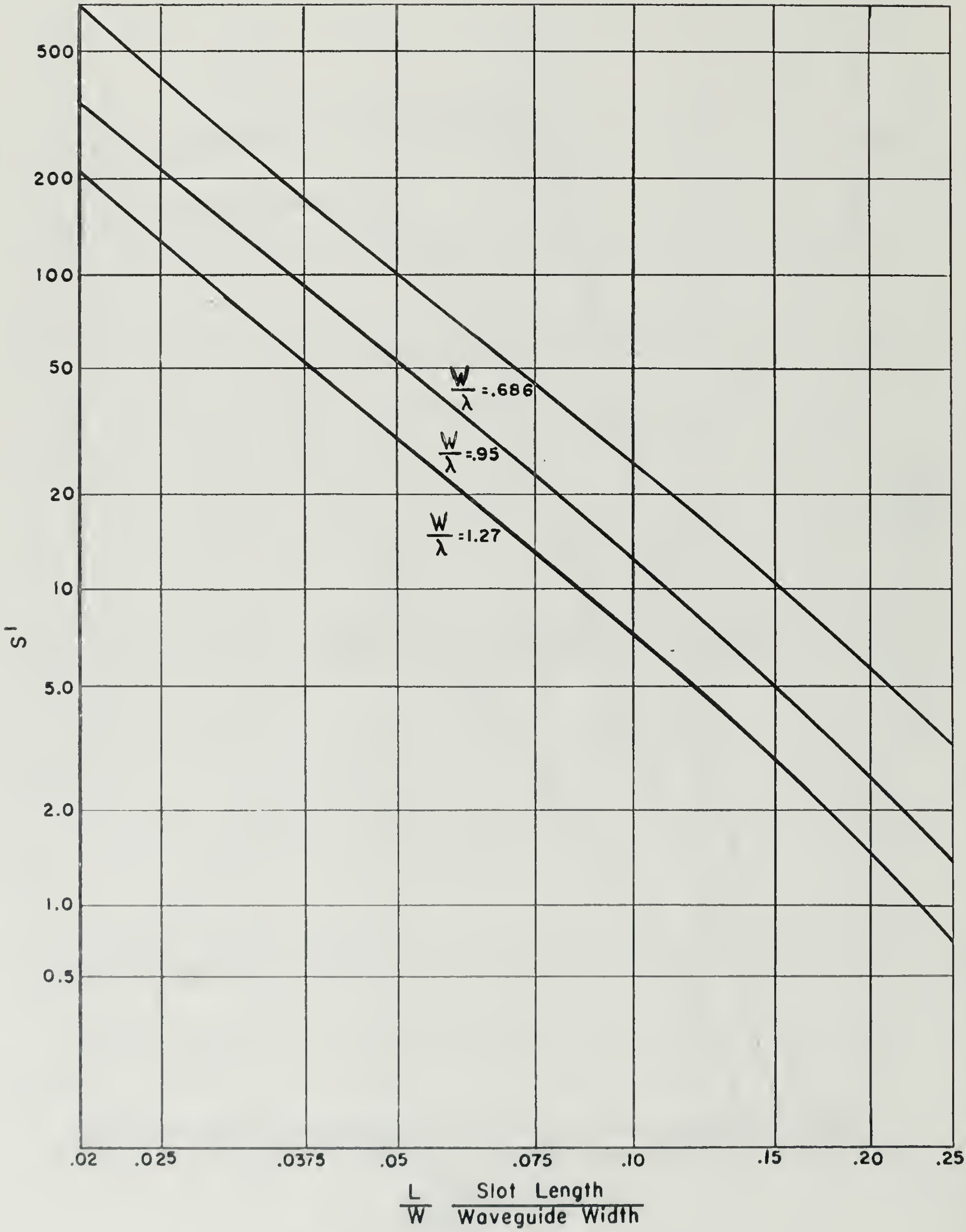

Figure 25 $S' = \sum_{m=3}^{\infty} \frac{\cos^2 \frac{m\pi L}{2W}}{\left(1 - \frac{m^2 L^2}{W^2}\right)^2} \frac{\left(\frac{m^2\lambda^2}{4W^2} - 1\right)}{(m^2 - 1)^{\frac{1}{2}}}$

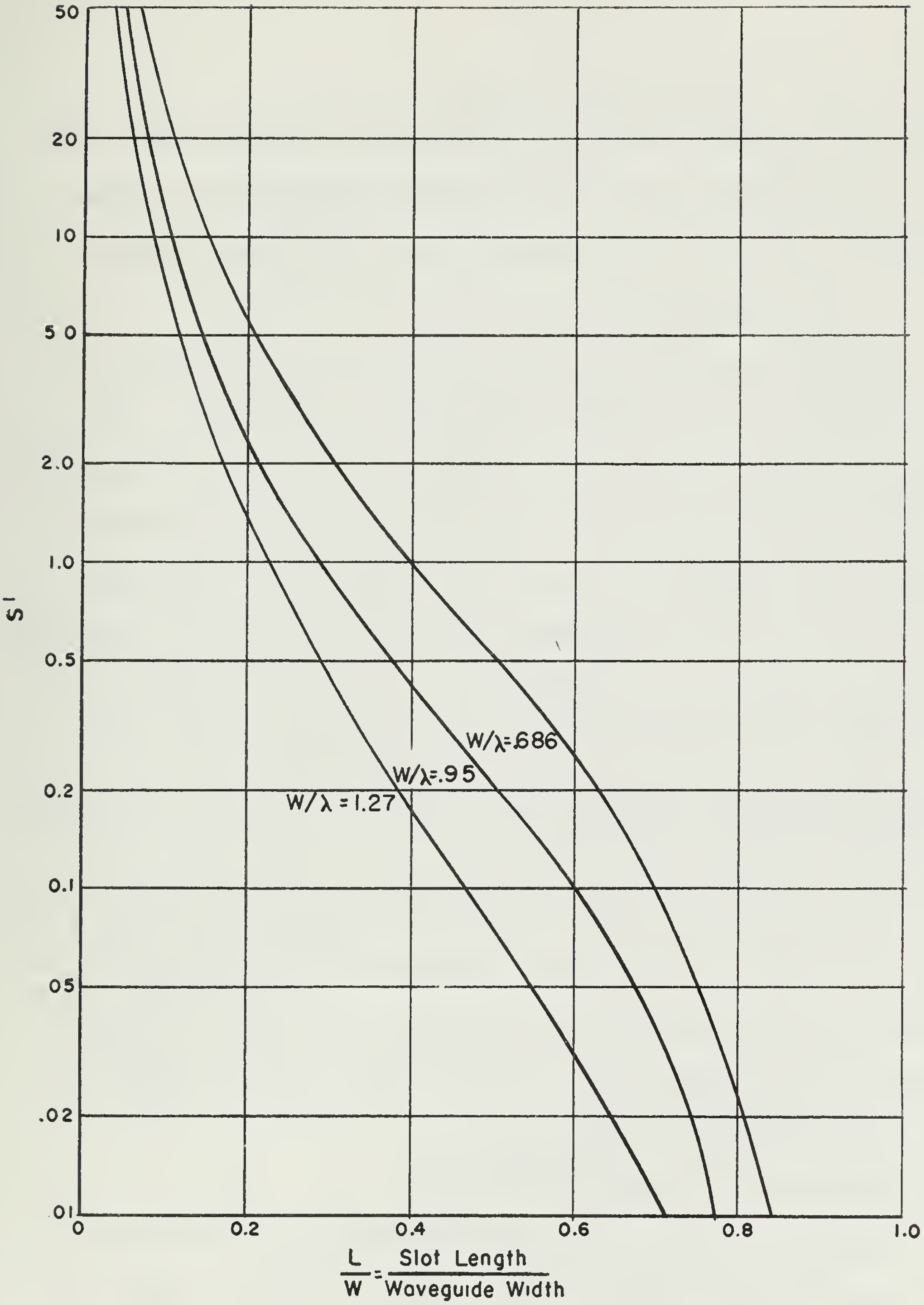

Figure 26 $$S' = \sum_{m=3}^{\infty} \frac{\cos^2 \frac{m\pi L}{2W}}{\left(1-\frac{m^2L^2}{W^2}\right)^2} \; \frac{\left(\frac{m^2\lambda^2}{4W^2}-1\right)}{(m^2-1)^{\frac{1}{2}}}$$

Figures 27-30. Convergence of the iterative process was sufficiently rapid that the results for $\delta(\gamma)$ are estimated to be within about 10% of the values obtained by an exact solution of Equation 4-1. Since Equation 4-1 is based on an assumed aperture distribution, further iteration does not appear warranted.

Of some interest is the fact that γ is practically insensitive to variations of L above about $\lambda/2$. Effective control over α thus is obtained only with relatively small values of L. In this connection, it should be noted that for $L < \lambda/2$, α is quite sensitive to finite values of wall thickness, because of the evanescence of the fields in the slot region. Thus for cases of moderate wall thickness, significant discrepancies may exist between the actual values of α and those predicted by the approximate analysis. The experimental data given in Figures 27-30 were obtained under an effective condition of vanishingly small wall thickness (see Section 5.1)

The technique of aperture illumination control is as outlined in Section 3.3. Since in the case of infinitesimal slot spacing, there is no essential difference between the results obtained with the transversely slotted and the axially slotted guides, detailed examples of this application are not necessary.

4.3 Surface Wave Solution

Equation 4-1 admits an unattenuated surface wave solution for L less than a critical value near $\lambda/2$. As in Section 3.5, assume $\gamma/k = c/v > 1$.

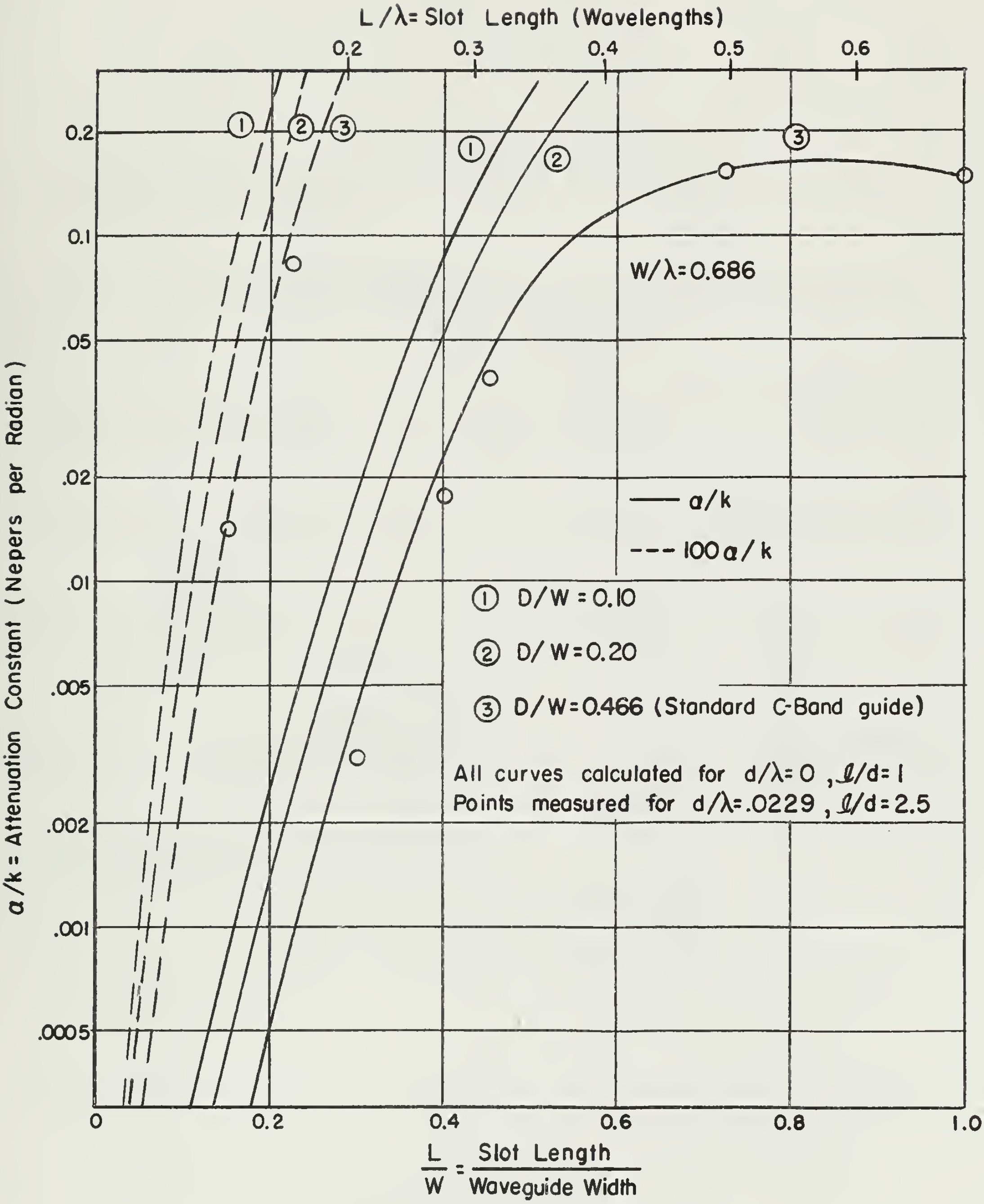

Figure 27 Attenuation Constant versus Slot Length for Infinitesimally Spaced Slots, W/λ = 0.686

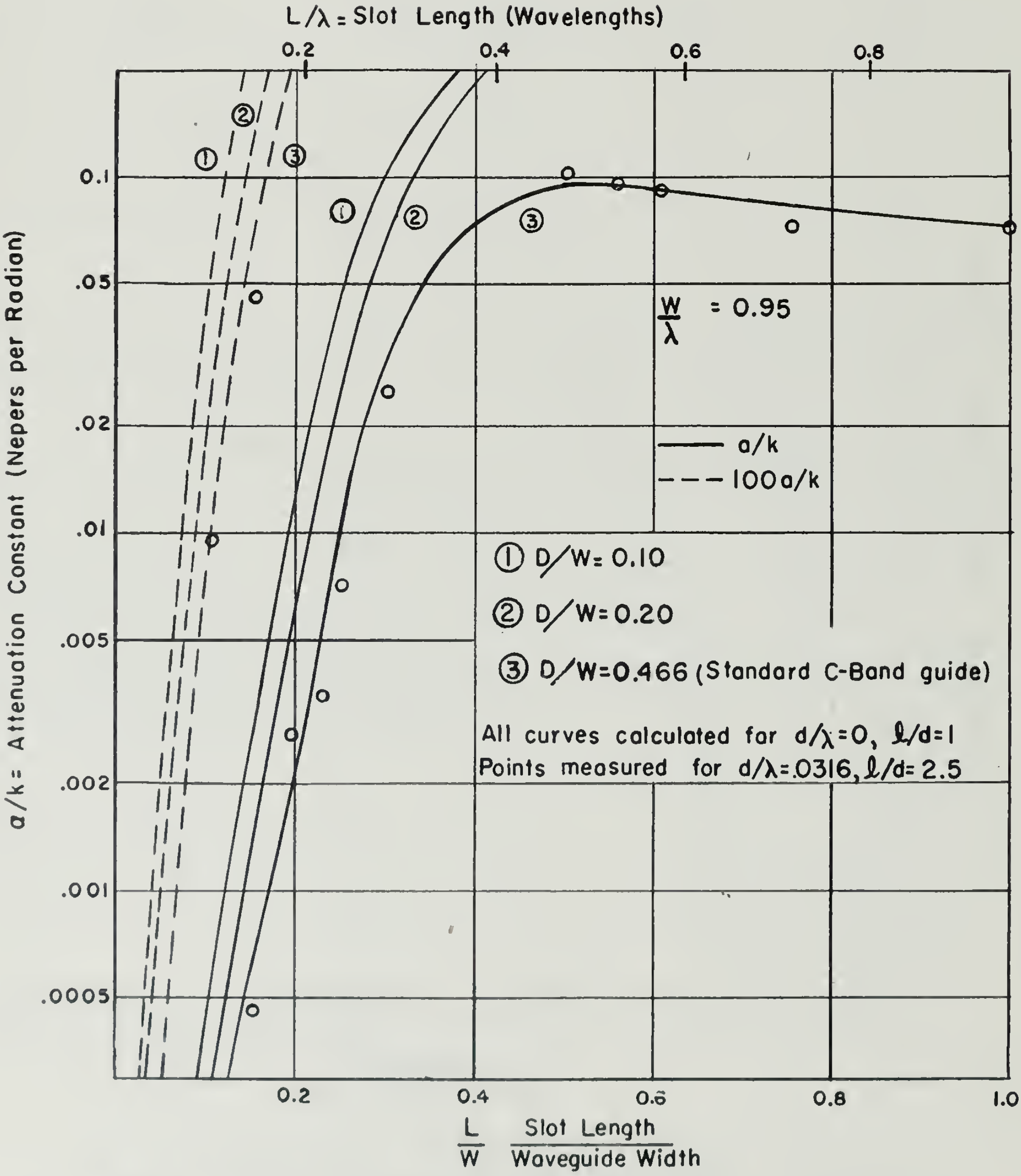

Figure 28 Attenuation Constant versus Slot Length for Infinitesimally Spaced Slots, W/λ ≐ 0.95

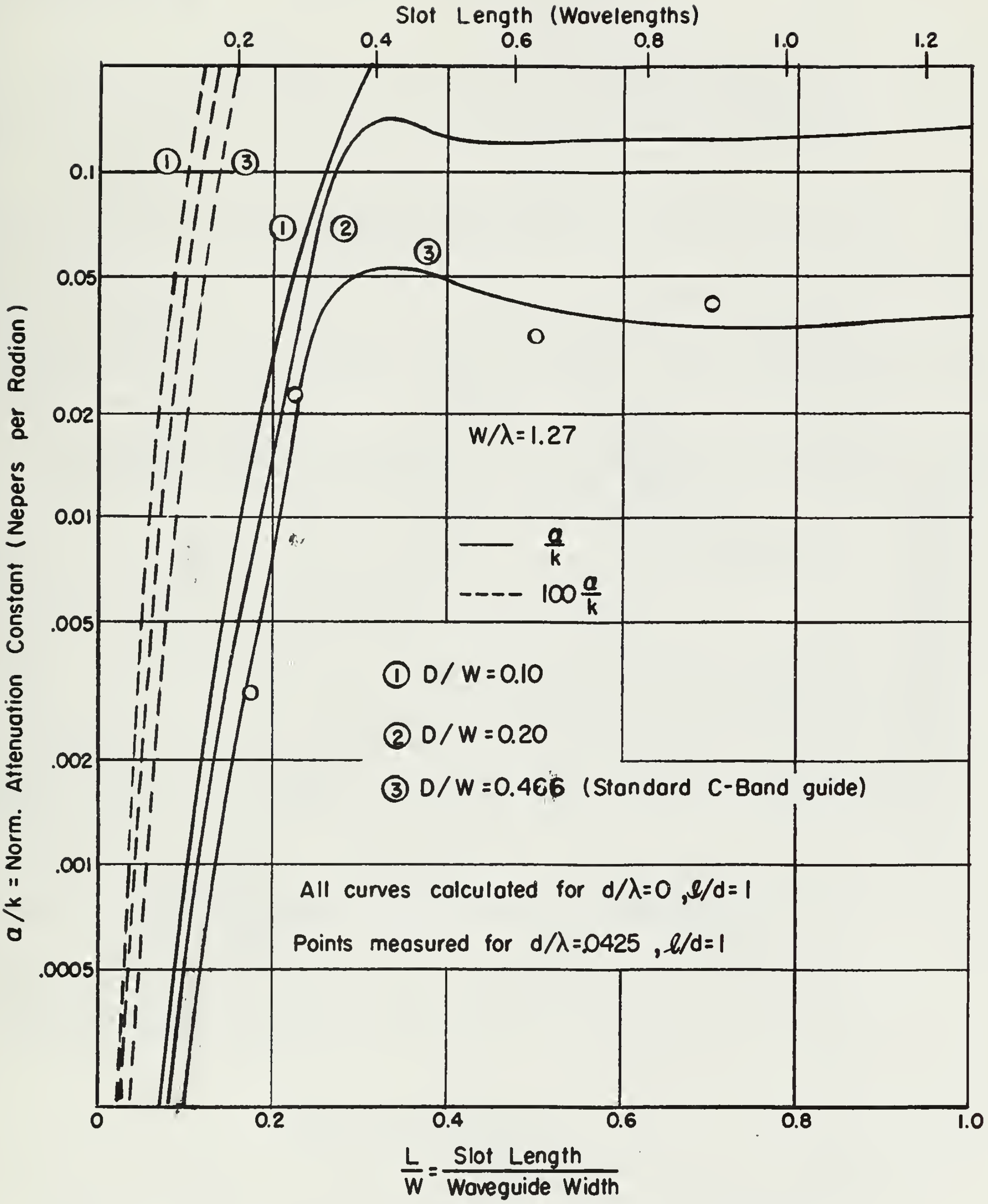

Figure 29 Attenuation Constant versus Slot Length for Infinitesimally Spaced Slots. W/λ = 1.27

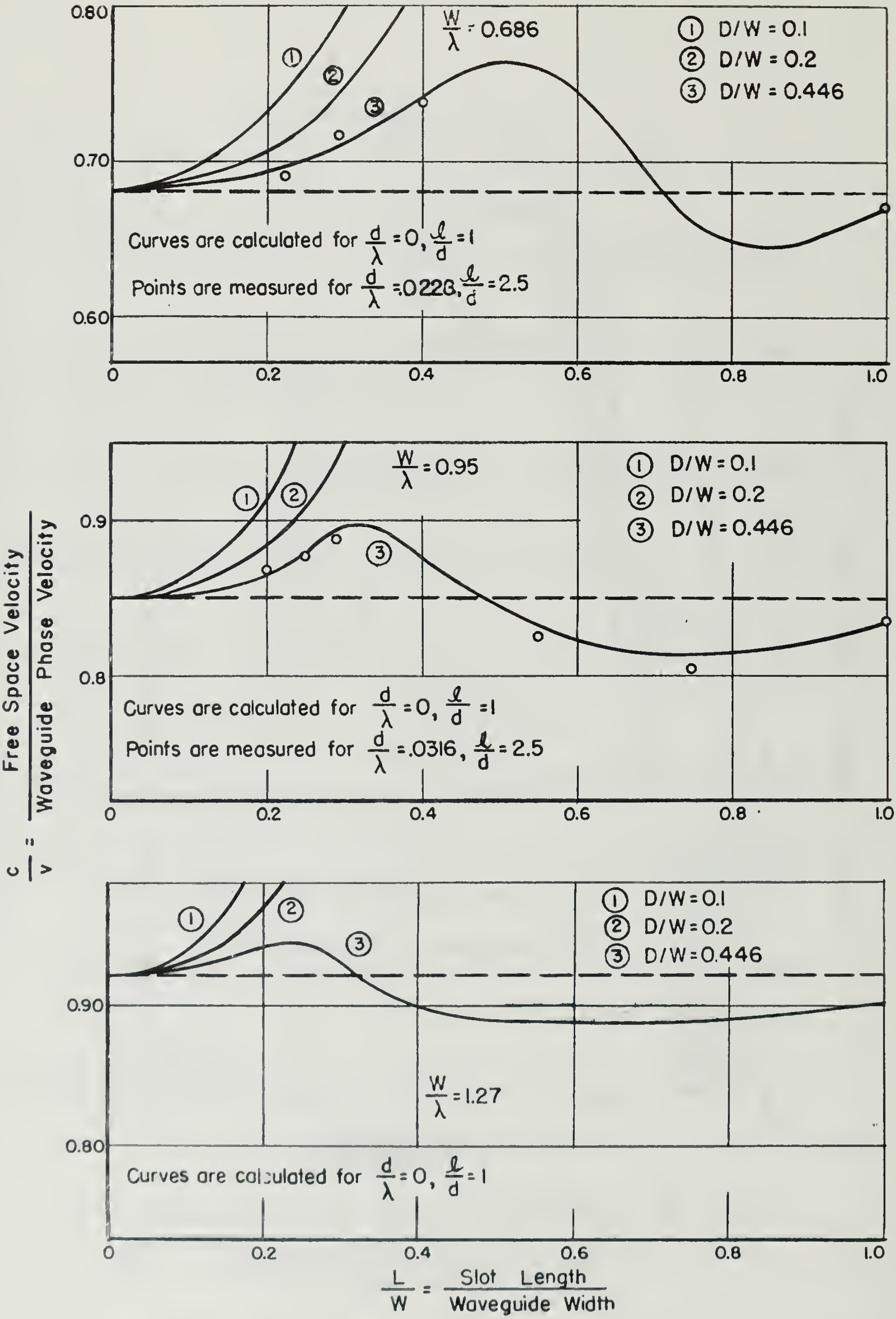

Figure 30 Velocity Ratio versus Slot Length for Infinitesimally Spaced Slots.

Then

$$\beta = -j\,\sigma = -j\,k\sqrt{(c/v)^2 - 1},$$
$$\kappa = -j\,\zeta = -j\,k\sqrt{(c/v)^2 + (\lambda/2W)^2 - 1}.$$

With these substitutions, Equation 4-1 becomes

$$\frac{\coth \zeta D}{\zeta D} = \frac{(1-L^2/W^2)^2}{\cos^2(\pi L/2W)}\ \frac{1}{1-(\lambda^2/4W^2)}\ \frac{\lambda}{2\pi D}\sum_{m=3}^{\infty}\left(\frac{m^2\lambda^2}{4W^2} - 1\right)\frac{\cos^2(m\pi L/2W)}{(1 - m^2L^2/W^2)^2}\ \frac{k}{\zeta_m}.$$

$$\cdot \coth \zeta_m D + j\,\frac{\pi W}{16D}\ \frac{[1-(L^2/W^2)^2]}{\cos^2(\pi L/2W)}\ \frac{1}{[1-(\lambda^2/4W^2)]}\ I_o(-j\,\frac{\sigma}{k}, \frac{L}{\lambda}), \qquad (4\text{-}4)$$

where

$$\zeta_m = k\sqrt{(c/v)^2 + (m\pi/2W)^2 - 1}.$$

Since $c/v > 1$, the perturbation of c/v from that of the $TE_{1,0}$ closed waveguide mode is in most cases relatively large. Hence the iterative method of solution using Equation 4-3 is of little value, while the direct solution of Equation 4-4 is quite tedious. However, an asymptotic expression valid for small L/λ which is a slight extension of Equation 3-17 is easily developed.

From Equations 3-14, 15, Section 3.4, we have as $c/v \to 1$,

$$\frac{\coth \zeta D}{\zeta D} \simeq \frac{\coth(\pi D/W)}{\pi D/W},$$

$$I_o\left(-j\,\frac{\sigma}{k}, \frac{W}{\lambda}\right) \simeq -j\,\frac{2}{\pi}\left\{(1.273)\left[\bar{\gamma} + \ln \frac{\sigma}{k}\frac{L}{\lambda}\right] - .807 + 1.215\,\frac{\lambda^2}{4W^2}\right\},$$

$$\sigma = k\sqrt{(c/v)^2 - 1} \simeq k\sqrt{2(c/v - 1)}.$$

Substitution into Equation 4-4 gives

$$\frac{\coth \pi D/W}{\pi} \frac{\cos^2(\pi L/2W)}{\left[1-(L^2/W^2)\right]^2}\left[1-(\lambda^2/4W^2)\right] \simeq \lambda/2\pi W \quad S + \frac{1}{8}\left\{1.273\left[\bar{\gamma} + \tfrac{1}{2}\ln\left(\frac{c}{v}-1\right) + - \tfrac{1}{2}\ln\frac{\lambda^2}{4L^2} - \tfrac{1}{2}\ln 2\right] + .807 + 1.215\,\frac{\lambda^2}{4L^2}\right\},$$

where S has been written for the infinite summation over m. Simplifying,

$$c/v = 1 + \exp\left\{.808 - (2\lambda/W)\,S - 1.91\left(\lambda^2/4L^2\right) + \ln\left(\lambda^2/4L^2\right) + 4\left[1-(\lambda^2/4W^2)\right] \cdot \frac{\cos^2(\pi L/2W)}{\left[1-(L^2/W^2)\right]^2}\coth \pi D/W\right\}. \tag{4-5}$$

From Equation 4-4, S increases indefinitely for fixed L/W as $W/\lambda \to 0$. Thus, since $c/v \to 1$ as $\omega \to 0$, there is no lower frequency limit for propagation of this mode. Similarly, from Figure 25, S increases without limit as $L/W \to 0$. Thus for fixed W and D, the mode continues to propagate as $L \to 0$. However, for $L \ll \lambda/2$, the fields are quite loosely bound to the aperture surface with the principal energy content being in the external region. Under this condition, the mode is inappreciably excited by an incident internal $TE_{1,0}$ field.

The sequence of axial field distribution diagrams in Figures 31-32 gives an indication of the relative excitation of the surface wave and the fundamental modes as L/λ is increased, frequency and all other dimensions being held constant. Presence of the surface wave is indicated by the deviation of the measured db field amplitude from a straight line dependence on axial distance. For these curves, the field amplitude was measured at the back wall of the waveguide. The E_x component of the surface wave varies approximately as $e^{\zeta x}$ as $x \to -D$, while the

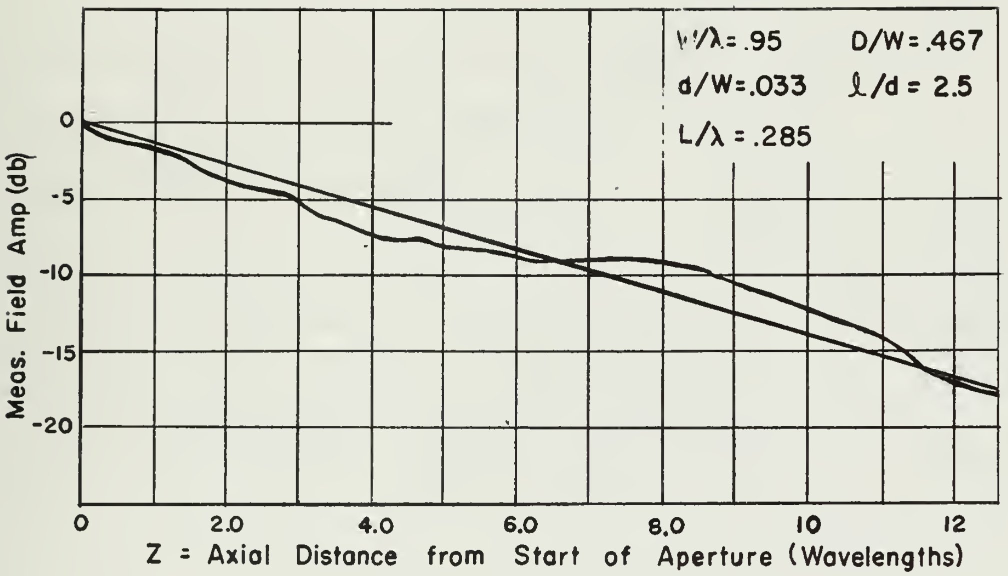

a) L/λ = .285

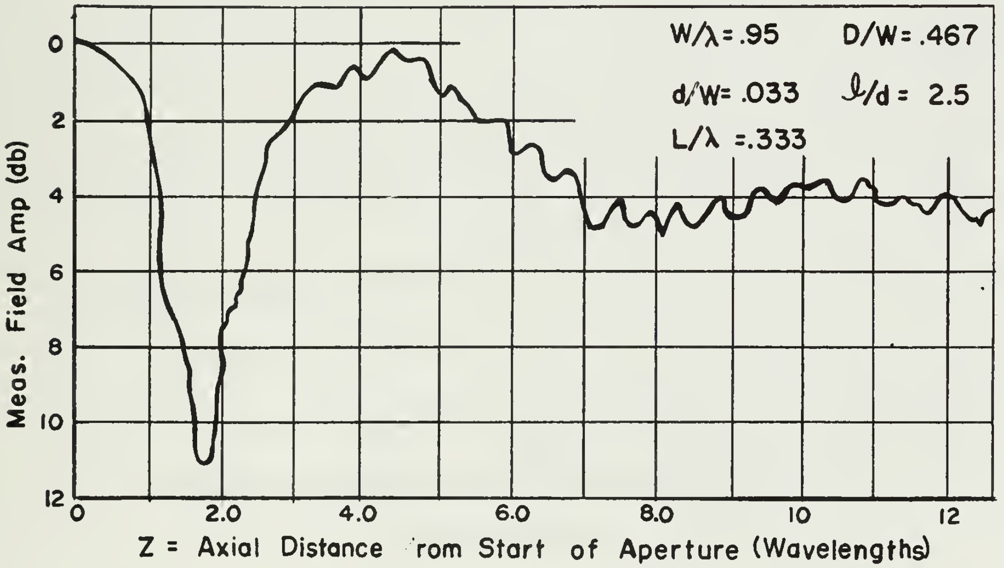

b) L/λ = .333

Figure 31. Measured Axial Amplitude Distributions with Fundamental and Surface Wave Modes Present. (Also see Figure 32.)

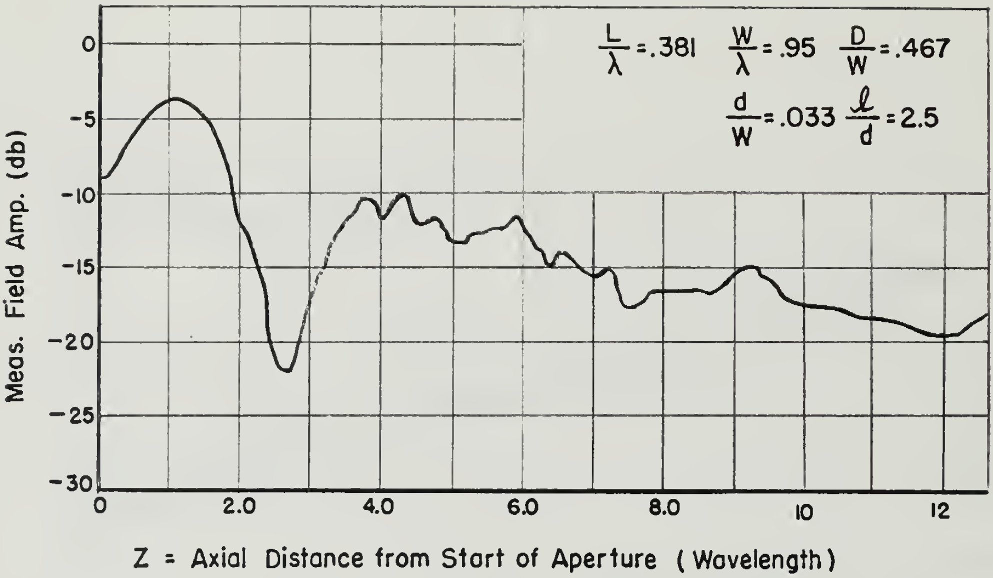

c) L/λ = .381

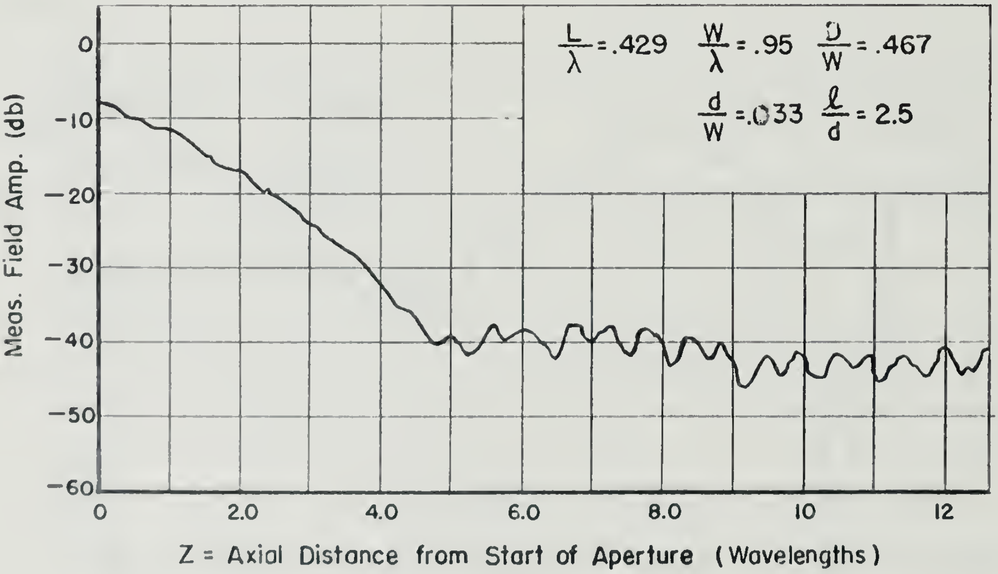

d) L/λ = .429

Figure 32. Measured Axial Amplitude Distributions with Fundamental and Surface Wave Modes Present

same component of the fundamental mode reaches a maximum at the point of measurement. Thus, since ζ increases with increasing L/λ, the apparent decrease in excitation of the surface wave mode after L exceeds about 0.3 λ is somewhat exaggerated.

A more reliable indication of the process is given by the radiation patterns ($\varphi = 0$, E_θ polarization) in Figure 33. Frequency is varied with all other dimensions held constant. The presence of the surface wave is indicated by the appearance of a second lobe near $\theta = 0$ in pattern 33b, and by the interference pattern in 33c. In 33d, for $L = .45\lambda$, evidence of the surface wave has again disappeared. From this sequence, it appears that for these particular transverse dimensions, excitation of the surface wave reaches a maximum for L near $.35\lambda$.

A possible reason for the peak in the relative excitation of this mode can be drawn from curve 3 in Figure 30b, for which the transverse waveguide dimensions are approximately the same as for the patterns in 33b, c. The velocity ratio c/v for the fundamental mode reaches a maximum for $L = .34\lambda$. Since c/v has been increased from its unperturbed value, the fields for the fundamental mode are evanescent with x, i.e., decay approximately exponentially as $x \to -D$. Thus the transverse distribution of the internal fields of the fundamental mode most closely approaches that of the surface wave mode when $L \simeq .34\lambda$, and the relative excitation of the latter mode is thus increased in this region.

Following the same reasoning, it would appear from curves 1 and 2 in Figure 30b that excitation of the surface wave would be further

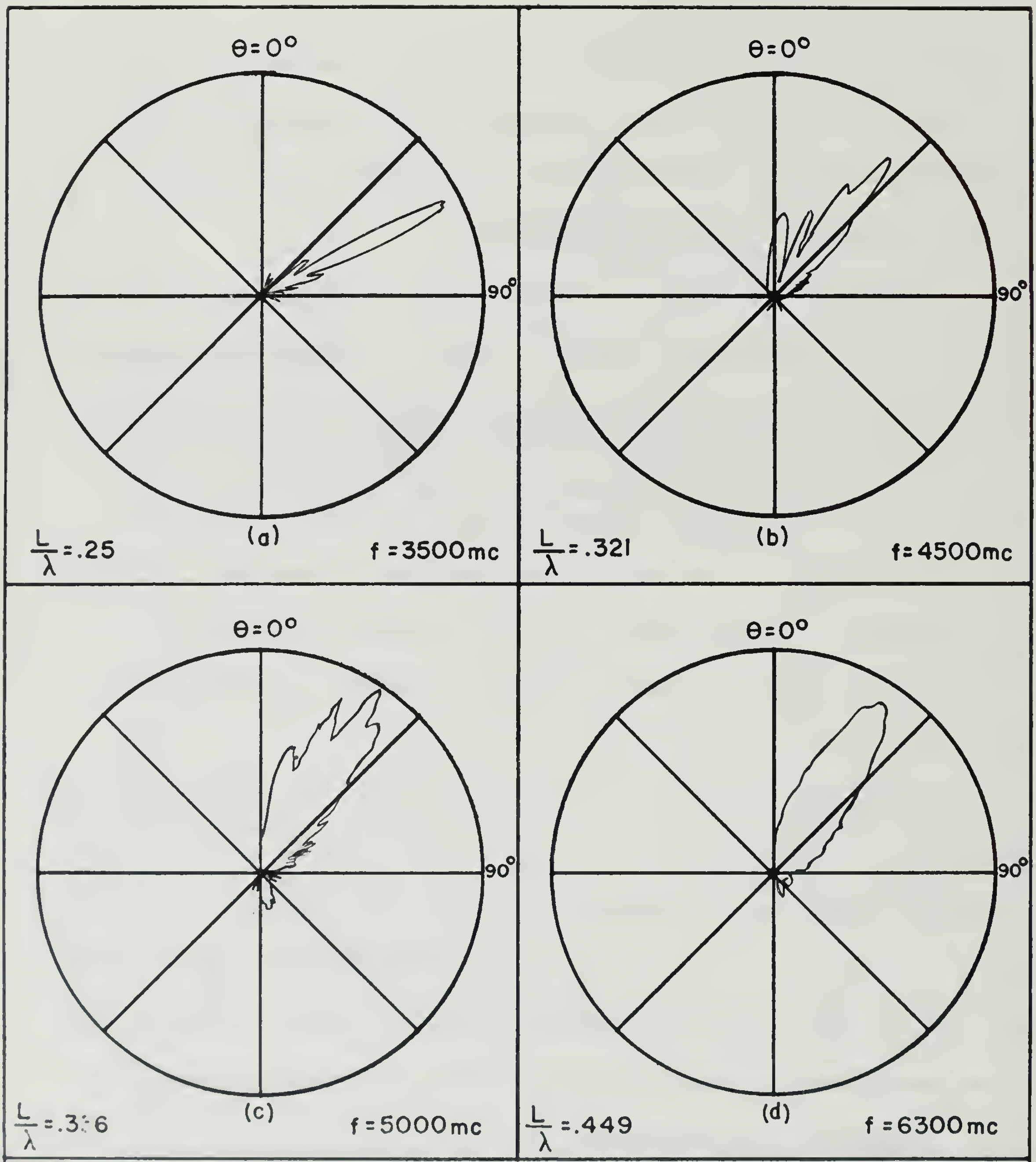

W=4.76 cm D=2.22 cm L=2.14 cm d=.397 cm $\ell/d=2.5$ $\mathcal{L}=76$ cm

All patterns are voltage measurements with $\phi=0^\circ$.

Figure 33 E-Plane Radiation Patterns Showing Relative Excitation of Surface Wave versus L/λ as Frequency is Varied

increased by a reduction in D, since this results in a greater perturbation of c/v for the fundamental mode. The patterns in Figure 34, with (c) and (d) being obtained with decreased D/λ, show this to be the case. In addition, patterns (a) and (c) indicate excessive c/v ratio of the surface wave for the given aperture length, L. Patterns (b) and (d) are for the same conditions as, respectively, (a) and (c), except for a reduction in L/λ.

Alternatively, when effective suppression of the surface wave mode is required, L must be held to relatively small values. The upper limit is dependent on the transverse dimensions of the waveguide. For $D/W = .467$, $L = 15\lambda$ and for uniform L/λ, approximately 12db suppression of the end-fire lobe is obtained with $L \leq .27\lambda$ for $W = .7\lambda$, or with $L \leq .18\lambda$ for $W = 1.4\lambda$. The result is an effective upper limit on the value of α which may be obtained. For use in antennas of short aperture length where relatively high α is required, control by means of variation of ℓ/λ is to be preferred (Section III).

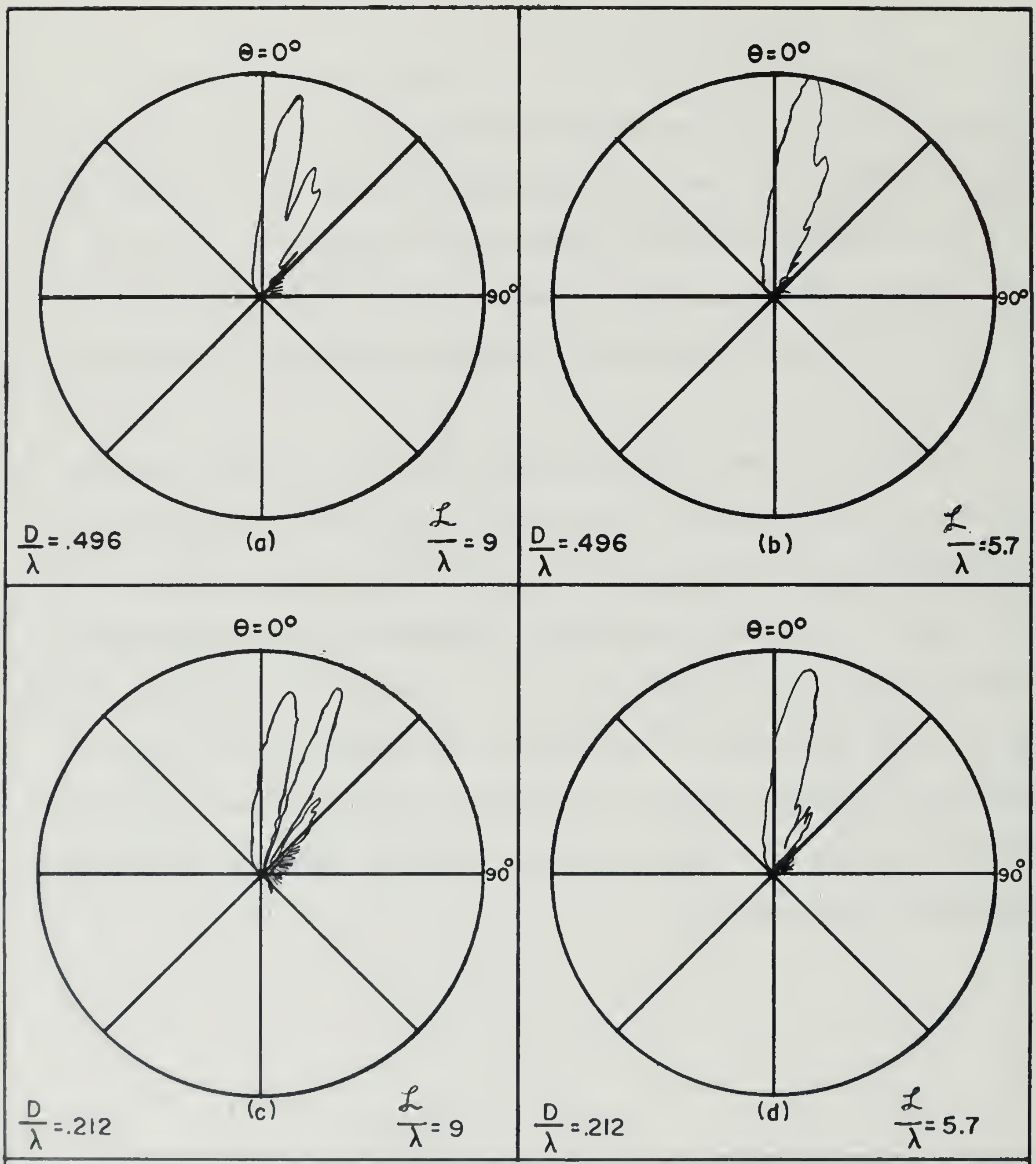

$W/\lambda = 1.06$ $L/\lambda = .32$ $d/\lambda = .035$ $\ell/d = 2.5$

All patterns are voltage measurements with $\phi = 0°$

Figure 34 E-Plane Radiation Patterns Showing Increase in Surface Wave Excitation with Decrease in D/λ

V. EXPERIMENTAL VERIFICATION OF THE THEORY

The validity of the approximate theory was checked by measurements of the propagation constant on a laboratory model. The results of these measurements were reported in previous sections. A brief discussion of the experimental procedure is included below.

5.1 Details of Construction of the Model.

A view of the model including the important dimensions is given in Figure 35. All measurements were performed in the 2-7 kmc frequency range.

Sectional construction of the model was employed in order to allow variations in the transverse dimensions of the waveguide. In the course of assembly, the interior seams which resulted were covered with adhesive-backed aluminum foil tape.

The slots were milled in a separate 1/32 inch thick aperture plate. In order to reduce the number of mechanical operations, the slots were cut in each case to a uniform length equal to the width of the assembled waveguide. The effective slot length was then varied by masking part of the outside surface of the aperture plated with foil tape. While the actual thickness of the aperture plate was about .02λ at 7 kmc, it should be noted that for small L/W, the masking process gave an effective wall thickness which was considerably less and roughly corresponded with the 10^{-3} inch thickness of the foil.

The fields were probed at discrete intervals through a series of closely spaced holes located along the center of the back wall of the

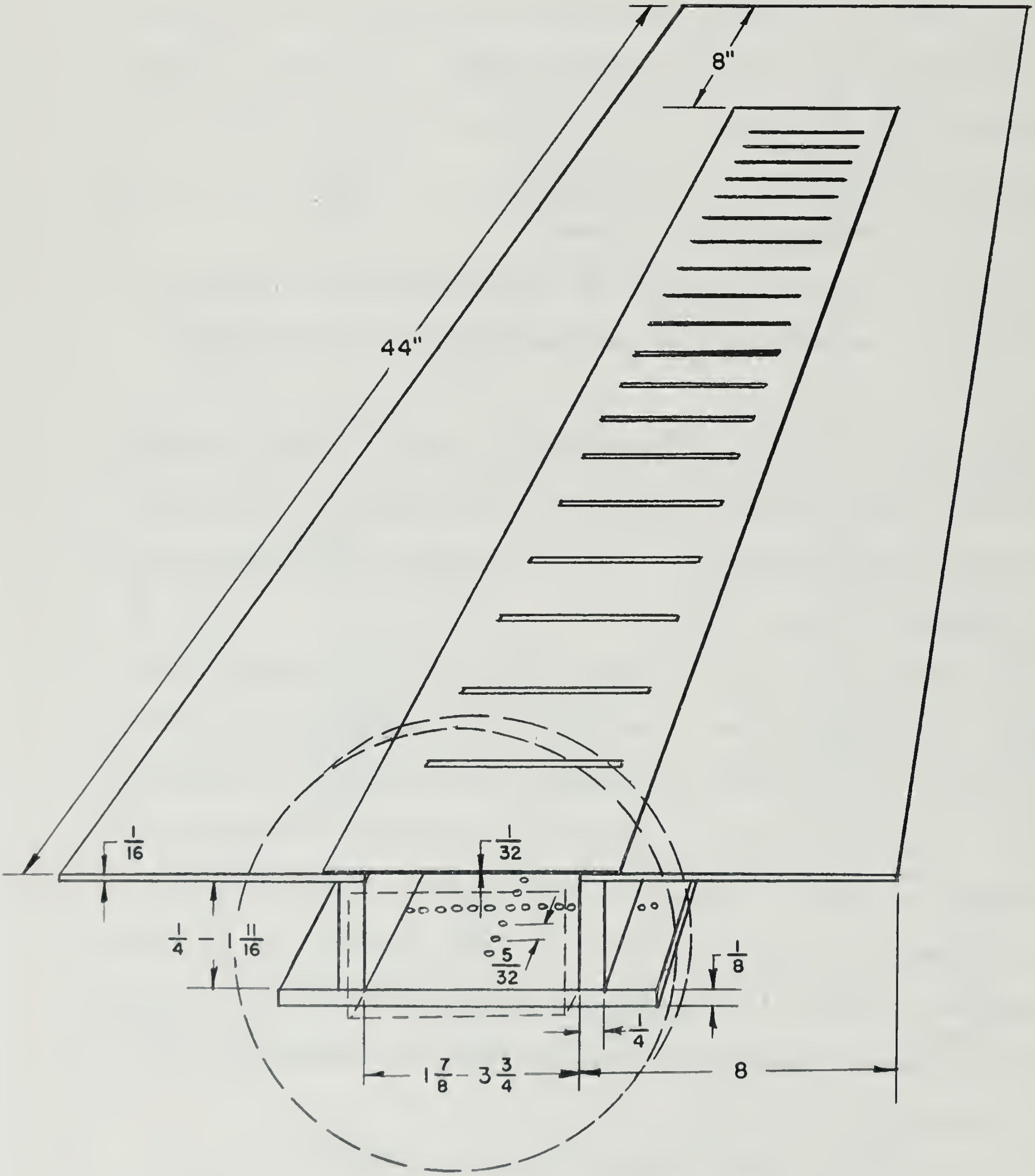

Figure 35. The Experimental Model

waveguide, as shown in Figure 34. The use of an array of holes instead of the usual longitudinal slot improved the mechanical stability of the model and eliminated the possible excitation of an asymmetrical slot mode resulting from a dissymmetrical location of the slot. At several points along the guide axis, transverse arrays of holes were provided to enable observation of the transverse distribution of the fields. Since the thickness of this back wall was somewhat greater than the hole diameter, radiation losses through the holes were negligible.

5.2 Measurement of γ in Cases of Large α.

Two separate procedures were employed in the measurement of γ. Under conditions where α was relatively large, the slotted waveguide was terminated in a matched load to give an approximately pure exponential mode of propagation. The value of γ was then obtained from direct phase-amplitude field measurements along the axis of the guide. As a general rule, this method was employed in those cases for which the reported value of $\frac{\alpha}{k}$ was greater than .005. A schematic diagram of the phase comparison setup employed in the measurement of the phase velocity appears in Figure 36. The principal limitation on the accuracy of this method arose from the occasional presence of extraneous surface wave modes. In these cases, the measured phase and db amplitude of the fields did not bear their usual linear relationship with axial distance, and an accurate determination of γ was not possible.

Under conditions of single mode propagation, the experimental values of γ are believed to be accurate to within about 5%. Under conditions favorable for the excitation of surface waves, in particular for $1.3\,\lambda \leq W \leq 1.5\,\lambda$ for the results in Section III, and for $0.3\lambda \leq L \leq 0.5\lambda$

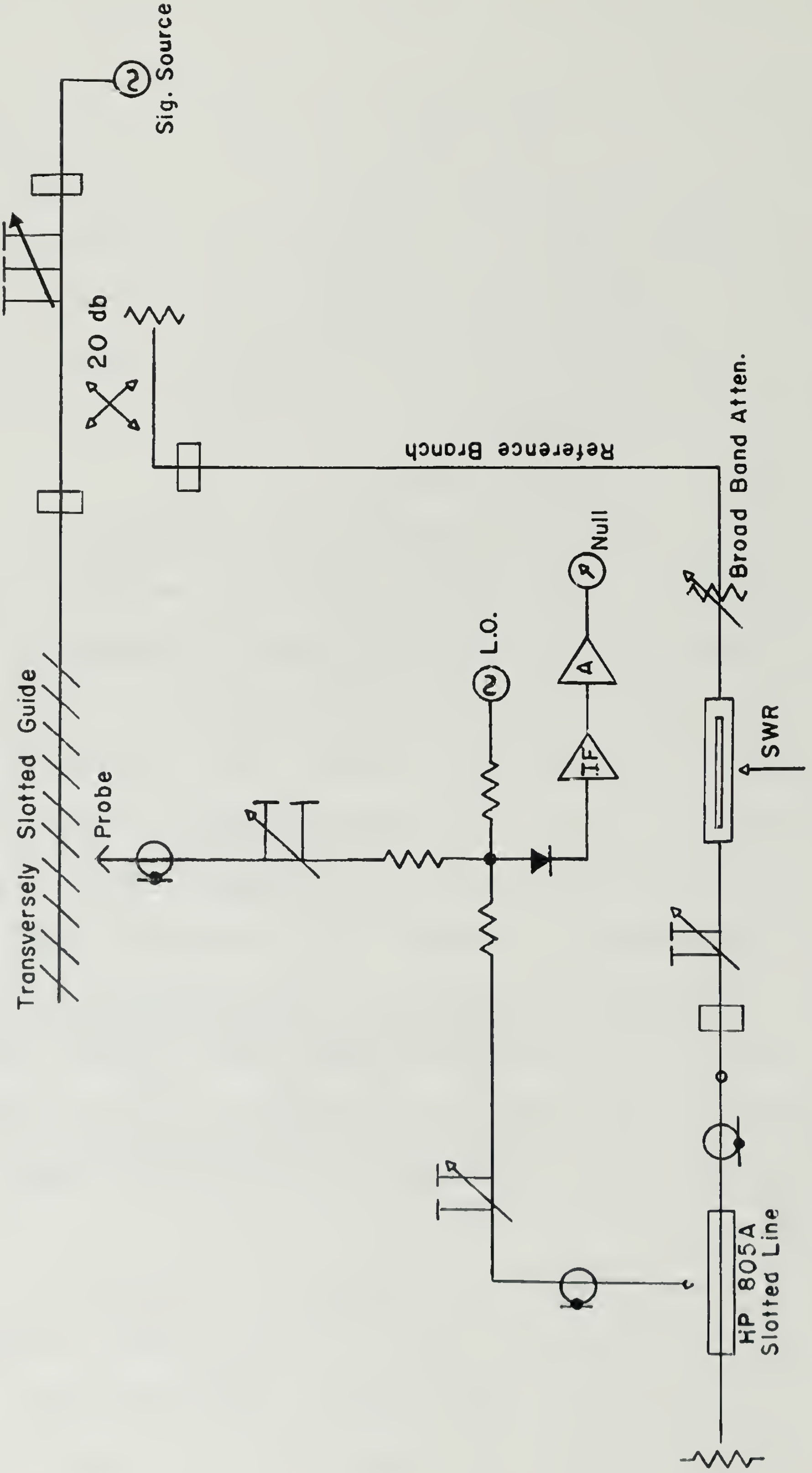

Figure 36. Schematic of Experimental Setup for Phase — Amplitude Measurements

for the results in Section IV, the accuracy is somewhat less.

5.3 Measurement of γ in Cases of Small α.

For the cases of small L/W in Section IV where the reported value of $\frac{\alpha}{k}$ was less than approximately .01, α was determined indirectly from a standing-wave-ratio measurement. For this case, the transversely slotted waveguide was terminated in a short circuit, and the input voltage-standing-wave-ratio (VSWR) was measured at a point prior to the beginning of the aperture. Since this method assumes negligible reflections at the beginning and end of the aperture, the magnitudes of these discontinuities were reduced by tapering the slot length gradually from zero to the desired L over a short distance at the aperture end points. The residual VSWR (measured with the waveguide terminated in a matched load beyond the end of the aperture) was then found to be less than 1.03 for all cases of interest.

Since the tapered endpoints contributed an unknown amount to the total radiation loss, the short circuit VSWR measurements were performed for two cases of differing lengths of the uniform portion of the aperture. In addition, conductivity losses were approximately taken into account by performing a third short circuit VSWR measurement with the aperture completely covered over. Assuming that the conductivity losses are only slightly affected by the presence of the slots, and assuming that the radiation losses from the uniform portion of the aperture are directly proportional to the aperture length, these three measurements gave a corrected radiation loss for a length of uniform aperture.

The value of α determined in this way is estimated to be accurate to within about 10% for the largest values of α reported ($\frac{\alpha}{k}$ of the order of .01) and about 20% for the smallest.

For convenience, the associated value of c/v in these cases was determined from the distance between two well spaced minima measured along the aperture under short circuit conditions. Since observation of the fields was possible only at discrete intervals, the exact location of the minimum was estimated from plots of the measured amplitude distribution. The values of c/v so derived are estimated to be accurate to within about 5%.

VI. CONCLUSIONS AND RECOMMENDATIONS FOR FURTHER INVESTIGATION

The propagation constant of the transversely slotted waveguide can be effectively controlled through the variation of the transverse dimensions of the waveguide and the dimensions and spacing of the slots. Thus, for antenna applications, the aperture illumination can be adjusted by appropriately varying these parameters. The phase velocity is affected primarily by the waveguide width and to the first order is independent of the slot length and spacing and of the waveguide depth. The attenuation constant is primarily a function of the latter three parameters, being to the first order independent of the waveguide width.

The normalized attenuation constant, α/k, is strongly dependent on the slot length, L, for $L < \lambda/2$. Above this point, α/k is practically insensitive to further increase of L. The maximum α/k obtainable in this manner is of the order of 0.1 for a standard waveguide aspect ratio. However, in the usual case where single mode propagation is required, the existence of a surface wave, which is strongly excited for L of the order of $.35\lambda$, imposes a further limitation of about .01 on the maximum value of α/k obtainable. While decreasing the waveguide depth, D, gives an increase in α/k for a fixed L, it also tends to increase excitation of the surface wave, so that this method is of little value in extending the upper range of α/k. Instead, increased α/k can be obtained by employing the slot spacing as the controlling parameter with $L > \lambda/2$, since the surface wave does not exist for L in this range. Since α/k is approximately independent of L for $L > \lambda/2$, the results for the particular case of L equal to the waveguide width, W, are sufficiently general. In this case the range of α/k for variation of the slot spacing, ℓ, alone is about 10:1, although α/k can be increased without limit by decreasing D. The minimum value of α/k obtainable for L=W is of the order of .01, which roughly corresponds with the upper limit imposed by the existence of the surface wave when $L > \lambda/2$. Consequently, practically any value of α/k is obtainable if all three parameters are allowed to vary. The remaining parameter, the slot width, has relatively little effect on either α/k or the velocity ratio c/v.

Further investigation of the surface wave supporting properties of the structure is indicated. Of importance are methods of surface wave excitation which give high excitation efficiencies without the need for external launching devices. Alternatively, the characteristics of different periodic coupling mechanisms, e.g., closely spaced circular holes, should be studied from the standpoint of attempting to decrease the surface wave excitation.

Since the pattern of a traveling wave line source is conical when $c/v>1$, a broadside array of slotted waveguides is ordinarily employed to give the required pattern characteristics. Thus, the effect on the propagation constant and on the individual element radiation pattern when several slotted waveguides are in close proximity should be investigated.

Finally, the effects of finite wall thicknesses on the attenuation constant of the fundamental mode and on the excitation and phase velocity of the surface wave should also be considered. This parameter is of particular importance in cases of small slot length.

REFERENCES

1. Goubau, G. " On the Excitation of Surface Waves," *Proceedings of the IRE, Vol. 40, No. 7,* July 1952; p. 865.

2. Whitmer, R.M. " Radiation from a Dielectric Waveguide," *Journal of Applied Physics, Vol. 24, No. 9,* September 1953; p. 949.

3. Zucker, F.J. " The Guiding and Radiation of Surface Waves", *Proceedings of Symposium on Modern Advances in Microwave Techniques",* Polytechnic Institute of Brooklyn, 1954; p. 403.

4. Rotman, W. " A Study of Single Surface Corrugated Guides", *Proceedings of the IRE, Vol. 39, No. 8,* August 1951; p. 952.

5. Elliott, R.S. " On the Theory of Corrugated Plane Surfaces", *Transactions of the IRE, Vol. AP 2,* April 1954; p. 71.

6. Mueller, G.E. " A Broadside Dielectric Antenna," *Proceedings of the IRE, Vol. 40, No. 1,* January 1952; p. 71.

7. DuHamel, R.H., and Duncan, J.W . *A Technique for Controlling the Radiation from Dielectric Rod Waveguides,* Technical Report No. 11, Antenna Laboratory, University of Illinois, Urbana, Illinois, 15 July 1956.

8. Rotman, W. *The Channel Guide Antenna, Report No. E5054,* U.S. Air Force Cambridge Research Laboratories, January 1950.

9. Rumsey, V.H. " Traveling Wave Slot Antennas," *Journal of Applied Physics, Vol. 24, No. 11,* November 1953; p. 1358.

10. Harrington, Roger F. " Propagation Along A Slotted Cylinder", *Journal of Applied Physics, Vol. 24, No. 11,* November 1953; p. 1366.

11. Hines, Rumsey, and Walter " Traveling Wave Slot Antennas", *Proceedings of the IRE, Vol. 41, No. 11, November 1953;* p. 1624.

12. Kelly, K.C. and Elliott, R.S., " Serrated Waveguide, Theory and Experiment", *IRE Convention Record, Part I; Antennas and Propagation,* March 1955; p. 6.

13. Elliott, R.S. *Serrated Waveguide, Part I: Theory,* Technical Memorandum No. 354, Hughes Aircraft Co., Culver City, Cal.

14. Brillouin, L., *Wave Propagation in Periodic Structures,* Dover Publications, Inc., New York, 1953; p. 139.

15. Slater, J.C., *Microwave Electronics,* D. Van Nostrand Co., Inc., New York, 1950; p. 169.

REFERENCES (CONTINUED)

16. Schelkunoff , S.A., *Electromagnetic Waves,* D. Van Nostrand,Co., Inc., New York, 1943; p. 413.

17. Saxon, D S *Notes on Lectures by Julian Schwinger,* Massachusetts Institute of Technology, Cambridge, Mass., February 1945.

18. Morse and Feshbach, *Methods of Theoretical Physics, Section 9.4,* McGraw-Hill Book Co., Inc., New York, 1953.

19. Ibid, p. 1109

20. Rumsey, V.H. " Reaction Concept in Electromagnetic Theory" *Physical Review, Vol. 94, No. 6,* 15 June 1954; p. 1483.

21. Woodward, P.M. " A Method of Calculating the Field Over a Plane Aperture Required to Produce a Given Polar Diagram", *Journal of the IEE, Vol. 93, Part IIIa, No. 10,* March 1946; p. 1554.

22. Dunbar, A.S. *A Method for the Calculation of Progressive-Phase Antennas for Shaped Beams, Technical Report No. 10,* Stanford Research Institute, June 1950.

23. Rumsey, V.H. *Traveling Wave Slot Antennas,* Report No. 486-10, Ohio State University,Research Foundation, Antenna Laboratory, June 1953.

24. Montgomery, C.G., *Technique of Microwave Measurements,* McGraw-Hill Book Co., Inc., New York, 1947; p. 819.

25. Watson, G.N. *Theory of Bessel Functions,* The Macmillan Co., New York, 1944; p. 338.

26. Jahnke and Emde, *Tables of Functions,* Dover Publications, Inc., New York, 1945; p. 273.

APPENDIX A

PROOF OF THE STATIONARY PROPERTIES OF EQUATIONS 2-18 AND 2-21.

From Equation 2-18,

$$\iint_S h(s') h^*(s) K(s/s') \, ds \, ds' = 0, \qquad \text{(A-1)}$$

where S denotes the slot region and where s and s′ have been written for y, z and y′, z′, respectively.

Assume h differs from g by a small amount, i.e.,

$$h(s') = g(s') + \eta(s'),$$
$$h^*(s) = g^*(s) + \eta^*(s),$$

where η is small in absolute value. Let $K_a(s/s')$ be the kernel when the parameter γ has the value γ_c which satisfies Equation A-1. Thus

$$0 = \iint_S [g(s') + \eta(s')][g^*(s) + \eta^*(s)] K_a(s/s') \, ds \, ds'. \qquad \text{(A-2)}$$

Let

$$K_a = K_c + \frac{\partial K_c}{\partial \gamma} \delta\gamma + K. \; . \; . \; ,$$

where K_c is the kernel when γ has the correct value γ_c given by an exact solution of Equation 2-15. Substitution into Equation A-2, expanding, and neglecting terms of second order or greater gives

$$0 = \iint_S g(s') g^*(s) \left[K_c(s/s') + \frac{\partial K_c}{\partial \gamma} \delta\gamma\right] + [g(s')\eta^*(s) + g^*(s)\eta(s') \; K_c(s/s')] \, ds \, ds'$$

$$= \delta\gamma \iint_S g(s') g^*(s) \frac{\partial K_c}{\partial \gamma} ds \, ds' + \iint_S [g(s')\eta^*(s) + g^*(s)\eta(s')] K_c(s/s') \, ds \, ds', \qquad \text{(A-3)}$$

since, from Equation 2-15,

$$\int_S g(s') \, K_c \, (s/s') \, ds' = 0. \tag{A-4}$$

The last term of Equation A-3,

$$\iint_S g^*(s)\eta(s') \, K_c(s/s') \, ds \, ds' = \left\{ \iint_S g(s)\eta^*(s') \, K_c^*(s/s') \, ds \, ds' \right\}^*$$
$$= \left\{ \iint_S g(s')\eta^*(s) \, K_c \, (s/s') \, ds \, ds' \right\}^*,$$

since, from Equation 2-17,

$$K \, (s/s') = K^* \, (s'/s).$$

Substitution into Equation A-3 gives

$$0 = \delta \, \gamma \iint_S g(s')g^*(s) \, \frac{\partial K_c}{\partial \gamma} \, ds \, ds' + 2 \, Re \left\{ \int_S \eta^*(s) \, \left[\int_S g(s') \, K_c\left(\frac{s}{s'}\right) ds \right] ds \right\}.$$

The final term is zero by virtue of Equation A-4. Thus, assuming

$$\iint_S g(s') \, g^*(s) \, \frac{\partial K_c}{\partial \gamma} \, ds \, ds' \neq 0,$$

we have

$$\delta \, \gamma = 0,$$

and the stationary property of Equation 2-18 is proven.

The proof of the stationary property of Equation 2-21 is entirely analogous, although the z dependence has been eliminated and the problem is then two dimensional. The following is a repeat of the argument advanced by Rumsey[23].

Let γ be determined from the expression

$$\int_{-L/2}^{L/2} \underline{J_a}(y) \cdot [s]\, \underline{E_a}\,(y)\, dy = 0, \qquad \text{(A-5)}$$

where, from Equation 2-20, [s] is the matrix

$$[s] = \begin{bmatrix} 1 & 0 \\ 0 & 1 \end{bmatrix}.$$

Let $\underline{E_a}$ (y) be the assumed aperture distribution which differs by only a small amount from the correct aperture distribution, $\underline{E_c}$ (y), i.e.,

$$\underline{E_a}\,(y) = \underline{E_c}\,(y) + \delta\, \underline{E}.$$

Since $\underline{J_a}(y)$ is a function of γ , then to the first order

$$\underline{J_a}\,(\gamma) = \underline{J_a}\,(\gamma_c) + \frac{\partial\, \underline{J_a}\,(\gamma_c)}{\partial \gamma}\, \delta\, \gamma,$$

where, as before, γ_c is the correct value of γ. Substitution into Equation A-5 gives to the first order

$$0 = \int_{-\frac{L}{2}}^{\frac{L}{2}} \left[\underline{J_a}\,(\gamma_c) \cdot [s]\, \underline{E_c} + \underline{E_c} \cdot [s] \frac{\partial\, \underline{J_a}(\gamma_c)}{\partial \gamma}\, \delta\, \gamma + \underline{J_a}\,(\gamma_c) \cdot [s]\, \delta\, \underline{E} \right] dy. \qquad \text{(A-6)}$$

Since $\underline{J_a}$ is proportional to $\delta\, \underline{E}$, the final term of Equation A-6 is also second order. Also, from the reciprocity theorem for traveling wave line sources^9,

$$\int_{-\frac{L}{2}}^{\frac{L}{2}} \underline{J_a}\,(\gamma_c) \cdot [s]\, \underline{E_c}\,(\gamma_c)\, dy = \int_{-\frac{L}{2}}^{\frac{L}{2}} \underline{J_c}\,(\gamma_c) \cdot [s]\, \underline{E_a}\,(\gamma_c)\, dy = 0,$$

since J_c (γ_c) is identically zero. Therefore, assuming

$$\int_{-\frac{L}{2}}^{\frac{L}{2}} \underline{E_c} \cdot [s] \frac{\partial \underline{J_a} (\gamma_c)}{\partial \gamma} \, dy \neq 0,$$

we have

$$\delta \gamma = 0.$$

APPENDIX B

THE EVALUATION OF $I_n(\beta/k\ , L/\lambda)$.

From Equation 2-36,

$$I_n = 1/4\pi(\lambda/L)^2 \int_{-L/2}^{L/2}\int_{-L/2}^{L/2} \cos(\pi y/L)\cos(\pi y'/L)(k^2+\partial^2/\partial y^2)H_o^{(2)}(\beta_n\rho)\, dy dy', \qquad \text{(B-1)}$$

where

$$\beta_n = \sqrt{k^2 - \gamma_n^2},$$

$$\rho = |y - y'|.$$

Let

$$I_n = I_{n_1} + I_{n_2},$$

where

$$I_{n_2} = 1/4\pi\ (\lambda/L)^2 \int_{-L/2}^{L/2}\int_{-L/2}^{L/2} \cos(\pi y/L)\cos(\pi y'/L)(\partial^2/\partial y^2)\, H_o^{(2)}(\beta_n\rho)\, dy dy'. \qquad \text{(B-2)}$$

Integration by parts with

$$dv = (\partial^2/\partial y^2) H_o^{(2)}\ (\beta_n|y-y'|) = -(\partial^2/\partial y\, \partial y')\ H_o^{(2)}\ (\beta_n|y-y'|),$$

$$u = \cos(\pi y/L)\ \cos(\pi y'/L)$$

gives

$$I_{n_2} = (-1/4\pi)(\lambda/L)^2 \int_{-L/2}^{L/2} \left\{ \pi/L \int_{-L/2}^{L/2} (\partial/\partial y) H_o^{(2)}(\beta_n\rho)\cos(\pi y/L)\sin(\pi y'/L)\ dy' \right\} dy. \qquad \text{(B-3)}$$

Upon reversal of the order of integration, followed by a second integration by parts, Equation B-3 becomes

$$I_{n_2} = (-1/4\pi)(\lambda/L)^2 \int_{-L/2}^{L/2}\int_{-L/2}^{L/2} (\pi/L)^2\, H_o^{(2)}\,(\beta_n\rho)\,\sin(\pi y/L)\sin(\pi y'/L)\,dydy'.$$

Thus

$$I_n = k^2/4\pi(\lambda/L)^2 \int_{-L/2}^{L/2}\int_{-L/2}^{L/2} H_o^{(2)}\,(\beta_n\rho)\left[\cos(\pi y/L)\cos(\pi y'/L) + -(\lambda^2/4L^2)\sin(\pi y/L)\sin(\pi y'/L)\right] dydy'$$

$$= 1/\pi \int_{-\pi/2}^{\pi/2}\int_{-\pi/2}^{\pi/2} H_o^{(2)}\,(\beta_n\rho)\left[\cos y\cos y' - (\lambda^2/4L^2)\sin y\sin y'\right] dydy'. \qquad \text{(B-4')}$$

Since ρ is a function only of $y-y'$, Equation B-4' may be further simplified by first integrating with respect to y', with $y - y'$ held constant, and then integrating over all possible values of $y - y'$. If $r = y - y'$, then

$$I_n = 1/\pi \int_o H_o^{(2)}\,(\beta_n L\,|r|/\pi)\,dr \int_{-\pi/2}^{(\pi/2)-r} [\cos y'\cos(y'+r) + -(\lambda^2/4L^2)\sin y'\sin(y'+r)]\,dy +$$

$$+\, 1/\pi \int_o H_o^{(2)}\,(B_n L\,|r|/\pi)\,dr \int_{-(\pi/2)-r}^{\pi/2} [\cos y'\cos(y'+r) + -(\lambda^2/4L^2)\sin y'\sin(y'+r)]\,dy. \qquad \text{(B-5)}$$

Since

$$\cos y'\cos(y'+r) = \cos(-y')\cos(-y'-r),$$

$$\sin y'\sin(y'+r) = \sin(-y')\sin(-y'-r),$$

it is easily verified that the two terms of Equation B-5 are equal and

$$I_n = 2/\pi \int_0^{\pi} H_o^{(2)}\,(\beta_n L r/\pi)\,dr \int_{-\pi/2}^{(\pi/2)-r} [\cos y' \cos(y'+r) + (\lambda^2/4L^2) \sin y' \sin(y'+r)]\,dy'. \qquad \text{(B-6)}$$

Performing the indicated integration with respect to y' gives

$$I_n = \int_0^{\pi} H_o^{(2)}\,(\beta_n L r/\pi) \left[(1 - \lambda^2/4L^2) \cos r + 1/\pi\,(1 + \lambda^2/4L^2) \sin r \right] dr. \qquad \text{(B-7)}$$

For $n \neq 0$, Equation B-7 may be approximately evaluated in closed form. From Equation 2-34', β_n can be written

$$\beta_n = -j\sigma_n = -jk\sqrt{(n\lambda/\ell - \gamma/k)^2 - 1},$$

where σ_n is approximately real and positive for $n \neq 0$. With this substitution,

$$H_o^{(2)}\,(\beta_n \rho) = j\,(2/\pi)\,K_o(\sigma_n \rho).$$

Let

$$a = \pi/\sigma_n L.$$

Then, from Equation B-7,

$$I_n = j\,(2a/\pi) \int_0^{\pi/a} K_o(u) \left[[1 - (\lambda^2/4L^2)]\,[1 - (au/\pi)] \cos(au) + (1/\pi)[1 + (\lambda^2/4L^2)] \sin(au) \right] du$$

$$= j\,(2a/\pi) \left\{ \int_0^{\infty} f(u)\,du - \int_{\pi/a}^{\infty} f(u)\,du \right\}$$

$$= j\,(2a/\pi) \left\{ I_{n_3} - I_{n_4} \right\}, \qquad \text{(B-8)}$$

thus defining I_{n_3} and I_{n_4}.

Formulas for the evaluation of I_{n_3} are available[25]:

$$\int_o^\infty K_o\,(u)\;au\;du = (\pi/2)\,\frac{1}{\sqrt{1+a^2}}\;, \tag{B-9}$$

$$\int_o^\infty K_o(u)\sin\,au\;du = \frac{\text{arc sinh } a}{\sqrt{1+a^2}}\;, \tag{B-10}$$

$$\int_o^\infty u\,K_o\,(u)\cos\,au\;du = \int_o^\infty u\,K_o\,(u)\left[\left(e^{jau}+e^{-jau}\right)/2\right]du$$

$$= \tfrac{1}{2}\sqrt{\pi/2}\;[\Gamma\;(2)]^2\left\{\frac{P^{-3/2}_{-1/2}\;(ja)}{\sinh^{3/2}\;[\text{arc cosh } ja]} + \frac{P^{-3/2}_{-1/2}\;(-ja)}{\sinh^{3/2}\;[\text{arc cosh}(-ja)]}\right\}, \tag{B-11}$$

where P is the generalized Legendre Function. P may be expressed as

$$P^{-3/2}_{-1/2}\;(ja) = [1/\Gamma(5/2)]\;[(ja-1/ja+1)]^{3/4}\;F\;(\tfrac{1}{2},\tfrac{1}{2};5/2;(1-ja)/2) \tag{B-12}$$

where F is the Hypergeometric Function. The series representation of F is

$$F(\alpha,\beta;\gamma,z) = 1 + (\alpha\beta/\gamma)\;z + \frac{\alpha(\alpha+1)\;\beta\;(\beta+1)}{2!\;\gamma\;(\gamma+1)}\;z^2 + \ldots$$

In the following, it is assumed that

$$\sigma_n\;L > 2\pi,$$

and thus

$$a < 1/3. \tag{B-13}$$

Under this condition, and for the argument indicated in Equation B-12, F is given approximately by

$$F\left(\frac{1 \pm ja}{2}\right) \simeq 1.085 \pm .165\, ja.$$

Also

$$\left(\frac{\pm ja - 1}{\pm ja + 1}\right)^{3/4} \cong e^{\pm j(3\pi/4)}\,[1 \mp j\,(1 + 1/2)a - (1 + 1/8)a^2 \mp j(1 + 1/16)a^3 + \ldots]$$

$$\simeq e^{\pm j(3\pi/4)}\,[1 \mp j\,1.5a - 1.125\,a^2],$$

$$\text{arc cosh}\,(\pm ja) = \ln\,(a + \sqrt{a^2 + 1}) \pm j\,(\pi/2).$$

Since

$$\sqrt{1 + a^2} \simeq 1 + (a/2)^2,$$

then

$$\text{arc cosh}\,(\pm ja) \simeq a + \frac{a^2}{2} - \frac{\left(a + \frac{a^2}{2}\right)}{2} + \ldots \pm j\,\frac{\pi}{2}$$

$$\simeq a - \frac{a^3}{2} \pm j\,\frac{\pi}{2},$$

and

$$\sinh\,[\text{arc cosh}\,(\pm ja)] \simeq \pm j\,\cosh\left(a - a^3/2\right),$$

$$\sinh^{3/2}\,[\text{arc cosh}\,(\pm ja)] \simeq e^{\pm j(3\pi/4)}\,(1 + \tfrac{3}{4}a^2).$$

Upon substitution of these results, Equation B-11 becomes

$$\int_0^\infty u\,K_0\,(u)\,\cos au\,du \simeq$$

$$\simeq \frac{2}{3\sqrt{2}}\left\{\frac{(1 - j\,1.5a - 1.125a^2)(1.085 - .165ja)}{(1 + \frac{3}{4}a^2)} + \frac{(1 + j\,1.5a - 1.125a^2)(1.085 + .165ja)}{(1 + \frac{3}{4}a^2)}\right.$$

$$\simeq \frac{4}{3\sqrt{2}}\,(1.085 - 2.27\,a^2). \qquad \text{(B-14)}$$

From Equation B-9,

$$\int_0^\infty K_o\,(u)\,\cos au\,du \simeq \frac{\pi}{2}\,(1 - \frac{a^2}{2}). \qquad \text{(B-15)}$$

Also, since

$$\text{arc. sinh } a = \ln\,(\sqrt{1+a^2} + a) \simeq \ln\,(1 + a + \frac{a^2}{2})$$

$$\simeq a\,(1 - \frac{a^2}{2}),$$

then, from Equation B-10,

$$\int_0^\infty K_o\,(u)\,\sin au\,du \simeq a(1 - a^2). \qquad \text{(B-16)}$$

Collecting terms gives approximately

$$I_{n_3} \simeq \frac{\pi}{2}\left\{[1-(\lambda^2/4L^2)]\,[1 - .04a/2 - a^2/2 + (2.28a^3)/2] + 4/\pi^2(\lambda^2/4L^2)a(1-a^2)\right\}$$

$$\simeq \pi/2\left\{[1-(\lambda^2/4L^2)]\,(1 - a^2/2) + (\lambda^2/4L^2)(4/\pi^2)(a-a^3). \right. \qquad \text{(B-17)}$$

For I_{n_4}, from Equation B-8,

$$I_{n_4} = 1/a\int_\pi^\infty K_o\,(u/a)\left\{[1-(\lambda^2/4L^2)]\,(1 - u/\pi)\cos u + 1/\pi[1+(\lambda^2/4L^2)]\sin u\right\}du.$$

For

$$|a| < 1/3 \text{ and } 0 < Am\,(a) < 4',$$

$$|K_o(u/a)| < 2\sqrt{\pi/2}\,\sqrt{|a|}\;\frac{e^{-u/|a|\sqrt{2}}}{\sqrt{u}},$$

and

$$|I_{n_4}| < \sqrt{2\ |a|} \int_{\pi}^{\infty} e^{-u/|a|\sqrt{2}} \left\{ (2u/\pi)\ [1-(\lambda^2/4L^2)] + 2/\pi(\lambda^2/4L^2) \right\} du$$

$$= 2\ \sqrt{2|a|/\pi}\ \ [|a|(\pi+|a|)e^{-\pi/|a|\sqrt{2}}[1-(\lambda^2/4L^2) + |a|e^{-(\pi/|a|\sqrt{2}}(\lambda^2/4L^2)]$$

$$< 2\sqrt{2/(3\pi)}[1/3(\pi+1/3)e^{-3\pi/\sqrt{2}}[1-(\lambda^2/4L^2)]+1/3|a|e^{-3\pi/\sqrt{2}} + (.35)3\sqrt{2}\,(\lambda^2/4L^2)]$$

$$= \pi/2\ [1-(\lambda^2/4L^2)]\ (8.56)\ 10^{-4} + (\lambda^2/4L^2)(4/\pi^2)\ |a|\ (2.72)\ 10^{-3}].$$

Thus I_{n_4} is negligible compared with I_{n_3} and

$$I_n \simeq j(2a/\pi)\ I_{n_3} \simeq ja \left\{ [1-(\lambda^2/4L^2)][1-(a^2/2)] + (\lambda^2/4L^2)(4/\pi^2)(a-a^3) \right\}.$$

With the substitution

$$a = \pi/\sigma_n L,$$

$$I_n \simeq j[1-(\lambda^2/4L^2)]\ \frac{\pi}{\sigma_n L}\ [1-\pi^2/(2\sigma_n{}^2L^2)] + j(\lambda^2/4L^2)[4/(\sigma_n L)^2 - (4\pi/(\sigma_n L)^4\ ]$$

$$= j/kL \left\{ [1-(\lambda^2/4L^2)](k/\sigma_n)[1-(1/8)(\lambda^2/L^2)](k/\sigma_n)^2 + \right.$$
$$\left. + j(\lambda^3/L^3)[(1/2\pi^2)(k/\sigma_n)^2 - (1/8\pi^3)(\lambda^2/L^2)(k/\sigma_n)^4] \right\}. \tag{B-18}$$

This is Equation 2-37.

Because the limitation on σ_n stated in Equation B-13 is violated for $n=0$, a similar evaluation of Equation B-7 for this case is not possible. Instead the power series representation of $H_o^{(2)}(\beta\rho)$ may be used and the resulting series integrated term by term. Substitution of the power series and the collection of similar terms gives

$$I_o[(\beta/k),(L/\lambda)] = \sum_{i=0}^{\infty} (-1)^i[(\beta/k)(L/\lambda)]^{2i} \left\{ [1-j(2/\pi)\overline{\gamma}-j(2/\pi)\ln[(\beta/k)(L/\lambda)]Q_{2i} + \right.$$
$$\left. + j\ R_{2i} \right\},$$

with

$$Q_{2i} = (r_{2i} + s_{2i}) + \lambda^2/4L^2 \, (r_{2i} - s_{2i}),$$

$$R_{2i} = 2/\pi \left[Q_{2i} \sum_{r=1}^{i} 1/r - (t_{2i}+u_{2i}) - (\lambda^2/4L^2)(t_{2i} - u_{2i}) \right], \quad \text{(B-19)}$$

$$\bar{\gamma} = \text{Euler's constant} = .5772 \ldots,$$

and where

$$r_{2i} = 1/(i!)^2 \int_0^{\pi} (u^{2i}/\pi) \sin u \, du, \quad \text{(B-20a)}$$

$$s_{2i} = 1/(i!)^2 \int_0^{\pi} u^{2i} (1 - u/\pi) \cos u \, du, \quad \text{(B-20b)}$$

$$t_{2i} = 1/(i!)^2 \int_0^{\pi} (u^{2i}/\pi) \sin u \ln u \, du, \quad \text{(B-20c)}$$

$$u_{2i} = 1/(i!)^2 \int_0^{\pi} u^{2i} \cos u \ln u \, du. \quad \text{(B-20d)}$$

These integrals are in standard form and are readily evaluated through repeated application of the appropriate reduction formula. The results are

$$r_{2i} = \frac{(-1)^i}{\pi} \frac{(2i)!}{(i!)^2} \left[\sum_{r=0}^{i} \frac{(-1)^r \pi^{2r}}{(2r)!} + 1 \right], \quad \text{(B-21a)}$$

$$s_{2i} = (-1)^i \frac{(2i)!}{(i!)^2} \left[\sum_{r=0}^{i-1} \frac{(-1)^r \pi^{2r+1}}{(2r+1)!} \left(1 - \frac{2i+1}{2r+2}\right) + \frac{2(2i+1)}{\pi} \right], \quad \text{(B-21b)}$$

$$t_{2i} = \frac{(-1)^i}{\pi}\,\frac{(2i)!}{(i!)^2}\left\{\ln\pi\sum_{r=0}^{i}\frac{(-1)^r\,\pi^{2r}}{(2r)!} + \mathrm{Ci}\,(\pi) - \bar{\gamma} + \sum_{r=0}^{i-1}\frac{(-1)^r\,\pi^{2r}}{(2r)!}\sum_{j=r+1}^{i}\left(\frac{1}{2j}+\frac{1}{2j-1}\right) + \sum_{r=1}^{i}\left(\frac{1}{2r}+\frac{1}{2r-1}\right)\right\}, \tag{B-21c}$$

$$u_{2i} = (-1)^i\,\frac{(2i)!}{(i!)^2}\left\{\frac{2i+1}{\pi}\ln\pi + (-1)^i\,\frac{\pi^{2i-1}}{(2i)!}\,\xi_i + \sum_{r=1}^{i-1}\frac{(-1)^r\,\pi^{2r-1}}{(2r-1)!}\left(\frac{2i+1}{2r}-1\right)\left[\frac{1}{2i}+\frac{2r+2}{2r+1}+\sum_{j=r+1}^{i-1}\left(\frac{1}{2j}+\frac{1}{2j+1}\right)\right] + 2\,\frac{2i+1}{\pi}\left[1+\sum_{r=1}^{i}\left(\frac{1}{2r}+\frac{1}{2r+1}\right)\right] + \frac{2i+2}{\pi} - \mathrm{Si}\,(\pi) + \frac{\mathrm{Ci}(\pi)-\bar{\gamma}}{\pi}\right\}, \tag{B-21d}$$

where

$$\mathrm{Si}\,(\pi) = \int_0^{\pi}\frac{\sin x}{x}\,dx = \frac{\pi}{1\cdot 1!} - \frac{\pi^3}{3\cdot 3!} + \frac{\pi^5}{5\cdot 5!} - \dots,$$

$$\mathrm{Ci}\,(\pi) = \int_0^{\pi}\frac{\cos x}{x}\,dx = \bar{\gamma} + \ln\pi - \frac{\pi^2}{2\cdot 2!} + \frac{\pi^4}{4\cdot 4!} - \dots,$$

$$\xi_i = 0 \quad \text{for } i = 0,$$
$$\quad = 1 \quad \text{for } i \neq 0.$$

An alternative form (infinite series expansion) for the coefficients may be obtained by substituting the power series for sin u and cos u in Equations B-20a-d. The results are

$$r_{2i} = \frac{(-1)^{i+1}}{\pi}\,\frac{(2i)!}{(i!)^2}\sum_{r=i+1}^{\infty}\frac{(-1)^r\,\pi^{2r}}{(2r)!}, \tag{B-22a}$$

$$s_{2i} = (-1)^{i+1}\frac{(2i)!}{(i!)^2}\sum_{r=i}^{\infty}\frac{(-1)^r\,\pi^{2r+1}}{(2r+1)!}\left(1-\frac{2i+1}{2r+2}\right), \qquad \text{(B-22b)}$$

$$t_{2i} = \frac{(-1)^{i+1}}{\pi}\,\frac{(2i)!}{(i!)^2}\sum_{r=i+1}^{\infty}\frac{(-1)^r\,\pi^{2r}}{(2r)!}\left(\ln\pi-\sum_{j=2i+1}^{2r}\frac{1}{j}\right), \qquad \text{(B-22c)}$$

$$u_{2i} = (-1)^{i+1}\frac{(2i)!}{(i!)^2}\sum_{r=i}^{\infty}\frac{(-1)^r\,\pi^{2r+1}}{(2r+1)!}\left[\left(1-\frac{2i+1}{2r+2}\right)\left(\ln\pi-\sum_{j=2i+2}^{2r+1}\frac{1}{j}\right)-\frac{1}{2i+1}+\frac{2i+2}{(2r+2)^2}\right]. \qquad \text{(B-22d)}$$

In some cases, for large i, because of their rapid convergence, Equations B-22 are more readily evaluated than the corresponding Equations B-21.

Values of the coefficients for i up to 10 are tabulated in Table I.

Table I. Coefficients for $I_o\left(\frac{\beta}{k}, \frac{L}{\lambda}\right)$.

i	$r_{2i} + s_{2i}$	$r_{2i} - s_{2i}$	$t_{2i} + u_{2i}$	$t_{2i} - u_{2i}$
0	1.27324	0	-8.07572 (10^{-1})	1.21487
1	1.19022	2.54648	3.50990 (10^{-1})	2.20546
2	7.22338 (10^{-1})	3.57068	4.02443 (10^{-1})	3.13587
3	2.83234 (10^{-1})	2.40779	1.95932 (10^{-1})	2.22433
4	7.72136 (10^{-2})	9.91318 (10^{-1})	5.92386 (10^{-2})	9.51924 (10^{-1})
5	1.54708 (10^{-2})	2.77969 (10^{-1})	1.28820 (10^{-2})	2.74205 (10^{-1})
6	2.37413 (10^{-3})	5.67262 (10^{-2})	2.07623 (10^{-3})	5.71178 (10^{-2})
7	2.87979 (10^{-4})	8.81818 (10^{-3})	2.61044 (10^{-4})	9.01986 (10^{-3})
8	2.83059 (10^{-5})	1.07992 (10^{-3})	2.63714 (10^{-5})	1.11840 (10^{-3})
9	2.30023 (10^{-6})	1.06933 (10^{-4})	2.18994 (10^{-6})	1.11857 (10^{-4})
10	1.57123 (10^{-7})	8.74088 (10^{-5})	1.52188 (10^{-7})	9.21884 (10^{-6})

APPENDIX C

APPROXIMATIONS FOR THE SERIES S_3 AND S_5 IN EQUATION 3-3

We have

$$S_3 = \sum_{n=1}^{\infty} \left[\frac{\sin^2\left(\frac{n\pi d}{\ell} - \frac{\gamma d}{2}\right)}{n^3 \left(1 - \frac{1}{n}\frac{\ell}{\lambda}\frac{\gamma}{k}\right)^3} + \frac{\sin^2\left(\frac{n\pi d}{\ell} + \frac{\gamma d}{2}\right)}{n^3 \left(1 + \frac{1}{n}\frac{\ell}{\lambda}\frac{\gamma}{k}\right)^3} \right]. \qquad \text{(C-1)}$$

With the relations

$$(1 \pm x)^{-3} = 1 \mp 3x + 6x^2 \mp 10x^3 + \ldots$$

$$\sin^2 [(n\pi d/\ell)-(\gamma d/2)] - \sin^2 [(n\pi d/\ell)+(\gamma d/2)] = -(1/4) \sin (2n\pi d/\ell) \cdot \sin \gamma d,$$

$$\sin^2 [(n\pi d/\ell)-(\gamma d/2)] + \sin^2 [(n\pi d/\ell)+(\gamma d/2)] = 1-\cos \gamma d + 2 \cos \gamma d \cdot \sin^2 (n\pi d/\ell),$$

Equation C-1 becomes approximately

$$S_3 \simeq \sum_{n=1}^{\infty} \frac{1 - \cos \gamma d + 2 \cos \gamma d \sin^2 \frac{n\pi d}{\ell}}{n^3} \left[1 + 6\left(\frac{\ell}{\lambda}\frac{\gamma}{k}\right)^2 \frac{1}{n^2} + 15\left(\frac{\ell}{\lambda}\frac{\gamma}{k}\right)^4 \frac{1}{n^4} \right] + $$
$$- 3/4 \left(\frac{\ell}{\lambda}\frac{\gamma}{k}\right) \sin \gamma d \sum_{n=1}^{\infty} \frac{\sin \frac{2n\pi d}{\ell}}{n^4} \left[1 + \frac{10}{3}\left(\frac{\ell}{\lambda}\frac{\gamma}{k}\right)^2 \frac{1}{n^2} + 7\left(\frac{\ell\gamma}{\lambda k}\right)^4 \frac{1}{n^4} \right]. \qquad \text{(C-2)}$$

Several of the series in Equation C-2 are relatively slowly convergent for small values of d/ℓ. The following empirically modified asymptotic expressions which are accurate to within about 5% for $d/\ell \leq 1/2$ are used:

$$\sum_{n=1}^{\infty} \frac{\sin^2 \frac{n\pi d}{\ell}}{n^3} \simeq \left(\frac{\pi d}{\ell}\right)^2 \ln \frac{2.23\ell}{\pi d} + 3.2 \left(\frac{d}{\ell}\right)^4 ,$$

$$\sum_{n=1}^{\infty} \frac{\sin^2 \frac{n\pi d}{\ell}}{n^4} \simeq \zeta\ (2) \sin^2 \frac{\pi d}{\ell} \left(1 - .562 \sqrt{\frac{d}{\ell}}\right),$$

$$\sum_{n=1}^{\infty} \frac{\sin^2 \frac{n\pi d}{\ell}}{n^5} \simeq \zeta\ (3) \sin^2 \frac{\pi d}{\ell} \left(1 - .340 \frac{d}{\ell}\right),$$

$$\sum_{n=1}^{\infty} \frac{\sin^2 \frac{\nu\pi d}{\ell}}{\nu^2} \simeq \zeta\ (\nu-2) \sin^2 \frac{\pi d}{\ell}, \qquad \nu \geq 6,$$

$$\sum_{n=1}^{\infty} \frac{\sin \frac{2n\pi d}{\ell}}{n^4} \simeq \zeta\ (3) \sin \frac{2\pi d}{\ell} \left(1 - .680 \frac{d}{\ell}\right),$$

$$\sum_{n=1}^{\infty} \frac{\sin \frac{2\nu\pi d}{\ell}}{\nu} \simeq \zeta\ (\nu-1) \sin \frac{2\pi d}{\ell}, \qquad \nu \geq 6,$$

where $\zeta\ (\nu)$ is the Riemann zeta function,[26] having the following values:

ν	$\zeta(\nu)$
2	1.645
3	1.202
4	1.082
5	1.037
6	1.017
7	1.008
8	1.004

Since

$$\gamma d < \pi/4,$$

then

$$\sin \gamma d \simeq \gamma d \frac{(\gamma d)^3}{6},$$
$$\cos \gamma d \simeq 1 - \frac{(\gamma d)^2}{2}.$$

With these approximations, and upon dropping all terms involving $(\frac{\ell}{\lambda}\frac{\gamma}{k})$ to the fourth power or greater, S_3 is given approximately by

$$S_3 \simeq 2\pi^2 (d/\ell)^2 \sum_{1}^{2} \rho_{2i} \left(\frac{\ell}{\lambda}\frac{\gamma}{k}\right)^{2i}, \qquad \text{(C-3)}$$

where

$$\rho_o = \ln (2.23\ell/\pi d) + (3.2/\pi^2)(d/\ell)^2,$$
$$\rho_2 = 1.20 + (7.2/\pi^2)\sin^2(\pi d/\ell)[1 - .34(d/\ell)] - 2\pi^2 (\ell/d)^2 \ln (2.23\ell/\pi d) +$$
$$- 6.4(d/\ell)^4 + (.90/\pi^2)(\ell/d)[1 - .68(d/\ell)]\sin(2\pi d/\ell),$$
$$\rho_4 = 6.5 - (2.6/\pi)(\ell/d)\sin(2\pi d/\ell) + 0.6(\pi d/\ell)[1-.68(d/\ell)] \sin(2\pi d/\ell) +$$
$$+ (15/\pi^2)(\ell/d)^2 \sin^2 (\pi d/\ell) - 14.4[1-.34(d/\ell)]\sin^2(\pi d/\ell). \qquad \text{(C-4)}$$

From Equation 3-3, the coefficient of S_5 is small compared with that of S_3. Since, in addition, S_5 is rapidly convergent, only the n=1 term is taken as an approximation to the sum. Thus

$$S_5 \simeq \frac{\sin^2(\frac{\pi d}{\ell} - \frac{\gamma d}{2})}{(1 - \frac{\ell}{\lambda}\frac{\gamma}{k})^5} + \frac{\sin^2(\frac{\pi d}{\ell} + \frac{\gamma d}{2})}{(1 + \frac{\ell}{\lambda}\frac{\gamma}{k})^5}.$$

With the approximation

$$(1 \pm x)^{-5} \simeq 1 \mp 5x + 15x^2 \mp 35x^3 + 70x^4,$$

where $x = (\frac{\ell}{\lambda}\frac{\gamma}{k})$, S_5 is given approximately by

$$S_5 \simeq 4\left(\frac{\pi d}{\ell}\right)^2 \sum_{i=0}^{2} q_{2i} \left(\frac{\ell}{\lambda}\frac{\gamma}{k}\right)^{2i}, \qquad \text{(C-5)}$$

where

$$q_o = (1/2)(\ell/\pi d)^2 \sin^2 (\pi d/\ell),$$

$$q_2 = (15/2\pi^2)(\ell/d)^2 \sin^2(\pi d/\ell) + (1/2)\cos^2(\pi d/\ell) + (5/8\pi)(\ell/d)\sin(2\pi d/\ell),$$

$$q_4 = (35/\pi^2)(\ell/d)^2 \sin^2(\pi d/\ell) + (15/2)\cos^2(\pi d/\ell) + (35/8\pi)(\ell/d)\sin(2\pi d/\ell) +$$

$$- .416\, \pi\, (d/\ell) \sin (2\pi d/\ell). \qquad \text{(C-6)}$$

The coefficients p_{2i}, q_{2i} are plotted in Figures 37-42.

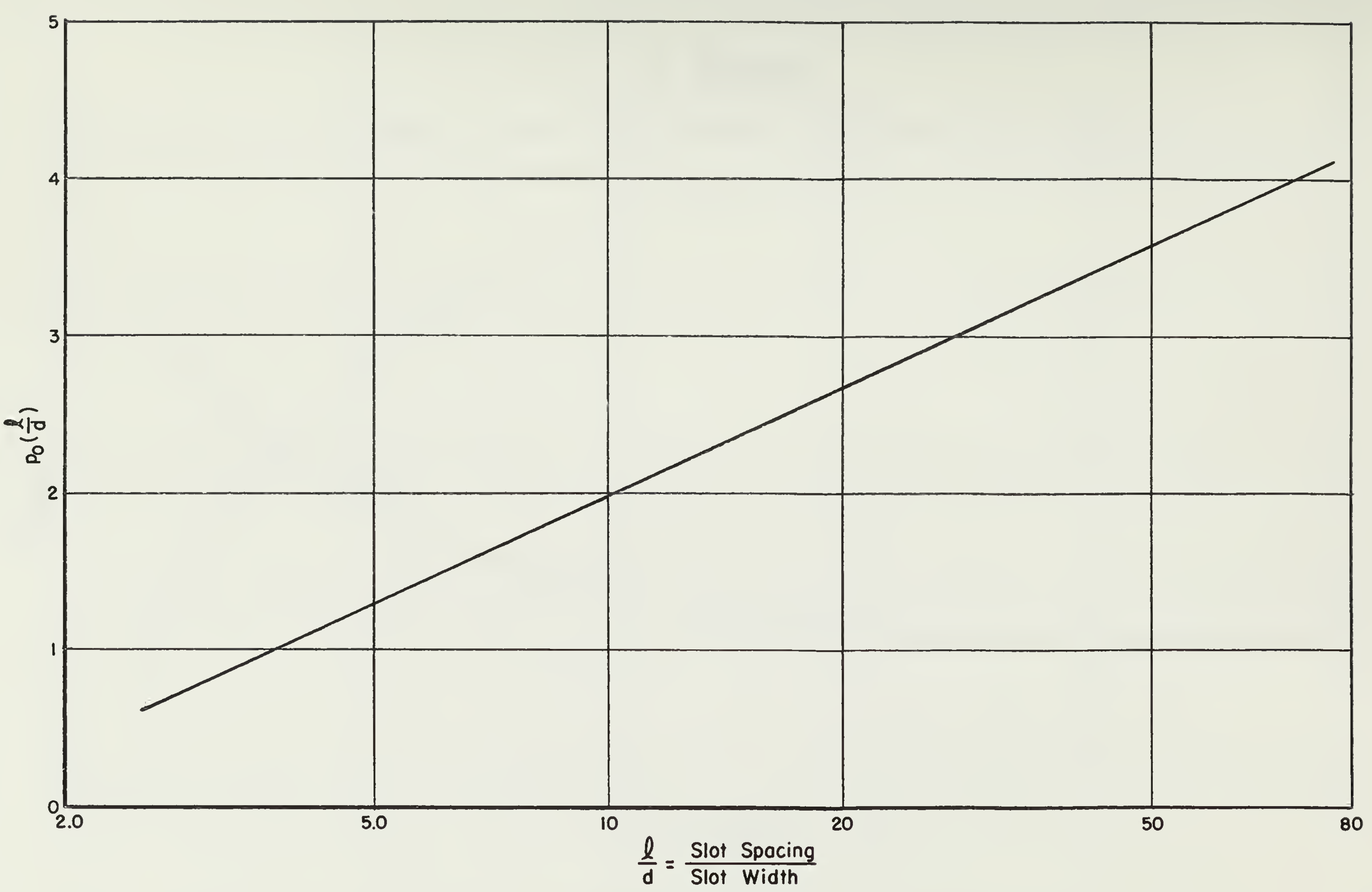

Figure 37. $p_o(\ell/d)$

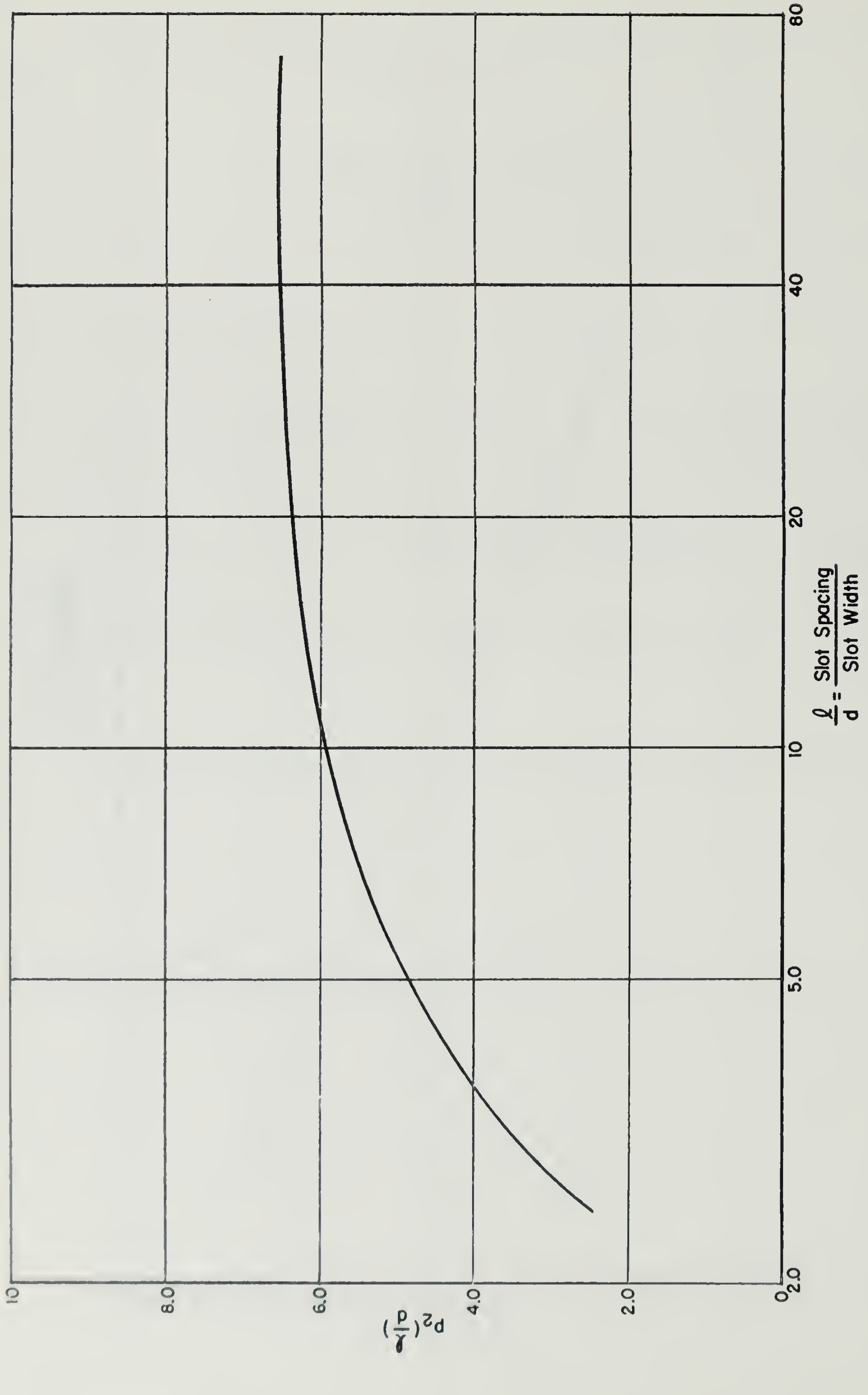

Figure 38. p_4 (ℓ/d)

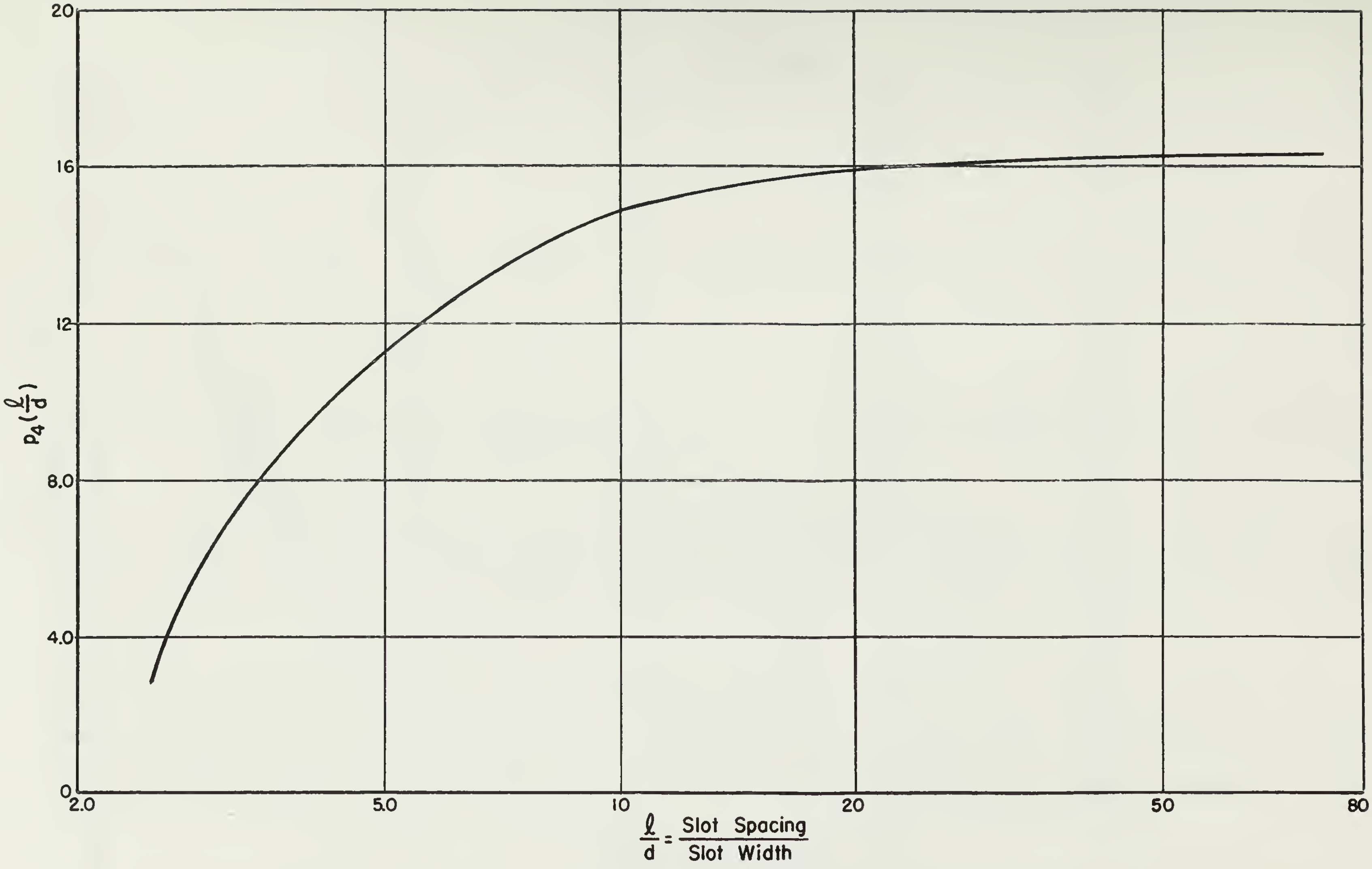

Figure 39. p_4 (ℓ/d)

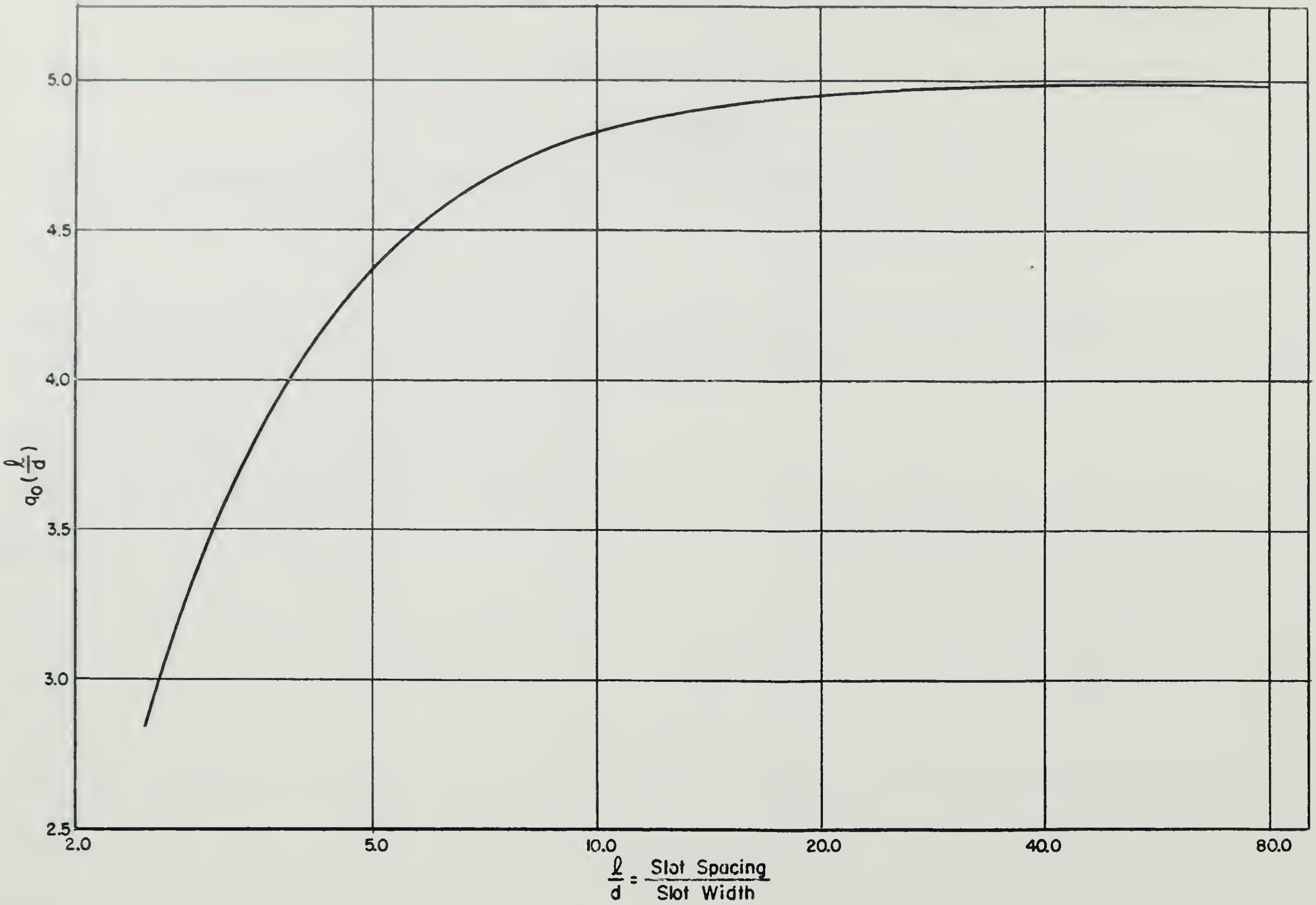

Figure 40. q_o (ℓ/d)

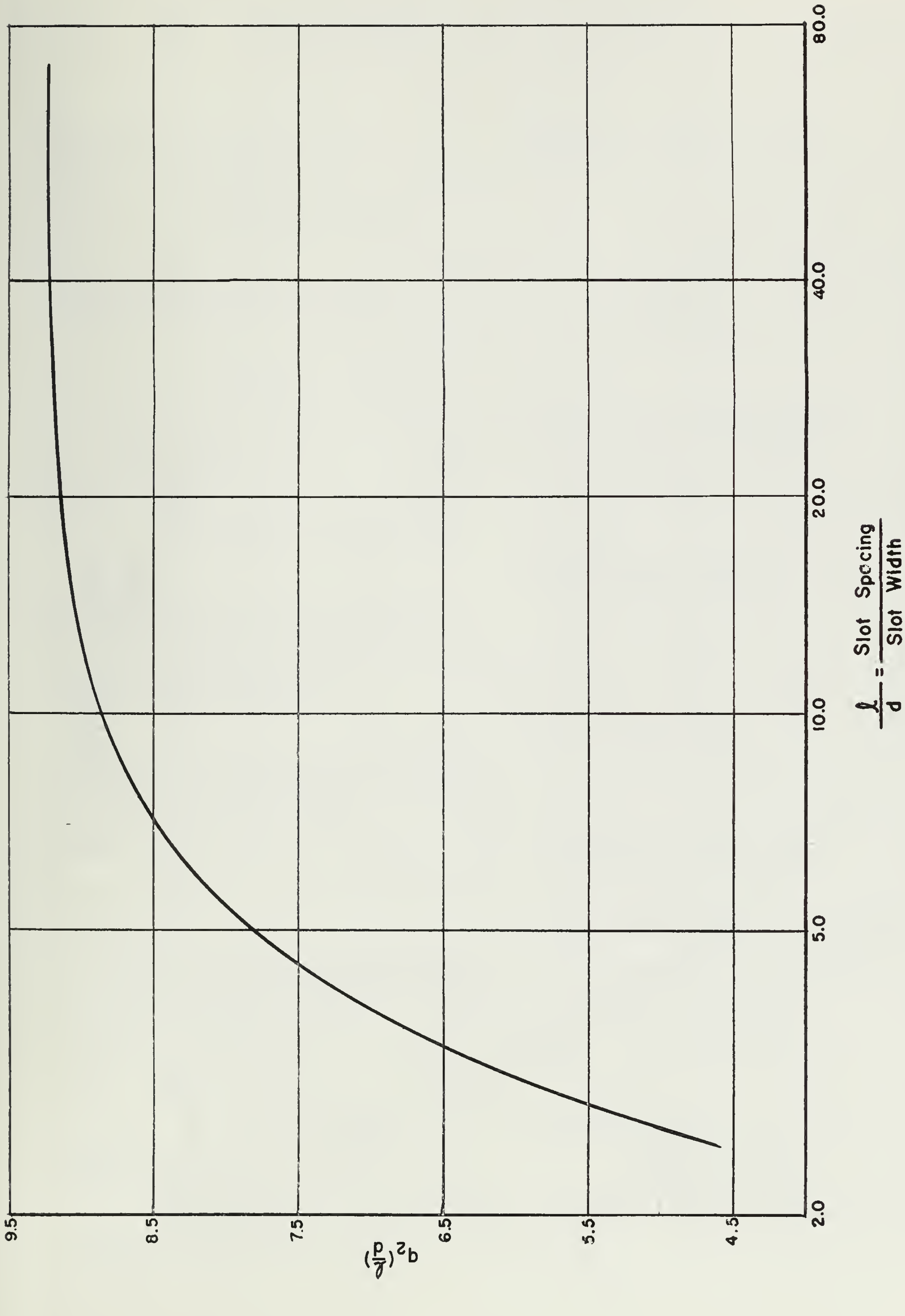

Figure 41. $q_2\ (\ell/d)$

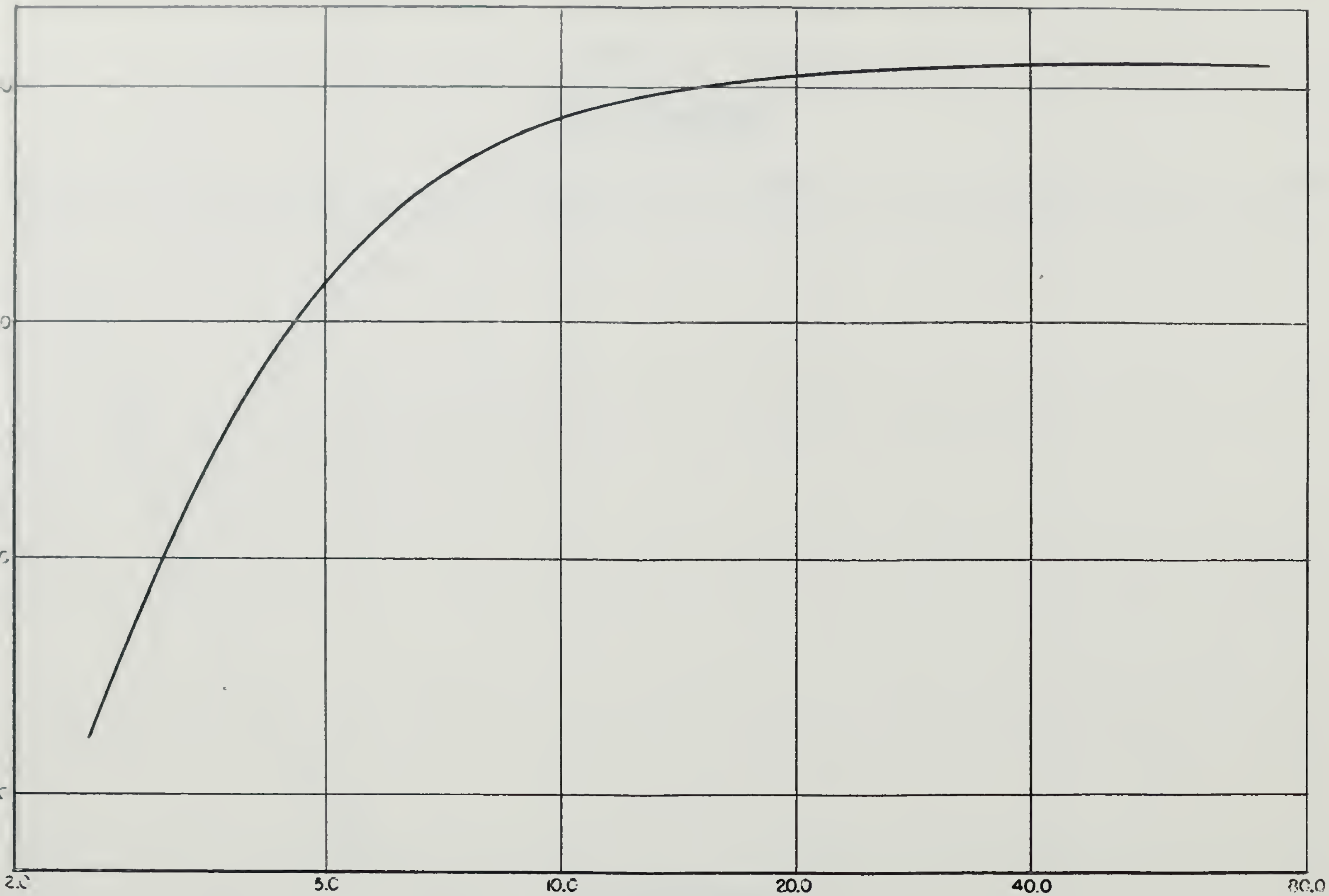

$\frac{\ell}{d} = \frac{\text{Slot Spacing}}{\text{Slot Width}}$

Figure 42. q_4 (ℓ/d)

DISTRIBUTION LIST FOR REPORTS ISSUED UNDER CONTRACT AF33(616)-3220

One copy each unless otherwise indicated

Commander
Wright Air Development Center
Wright-Patterson Air Force Base, Ohio

Attn: Mr. E.M. Turner, WCLRS-6
4 copies

Commander
Wright Air Development Center
Wright-Patterson Air Force Base, Ohio

Attn: Mr. N. Draganjac, WCLNT-4

Armed Services Technical Information Agency
Knott Building
4th and Main Streets 5 copies
Dayton 2, Ohio 1 repro

Attn: DSC-SA (Reference AFR205-43)

Commander
Hq. A.F. Cambridge Research Center
Air Research and Development Command
Laurence G. Hanscom Field
Bedford, Massachusetts

Commander
Hq. A.F. Cambridge Research Center
Air Research and Development Command
Laurence G. Hanscom Field
Bedford, Massachusetts

Attn: CRTOTL-1

Commander
Hq. A.F. Cambridge Research Center
Air Research and Development Command
Laurence G. Hanscom Field
Bedford, Massachusetts

Attn: CRRD, R.E. Hiatt

Air Force Development Field Representative
Attn: Capt. Carl B. Ausfahl
Code 1010
Naval Research Laboratory
Washington 25, D.C.

Director
Ballistics Research Lab.
Aberdeen Proving Ground, Maryland

Attn: Ballistics Measurement Lab.

Office of the Chief Signal Officer
Attn: SIGNET-5
Eng. & Technical Division
Washington 25, D.C.

Commander
Rome Air Development Center
Attn: RCERA-1, D. Mather
Griffiss Air Force Base
Rome, New York

Director
Evans Signal Laboratory
Belmar, New Jersey

Attn: Mr. O.C. Woodyard

Director
Evans Signal Laboratory
Belmar, New Jersey

Attn: Mr. S. Krevsky

Director
Evans Signal Laboratory
Belmar, New Jersey

Attn: Technical Document Center

Naval Air Missile Test Center
Point Mugu, California

Attn: Antenna Section

Commander
U.S. Naval Air Test Center
Attn: ET-315
Antenna Section
Patuxent River, Maryland

DISTRIBUTION LIST (Cont.)

Commander
Air Force Missile Test Center
Patrick Air Force Base, Florida

Attn: Technical Library

Chief
BuShips, Room 3345
Department of the Navy
Attn: Mr. A.W. Andrews
Code 883
Washington 25, D.C.

Director
Naval Research Laboratory
Attn: Dr. J.I. Bohnert
Anocostia
Washington 25, D.C.

National Bureau of Standards
Department of Commerce
Attn: Dr. A.G. McNish
Washington 25, D.C.

Director
U.S. Navy Electronics Lab.
Attn: Dr. T.J. Keary
Code 230
Point Loma
San Diego 52, California

Chief of Naval Research
Department of the Navy
Attn: Mr. Harry Harrison
Code 427, Room 2604
Bldg. T-3
Washington 25, D.C.

Airborne Instruments Lab., Inc.
Attn: Dr. E.G. Fubini
Antenna Section
160 Old Country Road
Mineola, New York
M/F Contract AF33(616)-2143

Andrew Alford Consulting Engrs.
Attn: Dr. A. Alford
299 Atlantic Ave.
Boston 10, Massachusetts
M/F Contract AF33(038)-23700

Chief
Bureau of Aeronautics
Department of the Navy
Attn: W.L. May, Aer-EL-4114
Washington 25, D.C.

Chance-Vought Aircraft Division
United Aircraft Corporation
Attn: Mr. F.N. Kickerman
Thru: BuAer Representative
Dallas, Texas

Consolidated-Vultee Aircraft Corp.
Attn: Mr. R. E. Honer
San Diego Division
San Diego 12, California
M/F Contract AF33(600)-26530

Consolidated-Vultee Aircraft Corp.
Fort Worth Division
Attn: C.R. Curnutt
Fort Worth, Texas
M/F Contract AF33(038)-21117

Textron American, Inc. Div.
Dalmo Victor Company
Attn: Mr. Glen Walters
1414 El Camino Real
San Carlos, California
M/F Contract AF33(038)-30525

Dorne & Margolin
30 Sylvester Street
Westbury
Long Island, New York
M/F Contract AF33(616)-2037

Douglas Aircraft Company, Inc.
Long Beach Plant
Attn: J.C. Buckwalter
Long Beach 1, California
M/F Contract AF33(600)-25669

Electronics Research, Inc.
2300 N. New York Avenue
P.O. Box 327
Evansville 4, Indiana
M/F Contract AF33(616)-2113

DISTRIBUTION LIST (Cont)

Beech Aircraft Corporation
Attn: Chief Engineer
6600 E. Central Avenue
Wichita 1, Kansas
M/F Contract AF33(600)-20910

Bell Aircraft Corporation
Attn: Mr. J.D. Shantz
Buffalo 5, New York
M/F Contract W-33(038)-14169

Boeing Airplane Company
Attn: G.L. Hollingsworth
7755 Marginal Way
Seattle, Washington
M/F Contract AF33(038)-21096

Grumman Aircraft Engineering Corp.
Attn: J.S. Erickson,
Chief Electronics Engineer
Bethpage
Long Island, New York
M/F Contract NOa(s) 51-118

Hallicrafters Corporation
Attn: Norman Foot
440 W. 5th Avenue
Chicago, Illinois
M/F Contract AF33(600)-26117

Hoffman Laboratories, Inc.
Mr. S. Varian
Los Angeles, California
M/F Contract AF33(600)-17529

Hughes Aircraft Corporation
Division of Hughes Tool Company
Attn: Dr. Vanatta
Florence Avenue at Teale
Culver City, California
M/F Contract AF33(600)-27615

Johns Hopkins University
Radiation Laboratory
Attn: Dr. D.D. King
1315 St. Paul Street
Baltimore 2, Maryland
M/F Contract AF33(616)-68

Fairchild Engine & Airplane Corp.
Fairchild Airplane Division
Attn: L. Fahnestock
Hagerstown, Maryland
M/F Contract AF33(038)-18499

Federal Telecommunications Lab.
Attn: Mr. A. Kandoian
500 Washington Avenue
Nutley 10, New Jersey
M/F Contract AF33(038)-13289

Glenn L. Martin Company
Baltimore 3, Maryland
M/F Contract AF33(600)-21703

Massachusetts Institute of Tech.
Attn: Prof. H.J. Zimmerman
Research Lab. of Electronics
Cambridge, Massachusetts
M/F Contract AF33(616)-2107

North American Aviation, Inc.
Aerophysics Laboratory
Attn: Dr. J.A. Marsh
12214 Lakewood Boulevard
Downey, California
M/F Contract AF33(038)-18319

North American Aviation, Inc.
Los Angeles International Airport
Attn. Mr. Dave Mason
Engineering Data Section
Los Angeles 45, California
M/F Contract AF33(038)-18319

Northrop Aircraft Incorporated
Attn: Northrop Library
Dept 2135
Hawthorne, California
M/F Contract AF33(600)-22313

Ohio State Univ. Research Foundation
Attn: Dr. T.C. Tice
310 Administration Bldg.
Ohio State University
Columbus 10, Ohio
M/F Contract AF18(600)-85

DISTRIBUTION LIST (Cont.)

Land-Air Incorporated
Cheyenne Division
Attn: Mr. R.J. Klessig
Chief Engineer
Cheyenne, Wyoming
M/F Contract AF33(600)-22964

Lockheed Aircraft Corporation
Attn: C.L. Johnson
P.O. Box 55
Burbank, California
M/F NOa(S)-52-763

McDonnell Aircraft Corporation
Attn: Engineering Library
Lambert Municipal Airport
St. Louis 21, Missouri
M/F Contract AF33(600)-8743

Michigan, University of
Aeronautical Research Center
Attn: Dr. R.D. O'Neill
Willow Run Airport
Ypsilanti, Michigan

Chief
Bureau of Ordnance
Department of the Navy
Attn: A.D. Bartelt
Washington 25, D.C.

Farnsworth Electronics Co.
3700 Pontiac Avenue
Ft. Wayne, Indiana
Attn: Tech. Librarian

Republic Aviation Corporation
Attn: Mr. Thatcher
Hicksville, Long Island, New York
M/F Contract AF18(600)-1602

Director, National Security Agency
RADE 1 GM, Attn: Lt. Manning
Washington 25, D.C.

Stanford Research Institute
Menlo Park, California
Attn: Mr J T Bolljahn
M/F Contract Af33(600)-25669

Radioplane Company
Van Nuys, California
M/F Contract AF33(600)-23893

Raytheon Manufacturing Company
Attn: Alice G. Anderson, Librarian
Wayland Laboratory
Wayland, Massachusetts

Republic Aviation Corporation
Attn: Engineering Library
Farmingdale
Long Island, New York
M/F Contract AF33(038)-14810

Ryan Aeronautical Company
Lindbergh Drive
San Diego 12, California
M/F Contract W-33(038)-ac-21370

Sperry Gyroscope Company
Attn: Mr. B. Berkowitz
Great Neck
Long Island, New York
M/F Contract AF33(038)-14524

Temco Aircraft Corp
Attn: Antenna Design Group
Dallas, Texas
M/F Contract AF33(600)-31714

North American Aviation, Inc.
4300 E. Fifth Avenue
Columbus, Ohio
Attn: Mr. James Leonard
M/F Contract AF33(038)-18319

General Electric Co.
French Road
Utica, New York
Attn: Mr. Grimm, LMEED
M/F Contract AF33(600)-30632

Westinghouse Electric Corporation
Post Office Box 746
Baltimore 3, Maryland
Attn: Mr. R.C. Digilio

AF33(616)-3220 UNCLASSIFIED REPORTS ONLY

Prof. J.R. Whinnery
Dept. of Electrical Engineering
University of California
Berkeley, California

Professor Morris Kline
Mathematics Research Group
New York University
45 Astor Place
New York, N.Y.

Prof. A.A. Oliner
Microwave Research Institute
Polytechnic Institute of Brooklyn
55 Johnson Street - 3rd Floor
Brooklyn 1, New York

Dr. C.H. Papas
Dept. of Electrical Engineering
California Institute of Technology
Pasadena, California

Radio Corporation of America
R.C.A. Laboratories Division
Princeton, New Jersey

Attn: Librarian

Electrical Engineering Res. Lab.
University of Texas
Box 8026, University Station
Austin, Texas

Exchange and Gift Division
The Library of Congress
Washington 25, D.C.

Dr. Robert Hansen
8356 Chase Avenue
Los Angeles 45, California

Technical Library
Bell Telephone Laboratories
463 West Street
New York 14, New York

Dr. R.E. Beam
Microwave Laboratory
Northwestern University
Evanston, Illinois

Department of Electrical Engineering
Cornell University
Ithaca, New York

Attn: Dr. H.G. Booker

Applied Physics Laboratory
Johns Hopkins University
8621 Georgia Avenue
Silver Spring, Maryland

Armed Services Technical Information Agency
Document Service Center
Knott Building
Dayton 2, Ohio 5 copies

Ennis Kuhlman
c/o Mc Donnell Aircraft
Lambert Municipal Airport
St. Louis 21, Missouri

Technical Reports Collection
303 A Pierce Hall
Harvard University
Cambridge 38, Massachusetts

Attn: Mrs. M.L. Cox, Librarian

Physical Science Laboratory
New Mexico College of A & MA
State College, New Mexico

Attn: R. Dressel

K.S. Kelleher
Melpar, Inc.
3000 Arlington Blvd.
Falls Church, Virginia

Electronics Research Laboratory
Stanford University
Stanford, California

Attn: Dr. F. E. Terman

ERRATA

Technical Report No 14

CLOSELY SPACED TRANSVERSE SLOTS
in
RECTANGULAR WAVEGUIDE

by

Richard F. Hyneman

Contract AF33(616)-3220
Project No. 6(7-4600) Task 40572

Page

6. Equation following (2-1) should read. $\underline{G}(x,y,z) = \underline{G}(x,y,z-\ell)$

15 The first sentence of the second paragraph starting on Page 15 should read: " ... the case of an aperture of finite extent, S."

17 Equation 2-30 should read.

$$H_{y_{ext}} = (1/j\omega\mu)[k^2+\partial^2/\partial^2y^2](-j/2\ell)\int_{-L/2}^{L/2}\left\{\sum_{n=-\infty}^{\infty}\int_{-d/2}^{d/2}\cos(\pi y'/L)\cdot\right.$$

$$\left.\cdot\, e^{j\gamma_n z}\, H_o^{(2)}(\beta_n\rho)\, dz'\right\} dy'.$$

18 The closing brace } follows the final term of Equation 2-33. In Equation 2-33, the differentials should be dy dy′ instead of dy dz′.

19 The closing brace } follows the final term of Equation 2-35. In Equation 2-35: $\mathcal{E}_{m,n} = 0$ for $m = 1$ when $n = 0$

$= 1$ otherwise.

22 The third equation is Equation 2-40, the fifth is Equation 2-41.

52 The last term of Equation 3-16 should be: "$1.215\ (\lambda^2/4W^2)$".
In the Equation following 3-16, the closing brace } follows the final term.

58 Equation 4-1 should read.

$$\frac{\cot\,\kappa D}{\kappa D} = \frac{1}{1-(\lambda^2/4W^2)}\ \frac{(1-L^2/W^2)^2}{\cos^2(\pi L/2W)}\left\{\sum_{m=3}^{\infty}{}'\left(\frac{m^2\lambda^2}{4W^2}-1\right)\ \ldots\right.$$

ERRATA (continued)

Page

60 The second equation on Page 60 should read:

$$(i+1)^{\beta} = k\sqrt{1 - (\gamma/k)^2_{i+1}} = k\sqrt{1 - [({}_o\gamma/k) + \delta_i(\gamma/k)]^2}.$$

70 Figure 30: D/W = 0.466.

71 The next-to-last equation should read:

$$I_o\left(-j\frac{\sigma}{k}, \frac{L}{\lambda}\right) = -j\frac{2}{\pi}\left\{(1.273)\left[\bar{\gamma} + \ln\frac{\sigma}{k}\frac{L}{\lambda}\right] - .807 + 1.215\frac{\lambda^2}{4L^2}\right\}$$

76. For Figure 33c: L/λ = .356.

89 The final term of the equation preceding Equation A-3 should read:

$$+[g(s')\eta^*(s) + g^*(s)\eta(s')]\, K_c(s/s')\Big\}\, ds\, ds'.$$

90 The final term of the fourth equation should read:

$$\ldots + 2Re\left\{\int_S \eta^*(s)\left[\int_S g(s')\, K_c(s/s')\, ds'\right] ds\right\}.$$

91 In the second equation: $s = \begin{bmatrix} 1 & 0 \\ 0 & -1 \end{bmatrix}$.

95 A plus (+) sign should precede the second line of Equation B-6.

96. The next-to-last equation should read: $\sigma_n L > 3\pi$.

98 The closing brace follows the final term of Equation B-17.

100 Equation B-20d should read:

$$u_{2i} = \frac{1}{(i!)^2}\int_o^{\pi} u^{2i}\left(1 - \frac{u}{\pi}\right)\cos u \ln u\, du.$$

105 Equation C-3 should read:

$$\sum_{i=o}^{2}.$$